corrected

Cranfield University

ANNI KAISA VUORENKOSKI

Development of a liquid-phase LPG MPI conversion system

School of Engineering

PhD Thesis

Cranfield University

School of Engineering

PhD Thesis

2004

ANNI KAISA VUORENKOSKI

Development of a liquid-phase LPG MPI conversion system

Supervisors: Dr. Mark Jermy and Dr. Matthew Harrison

October 2004

This thesis is submitted in partial fulfilment of the requirements for the degree of Doctor in Philosophy

ABSTRACT

For decades Liquefied Petroleum Gas (LPG) has been considered as one of the most prominent alternative fuels to petrol. LPG typically consists of propane, butane and propylene, but also smaller quantities of methane and ethane. LPG has a low price compared to petrol, the potential of low emissions and has indigenous availability. It possesses approximately the same energy density, on a gravimetric basis, as petrol, vaporises easily, mixes readily with air, is resistant to auto-ignition, has wide flammability limits and a good laminar burning speed. Therefore it is also possible to achieve an acceptable efficiency and power from a spark ignition engine run with LPG. The state-of-the-art LPG systems used in spark-ignition engines are either mono-fuel systems, where the vehicle is solely operated using LPG, or bi-fuel vehicles, capable of using either petrol or LPG.

The objectives of this work were to develop an aftermarket conversion bi-fuel LPG system, which would improve the efficiency of the engine during LPG operation, with further improvements in the mixture preparation and control, the methods for LPG fuelling calibration and the methods to prevent premature vaporisation in the fuel rail. An additional objective of this study was to investigate the performance and combustion of LPG in a non-optimised spark-ignition engine.

A prototype system was developed and demonstrated in a 4-cylinder research engine. This novel system uses a liquid LPG injection system, in contrast to the conventional vapour injection systems used in aftermarket LPG bi-fuel conversions. A significant improvement in engine power output was shown, as well as an improvement in mixture control. An optical diagnostics method was applied in order to study the mixture preparation using two alternative LPG fuel injection configurations. The results from both the mixture formation study and the engine experiments showed that the charge cooling effect can be used to improve the efficiency of a non-optimised bi-fuel engine. It was also shown that from the mixture control point of view, injecting the fuel directly to the manifold gives a significant advantage over systems where the fuel is injected to the manifold through coupling pipes.

This novel LPG system also uses a fuel pressurising method that improves the fuel system performance in extreme conditions. In addition, a control method to prevent the premature vaporisation of the LPG fuel in the fuel supply line was developed. The method comprises an optical sensor which can detect migrating vapour bubbles in addition to complete phase changes in the fuel line. It was noticed during validation of the sensor that vaporisation in the fuel rail starts in local hot spots, before the global saturation conditions in the fuel rail are met.

This work has demonstrated the potential of using non-optimised LPG systems in bi-fuel vehicles. However, the final validation of the novel control system requires extensive testing on a fleet of test vehicles, and this was not possible within the scope of the work.

ACKNOWLEDGEMENTS

I would like to take this opportunity to thank my supervisors, Dr Mark Jermy and Dr Matthew Harrison, for their support and advice during my studies. Thank you both for making it possible. Also, I would like to thank Dr Glenn Sherwood for his advice and help with the schlieren imaging, and I would also like to thank Professor Doug Greenhalgh for encouragement throughout.

I would like to thank DTI and Jaymic Ltd for supporting this project through the TCS scheme. Also, I would like to thank Steve Chambers at Jaymic for his practical advice and help.

A very special thank you goes to the technicians Tim Lee and the late Bob Wilson, whose help and effort throughout this work has been huge. I would also like to thank Eric Lepot and Stathis Kaparis, who contributed to the development of the LPG system. Finally, I would like to thank my fellow PhD candidates for valuable friendship throughout these three years, Thierry, Andreas, Eudoxios, Christian, Damien, Fatiha, Taib, Edouard, Dmitry, Adam, Alessio and all the others.

The biggest thank you goes to my family, my husband Fraser and my son Felix, for being the ultimate motivation. "Get your motor running, head out on the highway, lookin' for adventure in whatever comes our way"...

LIST OF CONTENTS

LIST OF FIGURES

UNITS

c	Speed of light [m/s]
c_o	Speed of light in a vacuum (3×10^8 m/s)
n	refractive index
ε	light ray deflection angle produced by schlieren [rad or arcs]
p	pressure [kPa]
ρ	density [kg/m^3]
Δ	increment or change in the quantity which follows
T	temperature in degrees [°K]
R	specific gas constant [J/(kg x °K)]
k	Gladstone-Dale coefficient [m^3/kg]
N	number of samples

NOTATION

°CA	degrees of Crank Angle
ATDC	After Top-Dead Centre
AFTDC	After Firing Top-Dead Centre
ASOI	After Start Of the Injection
BTDC	Before Top-Dead Centre
CARS	Coherent Anti-Stokes Raman Spectroscopy
CCLIS	Close-Coupled Liquid Injection System
CVI	Closed-valve injection
DEMA	Diethyl Methylamine
DISI	Direct Injection Spark Ignition
GDI	Gasoline Direct Injection
DI	Direct Injection
ECU	Engine Control Unit
EGR	Exhaust Gas Recirculation
FI	Fluctuation intensity
GRT	Global Rainbow Thermometry
IR	Infra Red
IVC	Intake Valve Closing
IVO	Intake Valve Opening
LBF	LPG Blended Fuel
LIF	Laser Induced Fluorescence
LII	Laser Induced Incandescence
LPG	Liquefied Petroleum Gas
LPLI	Liquefied Petroleum gas Liquid Injection
MBT	Maximum Brake Torque – timing
MFB	Mass Fraction Burned
MPI	Multi-point Port-Injection
NMHC	Non Methane Hydro Carbons
OBD	On-Board Diagnostics
OEM	Original Equipment Manufacturer
OFP	Oxygen Forming Potential

OVI	Open-valve injection
PCLIS	Pipe-Coupled Liquid Injection System
ROHR	Rate Of Heat Release
SI	Spark Ignition
SOI	Start Of the Injection
TDC	Top-Dead Centre
WOT	Wide-Open Throttle

I. INTRODUCTION AND OBJECTIVES

I.1 REDUCING EMISSIONS

The stringent emission legislation in the European Community (EC) area and in many other countries around the world has steered the local governments and car manufacturers to develop the current petrol and diesel vehicle technology, but also to look for alternative fuel for internal combustion engines used in road vehicles. The current emission legislation in the European Union (EU) is based on EU directive 70/220/EC, which stated the first official limits on exhaust emissions. The most recent emission standards define limits for carbon monoxide (CO), hydrocarbons (HC), nitrous oxides (NO_X) and particulates (only for diesel vehicles). The limits are defined in grams per kilometre (Table I-I).

Table I-I. Emission limits in EU legislation (vehicles with spark-ignition engines).

Regulation	From	CO [g/km]	HC+NO_X [g/km]	HC [g/km]	NO_X [g/km]
Euro I	1 Jul, 1992	2.72	0.97	-	-
Euro II	1 Jan, 1996	2.2	0.5	-	-
Euro III	1 Jan, 2000	2.3	-	0.2	0.15
Euro IV	1 Jan, 2005	1.0	-	0.1	0.08

Source: (European Union, 2004).

The current regulation, commonly called the Euro III, came into force in January 2000. In addition to the limits for the pollutant emissions, the Euro III regulations limit the carbon dioxide (CO_2) emissions by regulating the fuel economy and also require the integration of On-Board Diagnosis (OBD) equipment. The purpose of this equipment is to detect any malfunction in engine operation, which might lead to an increase in pollutant exhaust emissions, by constantly monitoring the signals from several engine sensors and actuators.

The main strategy to reduce pollutant emissions in spark-ignition (SI) engines has been to develop the engine management systems, mixture formation systems and emissions after-treatment equipment. The development of the injection and ignition control has made it possible to provide precise control of injected fuel quantities and

ignition timing, which are the most essential factors concerning the raw emissions. Modern Engine Control Units (ECUs) have also been equipped with adaptive control algorithms to compensate for varying fuel quality and ageing engines. There has also been a significant effort to improve the fuel quality and the introduction and development of catalytic converters have made it possible to considerably further reduce exhaust emission components. New engine technologies have also been adapted in order to achieve compliance with the emission legislation, such as variable valve timing, multi-valve technology, improved combustion chamber geometry and lean-burn and Direct Injection Spark Ignition (DISI) technology.

The prospect of using alternative fuels has also been actively investigated during the past decades. The strongest research effort is aimed at developing solutions for electrically (hydrogen) powered vehicles, but the development is slow and the results in reduction of harmful pollutants are expected to be seen after a long period of time. The use of alternative, less polluting fuels for internal combustion engines has often been referred to as a bridging technology and a short-term solution for urban pollution.

The main challenge from the view of car manufacturers is to meet the emission legislation limits without compromising the customer requirements for efficiency and performance. Petrol and diesel have both high energy density, which gives these conventional fuels advantages not only in performance but also in fuel consumption and operating distance.

Liquefied Petroleum Gas (LPG) gas has for decades been considered as one of the most promising alternative fuels for internal combustion engines mainly due to its relatively high energy density, high octane rating and low emissions. LPG can be stored in the tank as liquid at a moderate pressure, which gives it major benefit over most other alternative fuels. It has been recognised in many countries as a "green fuel", and its use as an alternative fuel for road vehicles has been supported by many governments by fuel tax reductions.

Natural gas, which essentially consists of methane, has also been referred as a clean fuel, mainly due to its low CO_2 and particulate emissions. The use of natural gas as

automotive fuel is attractive also because natural gas has a high octane rating and higher autoignition temperature than petrol. Natural gas has the advantage of energy diversification and natural gas reserves have been estimated to be about the same order of magnitude as those of petroleum, but the current production is only 60% of crude oil production. Natural gas can be stored onboard vehicles in two ways, in gaseous form at atmospheric pressures and high pressures (the fuel stored this way is referred as Compressed Natural Gas or CNG), or in liquid at cryogenic temperatures and atmospheric pressures (referred as Liquefied Natural Gas or LNG). Energy diversification has also been a major reason for interest in using methanol as an alternative fuel in road vehicles. Methanol has also very high octane rating, but also very low heating value and stoichiometric air to fuel ratio, and the use of methanol leads to higher fuel consumption when compared to petrol. Methanol has also very high latent heat of vaporisation compared to petrol.

I.1.1 Government legislation and support

Several programs have been established by local governments to support the use of alternative fuels. The UK Government has recognised the need for a short term solution for reducing harmful pollutants resulting in both urban pollution and global warming. Transport is seen as the main cause for bad air quality in cities, which is considered a serious health risk, and is responsible for 25 % of total carbon dioxide emissions resulting in global warming. The government in the UK has established an Energy Saving Trust programme to help establish a sustainable market for alternative fuel vehicles in the UK. The focus of the programme is to create the conditions for clean fuel vehicles to be practically and economically viable. Similar programmes have been started by other local European governments (e.g. Netherlands, Germany, Italy and Switzerland) to support the use of cleaner fuels by, for example, reducing taxation on alternative fuels or vehicles that use alternative fuels.

Most of the programmes support the use of LPG in fleet vehicles, which is considered to contribute to the reduction of urban pollution. Government initiatives have been taken in the UK, Switzerland, Korea and Taiwan to convert taxis to use LPG. In some European countries, like the UK, the Netherlands and Italy, the government also promotes the installation of the bi-fuel conversion devices on petrol vehicles. This

however has recently been under criticism because it has been recognised that the emission benefits with the bi-fuel vehicles depend on the quality of the conversion (Chiu and Matthews, 1996; Energy Savings Trust, 2003).

I.1.2 Liquefied Petroleum Gas

LPG typically consists of propane, butane and propylene, but also smaller quantities of methane and ethane. LPG is one of the most popular and widely used alternative automotive fuel in the world due to its low price compared to petrol, potential to low emissions and indigenous availability. It possesses approximately the same energy density, on a gravimetric basis, as petrol, vaporises easily and mixes readily with air, is resistant to auto-ignition and has wide flammability limits and a good laminar burning speed. Therefore it is also possible to achieve an acceptable efficiency and power from a spark ignition engine run with LPG. LPG also offers advantages in mixture preparation and control during engine transients and cold-start over the conventional petrol due to the lack of wall wetting.

LPG is produced from two sources. In Europe and North America, most of the production sources from the refining of crude oil, while in the rest of the world, most the LPG results from the purification of natural gas during its extraction. Most countries, like the UK, designate the majority of their LPG production and import to domestic and industrial needs, and only a small fraction is reserved for road vehicle use. The total LPG production in the year 2002 was 210 million tonnes, of which 49% was used in the domestic sector, 25% in the chemical industry sector, 12% in other industry and 8% in transport. The majority of LPG markets are in North America and in Asia, which both have a 28% share of the total LPG consumption, while the consumption in Europe is 20% of total consumption (World LP Gas Association, 2004).

The composition of LPG varies significantly mainly depending on the geographical issues, but also on the local standards and regulations. The varying composition of C_3 and C_4 hydrocarbons in LPG has produced an additional challenge in the use of LPG as a motor fuel. In Europe, the lack of standards has been criticised for years by the LPG equipment manufacturers. The European standard EN589 does not exclude

significant variations in composition of LPG, and local European governments have adopted special legislation to limit the variation in LPG composition. In the UK, the LPG used both domestically and in motor vehicles is so called commercial propane, which typically comprises of 96% propane. In France, local legislation specifies that LPG must contain between 19 – 50% propane, while in Italy in Spain the LPG typically contains only 20% propane. In the Unites States, the standardisation is more advanced, and the fuel must contain at least 85% propane. In Asia, the LPG used consists of mainly butane (Guibet, 1999).

I.1.3 LPG systems

The LPG systems used nowadays in road vehicles can be roughly divided into two types: mono-fuel and bi-fuel vehicles. Mono-fuel, or often also called dedicated LPG vehicles, are designed to run exclusively on LPG fuel, while the bi-fuel vehicles can run both on LPG and petrol. While the vast majority of LPG vehicles have spark-ignition engines, technologies have been developed to enable LPG to be used in compression ignition engines.

Bi-fuel LPG vehicles can further be classified into two groups; Original Equipment Manufacturer (OEM) fitted systems and aftermarket (often called retrofit) systems. The OEM LPG systems have been designed exclusively for a particular type of petrol vehicle and are fitted to the vehicle by the car manufacturer. Aftermarket LPG systems on the other hand can be fitted in any type of vehicle with a spark ignition engine.

There are generally speaking two types of fuel supply systems, vapour or liquid systems. The conventional systems use LPG in its gaseous state; the fuel is mixed with air in the intake manifold of the engine as vapour. These systems are called vapour systems. The state-of-the-art fuel supply systems are either mono-point carburetion type systems or multi-point vapour injection systems. Recently, it has been shown that injecting LPG as liquid offers several advantages over vapour mixer or injection systems. The fuel metering is more accurate because of shorter injection durations, which leads to more accurate control over air to fuel ratio and prevention of manifold backfires. Also, when the fuel is vaporised in the intake manifold, the latent

heat for the phase change cools the intake air resulting in higher intake charge densities and hence improved engine power output. The intake air cooling affects also leads to lower combustion temperatures and lower emissions. These systems are called LPG Liquid Injection (LPLI) systems.

I.2 OBJECTIVES OF THE STUDY

I.2.1 State-of-the-art systems

Several studies in scientific literature cover LPG liquid injection systems. Most of the research concerns mono-fuel vehicles. Mono-fuel LPLI vehicles are fully optimised for the use of liquid injection LPG, which enables the increase in compression ratio, the optimisation of in-cylinder flow by optimising the manifold and combustion chamber geometry, and most importantly, the optimisation of the electronic engine control. Several researchers have demonstrated the potential of the use of liquid LPG as a sole fuel in conventional MPI engines, lean-burn engines and DISI engines. However, even though these systems offer obviously great opportunities in achieving the optimum engine performance and lowest emissions, the systems have significant limitations. First, all mono-fuel LPG vehicles are dependant on the local availability of the LPG fuel. Although LPG is increasingly available in urban areas due to increase in the use of LPG in fleet vehicles, in rural areas (even in the UK LPG distribution network) it is not widely available. Secondly, the mono-fuel vehicles are always vehicle model specific. Development of a mono-fuel LPG vehicle requires time and effort due to an elaborate optimisation process. Therefore, mono-fuel LPLI systems are solely used in fleet vehicles.

All the bi-fuel vehicle LPLI developments reported in scientific literature concern OEM installed systems. Obviously, these LPLI systems also have the disadvantage of being vehicle-specific, where only a few European car manufacturers offer a bi-fuel option for their models. The main difference compared to mono-fuel systems is obviously that the engine can use both petrol and LPG as a fuel. Another difference is in the engine optimisation; in the OEM installed bi-fuel LPLI engines the engine geometry, like the compression ratio and combustion chamber geometry, is optimised only for petrol operation. However, in these systems, the electronic control of the LPLI injection system is optimised for LPG (*fully software-optimised* system), where the fuel metering, injection phasing and ignition timing are all optimised for LPG operation. This requires the use of two engine control units, one for each fuel. The control units controlling the LPG are totally independent from the petrol control units, but have a constant communication link with the petrol control unit to prevent

interference with the OBD unit. Since LPG has different properties than petrol, the OBD is known to detect malfunctions during LPG operation even though there would be nothing wrong with the system. In OEM fitted bi-fuel systems this problem has been overcome by developing a bi-fuel specific OBD unit, which is able to detect the state of engine operation. Therefore, a modification to both the petrol ECU and the OBD unit is necessary.

There are no aftermarket conversions available as liquid injection LPG systems, but several vapour injection systems exist as aftermarket conversions. These bi-fuel systems have the benefit over the OEM fitted systems that they are essentially universal, and can be fitted to any type of vehicle, and the vast majority of LPG vehicles on European roads are aftermarket conversion bi-fuel vehicles. However, these systems lack the OBD compatibility. The fuel metering is usually carried out with a separate control unit, which has its own independent closed feed-back control, and there is no communication between the LPG control unit and the original OEM petrol control unit, as there is in the case of OEM fitted systems. This often leads to misinterpretation of the monitored signals by the petrol OBD unit. In the state-of-the-art bi-fuel aftermarket conversion systems this is avoided by sending dummy signals to the OBD during LPG operation. These systems are called "OBD-fix".

The aftermarket conversion systems have also been criticised for poor performance and emissions due to inadequate fuelling calibration (Chiu and Matthews, 1996). The LPG control units are calibrated by the installers, and the quality of these calibration systems vary significantly. In addition, in the vapour injection systems, the injection durations are significantly longer when compared to petrol injection durations due to considerably lower fuel density. This leads to a problem with backfiring when the intake manifold is filled with a combustible mixture most of the time.

The vapour mixer-type and injection systems have been reported to produce approximately 10-15% less brake power compared to petrol operation due to lower volumetric efficiency (Sierens, 1992; Shehata, 2001), and the vapour injection systems do not have many other benefits associated with the LPLI systems either. The LPLI systems offer a significant benefit in engine performance due to a different mixture formation mechanism; the intake air is cooled due to vaporising fuel and

hence the charge density and consequently, the volumetric efficiency are increased. This also has a beneficial effect on NO_X emissions and engine thermal efficiency. LPLI systems also do not suffer from backfiring problem. However, all LPLI systems are susceptible to problems with premature fuel vaporisation in the fuel rail, which is a consequence of the relatively low saturation temperature of LPG.

I.2.2 Objectives

The main objective of this work is to study the possibilities of significantly improving the aftermarket conversion systems. There are three main aspects:

1. All available aftermarket conversion systems have a performance penalty and the first objective of this study is to improve the engine performance of bi-fuel aftermarket LPG conversions by using a liquid injection system. The existing LPLI technology does not allow the systems to be installed in any other than specific vehicle models and as an OEM installation.
2. All the scientific literature concerning LPLI systems investigate systems that are fully software optimised or also engine geometry optimised, for LPG operation. One of the main objectives of this study is to understand the combustion and performance characteristics of *non-optimised* bi-fuel systems, where the engine operating parameters, like injection phasing and ignition timing are optimised for petrol operation.
3. To improve the mixture preparation and control of aftermarket LPG conversion systems in order to achieve faster and more accurate AFR control, but also prevent manifold backfires.
4. To improve both the compatibility with the OBD systems and the calibration process by using no additional control unit for LPG fuelling
5. To improve the methods to prevent the event of fuel vaporising in the fuel rail due to reaching saturation conditions in any LPLI system.

I.3 SYNOPSIS

I.3.1 Chapter II

The study of existing systems, in particular LPG properties, performance and emissions in spark ignition engines is described in Chapter II.

I.3.2 Chapter III

Chapter III describes the development of the system architecture. The objective is to develop an LPG conversion system, which would offer advantages over existing aftermarket systems by improving engine performance, mixture preparation and control, engine calibration and OBD compatibility. Also the system would improve the premature vaporisation control.

The injection control in the proposed aftermarket conversion systems is managed by the petrol control unit also during LPG operation. This prevents the interference with the OBD unit, as the petrol ECU is in control of all engine actuators and receives the actual signals from the monitored sensors. However, even though the fuel metering calibration would be fully carried out by using suitable hardware, the calibration could only be done in one load and engine speed conditions. It is believed that the adaptive algorithms of the ECU could compensate the minor differences in fuel metering during LPG operation in the rest of the engine operating range.

It is suggested that the fuel metering calibration of the system could be carried out by the installer, but methods would be sought within this study to calibrate only system hardware with no software calibration involved. This is believed to reduce significantly both the calibration effort and the risk of an unsuccessful calibration. Also, this fuelling control method would make the system universal, i.e. the conversion system could be fitted to virtually any type of petrol vehicle.

It is expected that the engine performance using this control method suffers compared to mono-fuel LPLI systems or the fully software-optimised, OEM fitted bi-fuel LPLI systems due to the lack of optimisation of the compression ratio or the ignition timing. However, a significant benefit in produced engine power is expected when compared

to the existing aftermarket conversion systems, which are all vapour injection systems.

Premature vaporisation is considered as one of the most significant issues in any type of LPLI systems. This occurs when the fuel pressure decreases below the saturation pressure, or the temperature increases above the saturation temperature. As a consequence, the fuel metering is affected by the presence of fuel vapour in the fuel rail. The method to overcome this problem has been to maintain the fuel pressure at a level of constant pressure difference between the fuel tank and the fuel rail. This is due to the fact that the fuel is stored in the fuel tank in its saturation conditions, and hence the pressure in the tank varies due to variations in the atmospheric temperature. The pressure in the fuel rail, in the presently available LPLI systems, is maintained at a constant 3-5 bar above the tank pressure, which means that the fuel rail pressure changes with the changing tank pressure. This in turn means that the pressure drop across the fuel injectors varies with the tank pressure, and therefore the injector flow rate varies due to varying tank pressure. Thus this strategy to prevent the saturation conditions in the fuel rail requires feed-back from the fuel rail pressure sensor to the fuel metering control unit to compensate the varying injector flow rate. Also, it has been reported in several studies that this method does not provide adequate margins to the saturation conditions. Within this study, it is suggested that a fuel pressurising method that would be able to use higher boost pressure and increase the margins to the saturation conditions would be sought.

Also, it is suggested that a method to detect the vapour bubble formation is developed. It is considered that the circumstances of vaporisation is very difficult to be totally avoided, but if a method to detect the condition could be found, it would make it more manageable to prevent the consequences of the event.

I.3.3 Chapter IV

In sequential bi-fuel vehicles, the location of the LPG injectors often addresses a practical problem. The space available in the intake manifold is not adequate to accommodate the LPG injectors beside the petrol injectors. In vapour injection bi-fuel systems, the fuel injectors and the fuel rail are installed remotely (away from the

manifold), where the fuel metering occurs. Fuel injectors are connected to the manifold via flexible pipes. While using vapour fuel, this configuration does not address any problems in terms of mixture formation, the fuel is vapour if it is injected directly to the manifold, or to the connecting pipes. However, in LPLI systems, mixture formation when using these types of coupling pipes causes a few potential problems. First, the fuel starts vaporising inside the pipes and the energy for vaporisation is taken from the pipe walls, rather than from the intake air, as would be the case if the fuel would be injected directly to the manifold. This reduces the charge cooling effect. Another potential problem is the fuel travelling time through the pipes; due to partial vaporisation, the travelling times might be so long that the fuel arrives in the manifold when the intake valve is already closed. This causes a problem concerning backfiring, but also the fuel metering suffers during engine transients. The problem of travelling time is particularly a problem within the proposed system control method, when the fuel injection is controlled solely by the petrol ECU.

To study the mixture formation in the pipe-coupled remote injection system, optical measurements of the fuel injection are carried out using Schlieren imaging in a constant volume chamber.

I.3.4 Chapter V

Chapter V describes the engine experiments carried out to demonstrate the operation of the LPLI bi-fuel system and also to evaluate the effect of certain system parameters. The main motivation for the study is to determine the extent of the expected engine power loss associated with the use of only one ECU to control both the petrol and LPG operation in the engine. Obviously, the existing petrol injection and ignition systems have been carefully calibrated for petrol operation, and the standard ignition control does not have an adaptive feedback control to be able to compensate the possible difference in optimum ignition timing. These differences in the combustion process are expected to result from the different thermochemical properties of LPG and petrol, the different intake temperature and resulting variation in the cylinder charge density and different processes of mixture formation using different injector configurations. The engine experiments were carried out in a small 4-cylinder engine equipped with both petrol and LPLI systems and controlled with a

programmable control unit in order to study the effects of different ignition timings on engine performance. The performance was evaluated by measuring both engine brake torque and cylinder pressure. The effect of charge cooling associated with the two LPG injection system configurations was investigated in order to understand the advantage of increasing the engine efficiency by using different injector configurations.

I.3.5 Chapter VI

Chapter VI describes the work carried out to develop and demonstrate the operation of a premature vaporisation control method. In order to detect saturation conditions in the fuel rail, a device to detect vapour bubbles on-line is developed. The detection of the bubbles is very difficult by using any conventional pressure and temperature monitoring methods. It is assumed that vaporisation starts in local hot spots in the fuel rail, and therefore the bubbles form before the average temperature or the average pressure of the fuel rail reaches the saturation conditions. The presence of the type of sensor which would be able to detect the vapour bubble formation would make it possible to obtain an additional means to control the fuelling. Also, the sensor would be very useful in the product development of LPLI systems when optimal solutions for fuel rail materials and other parameters are studied in order to reduce the heat transfer to the fuel rail.

I.3.6 Chapters VII and VIII

Chapter VII describes the achievements and contributions of this thesis work, while Chapter VIII includes the final conclusions, practical recommendation and suggestions for future work.

II. LITERATURE REVIEW

II.1 BASIC CONCEPTS OF MIXTURE FORMATION IN A SI ENGINE

II.1.1 Fuel – air composition requirement

The combustion in the cylinder is an oxidation process where the fuel compound, carbon and hydrogen react with oxygen. In order to achieve complete combustion, a certain amount of air mass is needed to react with the fuel mass. The stoichiometric air fuel mixture can be computed by considering the chemical equilibrium of the reaction process; the reactants, the chemical composition of the fuel (C_XH_Y) and the air, which contains by volume 21% oxygen (O_2) and 79% nitrogen (N_2), are converted to products, carbon dioxide (CO_2), water (H_2O) and nitrogen.(Heywood, 1988)

$$C_X H_Y + \frac{1}{\phi}(X + Y/4)\{O_2 + 3.76N_2\} \rightarrow products \qquad \textbf{Equation II-I}$$

The equivalence ratio ϕ characterises the stoichiometry of the reaction; in the case the where equivalence ratio $\phi = 1$, the reaction is stoichiometric. The reactant mixture composition can be determined in terms air to fuel ratio (AFR), the ratio of the air mass and the fuel mass. From the Equation II-1 and Equation II-2 one can derive the stoichimetric AFR for a given mixture composition

$$AFR_{stoich} = \frac{(X + Y/4) * \{32 + 3.76 * 28\}}{12X + Y} \qquad \textbf{Equation II-II}$$

For a common petrol fuel with carbon / hydrogen (X/Y) ratio of 8.6/14, this yields a chemically correct mixture ratio of $AFR_{Stoich} \cong 14.8$ (Lentz, 1992). The calculation could then be carried out using the carbon / hydrogen ratio of propane, which gives a value of $AFR_{Stoich} = 15.6$ for the pure propane compound. It should be noted that outside the UK, LPG also usually contains butane and smaller fractions of other substituents, which obviously changes the stoichiometric AFR. This is discussed in depth later in this chapter.

II.1.2 Engine control systems

II.1.2.1 Engine Control Units

In Multi-point Port Fuel Injection (MPI) spark ignition engines, the fuel is injected into the intake port of each cylinder and there is therefore one injector for each cylinder. The injector is usually located 50-100 mm from the valve, and it is positioned so that the spray aims towards the intake valve. The fuel flow rate through an injector is controlled by the pressure difference across the injector (solenoid valve). The pressure difference is maintained constant in order to make the fuel flow rate dependent only on injection duration. Because the manifold pressure varies with the varying throttle angle, the fuel system requires a pressure regulator that senses the manifold pressure and controls the pressure difference across the injector. As a result, the amount of fuel injected during one cycle is controlled by the injection pulse duration.

The Engine Control Unit (ECU) calculates the required amount of fuel by monitoring engine running conditions by acquiring signals from several sensors. The fundamental calculation routine is shown in Figure II-I. The base injection timing is calculated from the engine load signal and from the injector constants. This constant varies according to injector design and is multiplied by the injection duration time, which is obtained from the fuel mass corresponding to a particular air mass for each stroke. The effective injection timing results when the correction factors are included in the calculations. The correction factors also provide adjustment data for varying engine operating conditions. Conventionally, the fuel injection controllers use feed forward control based on a mass air flow (MAF) sensor located upstream from the throttle (or combined signal from engine speed and manifold absolute pressure) and a proportional integral (PI) type feed back control provided by an Exhaust Gas Oxygen (EGO) sensor and predetermined look-up tables (Bauer, 1999).

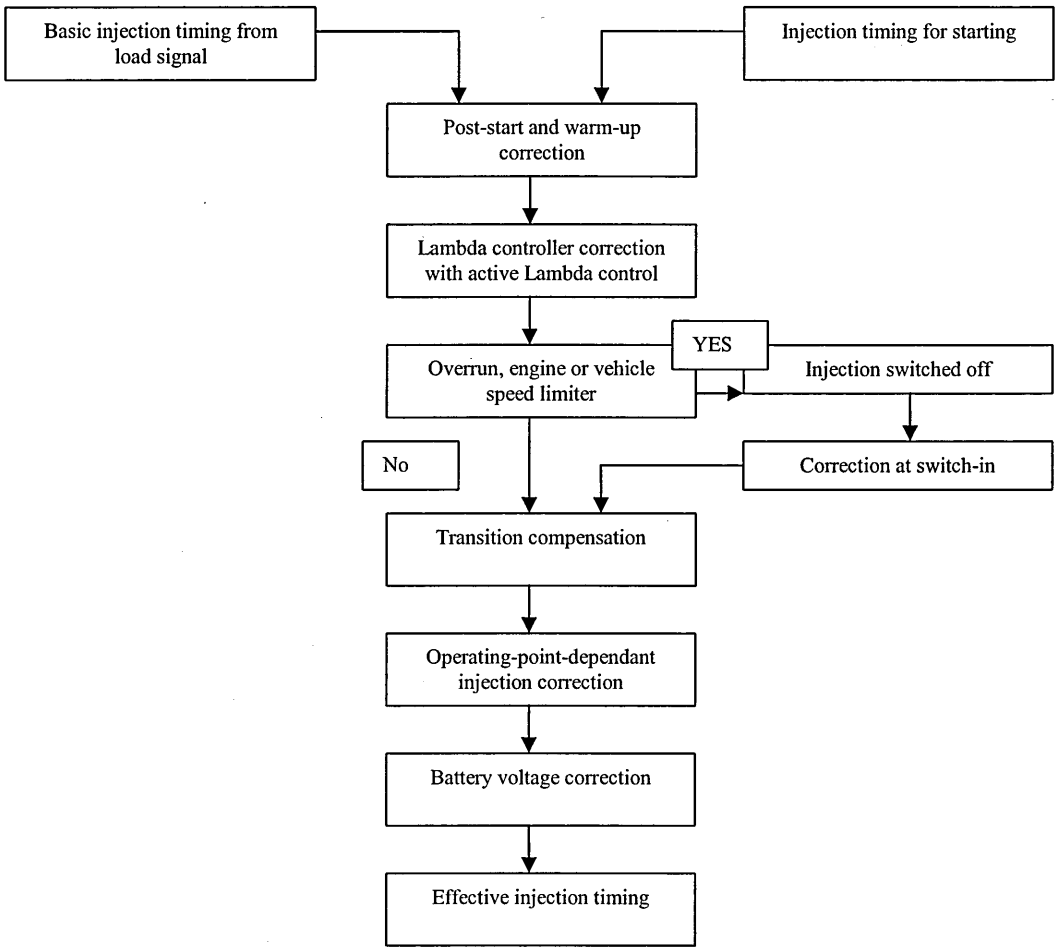

Figure II-I. Fuel injection calculation routine.

The ECU uses the signal from the air-mass meter and the monitored engine speed to generate an injection signal. At the same time, it generates a lambda-control factor from the EGO sensor signal to correct the injection time. The ECU reacts to the monitored signal by modifying the control variable with an initial jump followed by a ramp progression. The injection time is therefore shortened or lengthened, and the control factor reacts to the continuing data transfer by settling into a constant oscillation. The duration of the oscillation periods is determined by the flow times of the gas, while the magnitude of the ramp climb of the correction factor stays approximately constant within a particular load and speed range despite variations in the travel time of the gas.

The modern ECUs have also advanced algorithms to correct the injection signal and the AFR during transients and adapt to changing fuel properties and aging engines.

This control method is commonly called adaptive control. Several studies carried out during the past decade have showed that the fuel behaviour in the intake port lead to excursions in mixture formation and hence excursions in AFR in MPI engines. The fuel depositing in the manifold walls has a crucial effect on the excursions particularly during the period when the engine is still cold and during the transient driving conditions. During cold running conditions, the evaporation of the fuel deposited on the manifold walls and on the intake valve surface is insufficient due to the low temperature. This leads to fuel entering the cylinder as liquid and part of the fuel mass remaining in the manifold due to slow liquid fuel film velocity. During transient conditions, the fuel depositions on the wall accumulate causing the excursions in the AFR. This phenomenon, together with effects due to ageing and wear of engine mechanical parts and sensors, causes excursions in AFR, which can not be compensated with conventional closed-loop control (Bella et al., 1996; Imatake et al., 1997; Le Moyne and Moyne, 1999).

In petrol engine management systems, several methods have been developed to control the highly non-linear behaviour of fuel-air mixing and the consequent excursion in AFR. It has been suggested (Moraal, 1995) that a modulation method to reconstruct the AFR trace from the EGO signal to create an adaptation algorithm for injection control. The model called sliding mode controller is aimed at compensating the transient period AFR excursions and therefore is based on air transient detection and the parameters are updated only when transient operation has occurred. Artificial Neural Networks (ANN) and fuzzy systems have been shown to be capable of providing appropriate adaptive fuelling control algorithms and they have been reported to offer a capability to model the process non-linearity associated with transition periods. Some of the ANNs could be applied to use adaptive injection control only during the transient periods, but more advanced methods are capable of adjusting the injection duration in order to compensate for engine ageing, sensor drifts and changes in fuel quality (Frith et al., 1995). Some ANNs are based on predictive feed forward control (Tang et al., 1998) and some on pure feed back control, where inputs for the neural network are current and previous outputs (measured equivalence ratio), previous and current control (injected fuel mass) and desired equivalence ratio (Moraal, 1995). Shiraishi et al. (1995) suggest that the Cerebellar Model Articulation

Controller (CMAC) ANN requires minimal a priori knowledge of engine dynamics because it can learn and adapt to changing conditions in real time.

Alternative fuels such as LPG or CNG vaporise naturally, even if injected in liquid phase, to a low pressure intake manifold. Therefore it is not likely that the injected fuel forms a liquid film on the manifold wall and consequently cause transient period AFR excursions and adaptive control is not required to compensate transient fuelling. However, adaptive methods do have an important role when the LPG injection is controlled by a petrol injection control unit. The adaptive control might be capable of compensating for the different characteristics of the fuels, and the minor changes in injection pressure which result from varying engine load and the limitations of the hardware calibration method.

II.1.2.2Engine On-Board Diagnostics

An OBD system is standard equipment in new vehicles and is required by Euro III emission legislation. This unit monitors ECU commands and system responses, but it also checks some individual sensor signals for plausibility and stores recognised errors. It can detect malfunctions of the engine and the exhaust after-treatment system. The European emission legislation sets different requirements for the system monitoring and diagnostics than the US legislation. European OBD requirements are as follows (Bauer, 2004):

- Catalytic converter
- Combustion misses
- Lambda (oxygen) sensors
- "Comprehensive components"
- "Other emission-related components"

The purpose of the diagnostics system is to provide reliable monitoring of the emission control system performance on a continuous basis, so that faults can be detected as they occur, and the vehicle will continue to provide satisfactory emissions performance. An OBD system is designed to detect adverse behaviour of the engine management system, which would cause emissions to increase beyond the design

threshold. The definitions of the thresholds are based on empirical data on the pollutant emission concentration which would be expected as a result of a failure of the component. Thresholds are currently set so that a malfunction indicator light, fitted in the vehicle dashboard, will be switched on if the emissions exceed predefined limits the applicable emission standard.

The OBD monitors are designed for petrol operation. If an OBD equipped vehicle is operated on an alternative fuel, such as LPG, it is possible that the monitor indicates that a fault has occurred, even though the vehicle may be operating correctly with LPG. The monitor may turn the malfunction indicator light (MIL) on, when the vehicle is operating normally. The reason why monitors may set false codes when operating with LPG is obviously dependant on the system; this is one of the main reasons why the sequential liquid injection systems are developed for LPG. When the injection system for LPG operation is controlled by the same parameters and by the same control unit, one would expect that possibility for false codes should be minimised. However, when the AFR deviates from stoichiometric for extended periods of time, the OBD system recognises this state. If the deviations exceed specified programmed limits, this indicates that a fuel system or fuel-metering component has shifted outside its specified tolerance range. It is mainly dependant on that tolerance range, whether the OBD interprets the different stoichiometric air-fuel ratio as a fault in the injection device.

The correct function of the lambda sensor and the closed-loop control is one of the key issues in the emission control, and the system response to lambda signal is one of the functions monitored by the OBD. The most usual reason for incorrect function of lambda sensor is due to thermal ageing (Bauer, 1999). A lambda sensor that has been exposed to excessive heat for a considerable period of time may react more slowly to changes in the air-fuel mixture. This increases the period duration for the lambda-controller. The OBD monitors this control frequency and recognises an excessive delay as an error in sensor response. This delay might also be a result of long gas travel periods and this is the primary reason for the use of "OBD-fix" units in LPG systems.

II.1.2.3Emission control

A primary strategy to reduce pollutant emissions these days is a three-way catalyst. Three-way catalyst systems control CO, HC and NO_X emissions as a result of oxidation and reduction processes in the platinum/rhodium catalyst. Major limitations of three-way catalysts are that it does not reduce CO_2 emissions, which can be controlled only by controlling fuel consumption, and that the efficient conversion requires very accurate control of AFR. This is usually achieved by an electronic fuel injection system, which is controlled by measuring the oxygen concentration of the exhaust gas (closed loop control).

The EGO sensor is a device which essentially acts as a switch, indicating if the AFR ratio was either rich or lean of stoichiometry, but not by how much. For example, the sensor does not distinguish the AFR values of say 14.8 and 19. When using standard petrol, a value of 14.8 is perfectly acceptable, while the value of 19 results in a severe increase in exhaust NOx emissions, because the limitation of catalytic converter AFR operating range. In contrast, a wide-band AFR sensor, also called Universal Exhaust Gas Oxygen (UEGO), responds to the actual AFR, and therefore provides more accurate information than the switching EGO sensor, but this type of sensor is significantly more expensive and therefore not commonly used in production vehicles.

The EGO sensor monitors the relative air to fuel ratio as a function of the partial pressure of oxygen and produces an output voltage based on an electrochemical reaction, which is proportional to the differential partial pressure of oxygen which exists between the exhaust gas and atmosphere, where the partial pressure of oxygen in the exhaust (products) is proportional to the AFR of reactants. The sensor has a considerable time delay because of both the delay due to two engine crank revolutions elapsing from the fuel input and mixture output (cycle delay), and also a time delay due to the distance between the exhaust ports and the sensor location. As reported by Cottrill (1999), EGO sensors have a cross sensitivity to hydrocarbons above C_3H_8. Therefore, using propane as a reactant produces a comparable jump in EGO sensor output at stoichiometric mixtures with petrol and it has been shown (Gerini et al., 1996; Dill et al., 1997; Lynch and Smith, 1997; Newkirk et al., 1996) that standard EGO sensors can be used with propane fuelled vehicles.

II.2 REVIEW ON EXISTING LPG SYSTEMS

II.2.1 SI engines

II.2.1.1System evolution

Bi-fuel LPG systems are generally designed to run on petrol engines but have varying degrees of sophistication. First generation systems have simple venturi, which is controlled by open loop systems (no lambda control) with no electronic controls. Generally these simplest types of LPG systems are only installed on simple carburettor engines. Second generation systems are single point mixer type systems, and have a closed-loop control. The controllers have self-learning capability and a basic on-board diagnostic fault code storage. Third generation LPG systems have multi-point, sequential injection system with more accurate closed-loop control.

The vapour injection system consists of the following parts: A fuel tank, safety shut-off valves, a vaporiser/pressure regulator, injectors and an electrical control module (ECM). The fuel is fed from the tank into the vaporiser/pressure regulator, where it is vaporised and heated with engine coolant circulating through the component. When the fuel is flowing from the vaporiser/pressure regulator to the injectors, the pressure is set by the vaporiser/pressure regulator to a specific value relative to a reference pressure, which is the inlet manifold pressure. The injectors and the fuel rail are installed away from the manifold, and the fuel is injected to the manifold through coupling pipes thus enabling the fuel rail with the injectors to be installed remotely.

II.2.1.2Vapour injection bi-fuel control units

These state-of-the-art aftermarket conversion LPG systems, commonly called Sequential Gas Injection systems, use adaptive software techniques to build the LPG control system based on data from the vehicle's petrol ECU. The system reads the data sent to each petrol injector and uses this information to control the LPG injectors. Effectively the petrol engine management system is controlling the LPG fuel delivery via a computer interface that translates the raw data to compensate for the different characteristics between LPG and Petrol. These systems do not have any communication with the petrol ECU, and are fitted with OBD-fix units.

The OEM fitted bi-fuel systems use a microprocessor with learning capability to control the injection, which work as a stand-alone unit, independent from petrol ECU. The translator systems are highly compliant with the original petrol OBD with Controlled Area Network (CAN) connection, making the communication possible between the two control units. The draw back of these systems is that they are designed for only OEM installations and the current technology does not allow the after market installations.

II.2.1.3Liquid injection systems

Liquid LPG injection (LPLI) systems are considered to be the next generation LPG systems, both in bi-fuel and mono-fuel applications, because of the higher engine power output, lower NO_X emissions, better knocking characteristics and more accurate control over the mixture. It was first shown by Sierens (1992) that by injecting the LPG fuel into the intake manifold as liquid, in contrast to introducing the fuel as vapour as in conventional systems, the engine efficiency can be greatly improved and as a result, a power output similar to that with petrol operation is possible.

The improvement in the engine power output is a result of the improvement in volumetric efficiency. This is due to fuel vaporisation taking place after the injection event in the intake manifold. The low boiling point fuel vaporises fast in the manifold and the energy required for the vaporisation is acquired from the surroundings. At least some of the energy is taken as heat from the intake air, which consequently reduces the temperature of the intake air, and hence, the density of the fresh cylinder charge is increased. This phenomenon is well known in the scientific literature and is commonly called the charge cooling effect. The lower intake charge temperature also results in lower flame temperatures and exhaust temperatures. This in turn improves engine thermal efficiency and reduces NO_X emissions.

Another significant benefit of LPLI systems over the vapour mixer-type or vapour injection systems is in the prevention of backfire events. In vapour injection systems, the fuel introduction to the manifold occurs during a relatively long period of time due

to higher fuel volumes and longer injection durations. In mixer-type systems, the fuel flow to the manifold is obviously constant. This often is known to cause the mixture in the intake manifold to ignite as a result of the hot residual gases flowing from the cylinder into the intake manifold. This flow is commonly called backflow and occurs particularly at low engine speeds immediately after intake valve opening. The short injection durations and more accurate control over the injection timing associated with LPLI systems make it possible to prevent the combustible mixture from forming in the intake manifold.

References in scientific literature include both bi-fuel LPLI systems (Ferrera et al., 1999; Cipollone and Villante, 2000a; Stodart et al., 2001; Jaasma, 1999) and mono-fuel LPLI systems. While all the bi-fuel systems are conventional MPI systems, the LPLI mono-fuel systems include as well as conventional MPI systems (Kang et al., 2001b; Stanglmaier et al., 1998; Salomons et al., 1998) lean-burn (Oh et al, 2003) and DISI (Lee S-W et al, 2003) applications.

The LPLI MPI bi-fuel systems use very similar control system to the state-of-the-art OEM-fitted vapour injection systems, except that as well as controlling the fuel metering, the control units are able of controlling the injection phasing and ignition advance (Ferrera et al, 1999; Stodart et al, 2001). The LPLI bi-fuel systems have totally independent ECU for LPG operation, which can communicate with the petrol engine ECU to prevent OBD interference. Therefore, the existing LPLI bi-fuel systems, which are all OEM fitted, are considered to be fully software optimised. Another major difference between OEM-fitted LPLI and vapour injection control unit is due to different fuel pressure in the fuel line. The fuel is maintained in its liquid state until the injection event, unlike in the vapour injection systems, where the fuel is vaporised before the fuel metering event. All LPLI bi-fuel systems use the same strategy to supply the fuel to the fuel rail. The fuel is pressurised and circulated through the fuel system, the supply and return line, with a pump and regulated with a pressure regulator, which is located in the downstream of the regulator. Unlike in the case of vapour injection fuel pressure regulator, or in the case of a petrol MPI fuel pressure regulator, the fuel pressure is not referenced to the intake manifold pressure to maintain a constant pressure difference and hence a flow rate through the injectors, but instead it is referenced to the fuel tank pressure to maintain a constant pressure

difference between the fuel rail and the pressure in the tank (Jaasma, 1999; Cipollone and Villante, 2000a). This configuration is needed to maintain margins to the fuel saturation pressure. However, as a consequence, the injector flow rate changes due to changing saturation vapour pressure in the tank, and to compensate this, the fuel pressure in the fuel rail needs to be monitored and taken into account in the LGP fuelling map. Therefore, the LPLI bi-fuel controllers have an additional control parameter.

The most significant benefit of mono-fuel engines over the bi-fuel engines is that the engine compression ratio and the combustion chamber geometry can be optimised for LPG operation. The high octane rating allows higher compression ratios to be used. In addition, in mono-fuel lean-burn engines, the combustion chamber geometry can be optimised for LPG operation, which is particularly important in achieving favourable stratification in the combustion chamber.

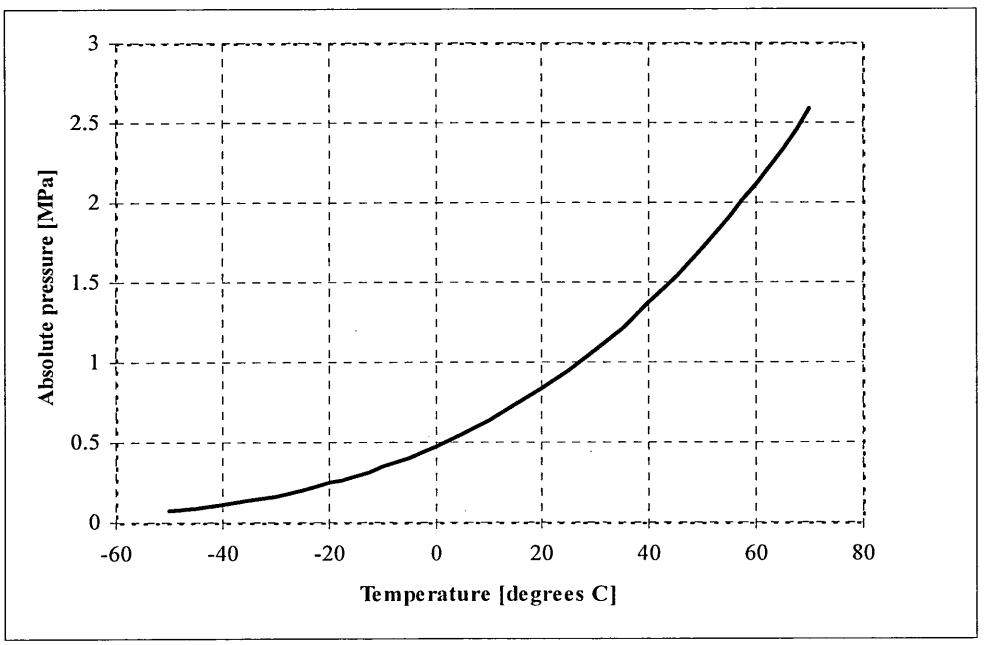

Figure II-II. Saturation curve of propane.

However, several technological challenges are associated with the LPLI systems. One of the greatest challenges in liquid-injection LPG systems is preventing premature vaporisation of the fuel in the supply system. The fuel is stored in the tank in liquid form at its saturation vapour pressure (Figure II-II). As the temperature of the fuel

inside the storage tank varies, the pressure in the fuel lines also varies. The varying temperature of the fuel in the tank is mainly caused by the heat transfer from the environment, but also by heat transfer from the fuel pump in the tank and from the engine. In order to maintain the fuel in its liquid phase until injection, the fuel should be above its saturation curve in the supply line and the fuel rail. The most critical aspect of premature vaporisation in the fuel line is the effect on fuel metering. Several solutions to the problem have been developed. These are reported in detail later in this chapter.

It is also reported that the high latent heat of vaporisation causes freezing of moisture in the air at the injector tip (Kim et al., 2003). Indeed, during the injection of liquid LPG into the inlet duct of an engine a large quantity of heat is extracted during the evaporation. This might lead to blockages of the outlet pipe of the injector because of freezing of moisture present in the air. The most critical effect of injector icing is the effect on injector flow rate and therefore on fuel metering.

The composition of LPG may vary world-wide from 100% butane to any mix of butane and propane up to 100% propane. Because of the different chemical and physical properties of its constituents, the saturation pressure of LPG varies depending on the composition. This should be taken into account in operation limits (margins to the saturation curve) of the fuel supply system. Also, the stoichiometric AFR of LPG varies with varying composition. The composition also varies due to tank emptying when the fuel is drawn to the engine. As the fuel is removed from the tank, more space is available for the fuel to vaporise in the tank and because the constituents have different volatility, the more volatile components will vaporise first, changing the composition in the liquid phase. This phenomenon has been reported to change the stoichiometry of the LPG in the tank (Cipollone and Villante, 2000b) and the pressure in the tank (Lutz et al., 1998).

Lean-burn-engines offer significant benefit in fuel economy, which is due to the possibility of combustion over all lean mixtures during part load engine operation. The mixture is ignited and combusted by forming a stratified charge in the cylinder by intake port and piston geometry. Intake port has a helical shape, which promotes in-cylinder swirl motion. The fuel is injected when the intake valve is open. This

injection phasing is commonly called Open-Valve Injection (OVI), in contrast to Close-Valve Injection (CVI). The swirl motion generated during the intake process promotes a non-uniform charge forming in the cylinder and pushes the rich part of the mixture (with the aid of tumble motion generated by the piston shape) to the top of the combustion chamber, in the vicinity of the spark plug. The combustion of the overall lean mixtures also results in lower exhaust temperatures, which in turn reduces the NO_X emissions, and increases the thermal efficiency. Gasoline Direct Injection (GDI) engines or Direct Injection Spark Ignition (DISI) engines use similar technology, in part load operation, the combustion occurs in overall lean conditions when the fuel is injected into the combustion chamber at the end of the compression stroke to form a rich mixture in the vicinity of the spark plug. During the full engine load operation the fuel is injected during the intake stroke to form more homogeneous, stoichiometric mixture in the cylinder combustion chamber. Several studies have been carried out on using LPG in both lean-burn engines and DISI engines. The advantages of these technologies largely depend on the mixture formation optimisation and the mixture formation process in LPG operation is potentially very different from the petrol operation due to differencies in fuel properties. The use of LPG in these stratified charge engines is discussed in detail later in this chapter.

II.2.2 CI engines

The main motivation for using LPG in diesel engines is the significantly lower particulate emissions and the lack of smoke-NO_X trade-off with LPG fuel compared to diesel fuel. However, high HC emissions and poor thermal efficiency compared to diesel operation is often associated with the use of LPG in compression ignition engines.

The use of LPG has been reported in at least three different types of compression ignition mixture formation systems. Due to the high auto-ignition temperature of LPG fuel compared to both petrol and diesel, the ignition process requires additional technology, while the LPG can be used in petrol SI engines without practically any modifications to the engine or to the fuel. The conventional method to ignite LPG fuel in a compression ignition engine, is to inject a small amount of diesel fuel to the combustion chamber to initiate the combustion (Bilcan et al, 2001). The type of

system where diesel fuel is used as a pilot fuel is commonly called the dual-fuel system. The major drawback of this system is the need for two fuel supply systems.

Another method is to use cetane enhancing additives mixed with the LPG, and also adding aliphatic hydrocarbon and lubricating additives to enable the use of LPG in compression ignition engine with only minor changes to the injection system (Sugiyama et al, 2003). The cetane enhanced LPG fuel is commonly called the LPG Blended Fuel (LBF). Also, the use of LBF in Homogeneous Charge Compression Ignition (HCCI) engines has been reported (Chen et al, 2001).

II.3 LIQUEFIED PETROLEUM GAS PROPERTIES

II.3.1 Table of properties

Table II-I. Table of properties of petrol, diesel and propane.

	Petrol	Diesel	Propane
Chemical formula	C_4 to C_{12}	C_3 to C_{25}	C_3H_8
Molecular weight	100-105	≈200	44.09
Composition, Weight %			
Carbon	85-88	84-87	82
Hydrogen	12-15	13-16	18
Oxygen	0	0	-
Specific gravity [15°C / 15°C]	0.69-0.79	0.81-0.89	0.5
Density [kg/m3 @15°C]	690-790	810-890	500
Boiling temperature [°C]	27-225	188-343	-42
Vapour pressure [kPa @38°C]	48-103	>1	1303
Octane no			
Research octane no	88-100	--	112
Motor octane no	80-90	--	97
Freezing point [°C]	-40	-40	-187.7
Viscosity [mPa s @20°C]	0.37-0.44	2.6-4.1	0.102
Flash point [°C]	-43	74	-104
Autoignition temperature [°C]	257	316	457
Flammability limits [volume %]			
Lower	1.4	1.0	2.1
Higher	7.6	6.0	9.5
Latent heat of vaporisation [kJ/kg @15°C]	349	233	426
Heating value			
Lower (liquid fuel-water vapour) [MJ/kg]	41.9-44.2	41.9-44.3	46.1
Lower (liquid fuel-water vapour) [MJ/l]	30-33	35-37	23
Specific heat of liquid [kJ/kg °K]	2.0	1.80	2.48
Stoichiometric air/fuel [weight]	14.7	14.7	15.7

Please note: All properties from Bechtold (1997).

The most relevant properties of petrol, diesel and propane are listed in Table II-I.

II.3.2 Performance

Several studies report that engine performance can be greatly improved by injecting the LPG fuel as liquid in the intake manifold in contrast to mixing the intake air with vapour phase LPG fuel. In optimised LPLI engines, the improvement in engine performance has been reported to be approximately 10% compared to vapour mixer-

type systems (Sierens, 1992; Kang et al, 2001a), but increase in engine output power as high as 17% has also been reported (Homeyer et al., 2002).

Kang et al (2001a) reported significant improvements in LPLI system performance in comparison with vapour mixer system. The results were based on single cylinder engine experiments, and it was shown that while the ignition timing was optimised in the case of LPLI using optimal timing for engine performance, in the case of vapour supply system the ignition timing was knock limited. This was attributed to lower charge temperatures, which also resulted in lower exhaust temperatures. The intake temperatures were measured by several thermocouples installed in the intake manifold and the results showed significantly lower intake temperatures in the case of LPLI system. Homeyer et al. (2002) also measured engine output power in a single cylinder engine using mixer-type system and LPLI system. They showed that optimising both the compression ratio and the ignition timing, the power output could be increased by 17% with the LPLI system. This was attributed to charge cooling.

The apparent charge cooling effect in LPLI systems is also reported in the study of Dutczak and Golek (2002). A mathematical model was created in order to simulate the effect of vaporising fuel to the charge density. The model results were compared to measurements in a single-cylinder engine operated with LPLI system. The model was applied to a small engine with single point fuel supply. The model predicted a 20 °K temperature drop in the inlet duct due to LPG liquid injection, and for petrol, a 10 °K temperature drop was predicted. For the vapour mixer case, there was a pressure increase in the fuel due to heat transfer from the inlet manifold walls. The experimental results showed that there was a similar, although more moderate tendency, where intake temperature was decreased in the case of LPLI approximately 10-20 °K depending on the engine load. There was a corresponding increase in the simultaneously measured engine torque. The measured engine torque was 9% higher for LPLI in comparison with the vapour mixer system and 3% higher than petrol. The authors do not report on fuelling or ignition control or the intake manifold measurement method.

The charge cooling effect is a well known tool to optimise injection timing and injection pressure and to improve volumetric efficiency of the engine. DISI engines in

full load (early injection mode) are known to have approximately 10 % benefit in volumetric efficiency when compared to MPI engines. This is considered to be attributed to the fact that in MPI engines, the enthalpy for fuel vaporisation is taken partly from the intake air. Both theoretical and experimental studies on charge cooling effect exist. Wyszynski et al. (2002) reported on measured volumetric efficiencies in a single cylinder engine, where it was shown that by optimising injection timing and injection pressure, volumetric efficiency can be increased. There was also a difference between different fuels, such as methanol, toluene and various petrol blends. For all the fuels it was also shown that the volumetric efficiency is increased when the fuel is injected directly to the cylinder, rather than in the intake manifold. It has also been reported that fuel wall impingement in the cylinder significantly decreases the charge cooling effect, and therefore volumetric efficiency is strongly dependant on amount of wall-wetting (Lippert et al., 2004). Also, charge cooling in HCCI engines have been studied (Sjoberg and Dec, 2004), and numerical model to predict the charge cooling effect on turbocharged engines has also been proposed (Andersson and Eriksson, 2004).

II.3.3 Mixture formation

As the mixture formation of vapour LPG mixer-type or MPI-type systems has not been studied widely in scientific literature, the mixture formation of liquid injection LPG systems, vaporisation and stratification, has been the subject of several recent studies as a response to the introduction of new technologies, such as lean-burn and direct-injection engines. The mixture formation has a great effect on combustion characteristics and also in engine emissions.

Cho et al (2000) measured the equivalence ratio and cyclic variation in the vicinity of the spark plug in a firing bi-fuel engine. The LPG system used in the measurements was a mixer-type, while the petrol system was a conventional MPI system. The measured equivalence ratio near the spark plug at the time of ignition was compared with the AFR measured with an UEGO sensor from the engine exhaust. The comparison showed that the local AFR in the spark plug location corresponds very well with the simultaneously sampled UEGO sensor signal when the engine was operated with LPG. However, when the engine was operated on petrol, the

equivalence ratio near the spark plug did not correspond to the UEGO signal, and showed very high cycle-to-cycle variation. This indicates that in the case of LPG, the mixture was more uniform and homogeneous in the vicinity of spark plug compared to the petrol operation. Brasoveanu and Gupta (1999) studied vapour propane fuel mixing with air gas turbine combustors by using a theoretical mixing model and concluded that mixing was greatly affected by the pressure and velocity divergence, which enhances fuel dispersion into the air flow.

Lee E, et al. (2003) simulated the droplet evaporation, wall impingement and droplet entrainment with surrounding air in MPI LPLI systems. The model was validated with wind tunnel experiments, which were considered to correspond to the conditions in an intake port. The experiments showed that although the injection pressure had only a small effect on the penetration depth, much greater effect was noticed with increasing the surrounding air velocity. The model was applied to investigate in-cylinder fuel distribution. The results suggested that by the time the piston reached the BDC, the fuel was fully evaporated and there were no liquid droplets present. Depending on the piston geometry, the mixture was stratified radially or axially in the cylinder by the time of the spark event. However, it was noticed that the injection during IVC resulted in stronger in-cylinder stratification and greater variation in equivalence ratio than injection during IVO, when despite of some noticeable stratification, the charge distribution was nearly uniform through the entire combustion chamber. The end of injection was 20°CA before IVO and 120°CA after IVO for IVC injection and IVO injection, respectively.

The effect of injection timing and in-cylinder flows on charge stratification in lean-burn petrol engines has been studied previously by Berckmuller et al (1996). The petrol mixture stratification in lean-burn engines was compared to mixer type LPG charge distribution by Fansler et al (2002), where it was noted that the equivalence ratio is essentially uniform during LPG fuelling, while mixture stratification is evident during petrol fuelling. Oh et al (2003) studied fuel stratification in a liquid LPG injection lean-burn optical engine. It was noted that fuel stratification was apparent using both CVI and OVI timings, but in the case of CVI, a lean mixture was observed in the vicinity of the spark plug, while a rich mixture near the spark plug at the time of ignition was apparent in the case of OVI. It was evident that the intensity of swirl

during the intake process had the greatest effect on achieving the favourable stratification in the cylinder.

Mixture formation of liquid injection LPG in DISI engines has also been studied by both simulations and experiments. Hyun et al. (2000) simulated the effect of piston cavity geometry, swirl and injection angle on mixture stratification. Oguma et al. (2003) compared spray characteristics and evaporation of pure butane, LBF and diesel in constant volume, high temperature and volume chamber. It was observed that while the evaporation rate of butane and LBF was higher than that of diesel, the spray penetration between the three fuels was very similar. Lee S-W et al. (2003) measured the LPG spray evaporation in a constant volume chamber. The geometry of the chamber was constructed to simulate the geometry of a DISI combustion chamber at the end of the compression stroke. The fuel was injected into the chamber at an ambient temperature of 293 K, and varying chamber ambient pressure. It was evident that the fuel evaporation rate was higher with lower chamber pressures, which reflects the saturation properties. In atmospheric pressure, there was still some liquid fuel present at 6 ms after the end of the injection, although the time for complete vaporisation of the spray was not reported. Also, when the temperature was increased both fuel penetration and the liquid phase decreased. At 800 K, the fuel was fully vaporised less than 1 ms after the end of injection. Lee S-W et al. (2001) also compared the effect of fuel evaporation on penetration depth using three different fuels for comparison, LPG, Dimethyl Ether (DME) and *n*-dodecane to represent diesel spray characteristics. It was found that the evaporation and hence spray penetration characteristics were considerably different in the case of the two low boiling point fuels when compared to *n*-dodecane. Also, the effect of increase in the ambient temperature was more radical in the case of LPG and DME spray. However, in another study, the same authors reported that even in high ambient temperatures the LPG spray contains a sufficient fraction of liquid to penetrate to the spark plug location in similar conditions found in DISI combustion chamber with the favourable interaction of an impingement wall, which represented the effect of a piston (Lee S-W et al., 2002).

II.3.4 Combustion

The flame propagation through the combustion chamber, in SI engines is primarily affected by the following parameters:

1. Combustion chamber geometry is a significant factor mainly due to the influence of spark plug location and combustion chamber volume and shape and the consequent flame surface area, but also the influence of in-cylinder flow motion.
2. Flow field characteristics affects on burning rate through turbulent motion of the unburned mixture. Turbulence is mainly promoted by swirl motion generated during induction and is mainly due to the intake manifold and valve geometries and flow velocities.
3. Unburned mixture composition and state affect the burn rate mainly because of the effect on laminar flame speed, which is essentially a function of the mixture equivalence ratio, temperature, pressure and burned gas fraction and fuel type.

The characteristics of the combustion process is important in an SI engine mainly because its effect on engine performance and emissions. The main combustion-related parameter concerning engine performance is ignition timing. Ignition timing affects primarily engine power and torque; the combustion process must be properly timed relative to the engine Top-Dead Centre (TDC) in order to obtain maximum torque. If combustion and the consequent pressure rise in the cylinder occur too early, the pressure rise in the cylinder acts to impede the compression stroke, and if the pressure rise due to combustion occurs too late, the magnitude of the pressure peak around TDC is reduced. The optimum timing for the ignition is called Maximum Brake Torque (MBT) – timing. It depends on the engine speed and load, and obviously on the combustion duration.

The AFR mixture quality has a significant effect on the combustion process. The combustion process in the cylinder can be roughly divided into three stages. The flame development angle, also called ignition delay is the first phase starting from the spark event. This early flame kernel development largely depends on the ignition energy, but also the local mixture composition in the vicinity of the spark plug. The

main fraction of the fuel is burned and the main fraction of chemical energy is released during the rapid burning phase. The combustion process during this phase is mainly affected by the turbulent intensity, the in-cylinder flow field and combustion chamber geometry, but also the mixture composition of the entire combustion chamber. Therefore, the greater flame development angle is an indication of mixture non-uniformities near the spark plug, while the rapid burning angle is not affected by these non-uniformities as the mixture through the entire combustion chamber is stoichiometric. The third stage of combustion is the flame termination. It has also been reported that lower charge temperatures lead to increased flame development time (Varde, 1992).

The differences in overall burning rates of LPG and petrol are widely reported in the scientific literature. The laminar flame speed of propane is higher than that of average petrol, iso-octane or methane (Metghalchi and Keck, 1980; Metghalchi and Keck, 1982; Thobois et al, 2003), and depends largely on the AFR (Kim et al, 1999). The laminar flame speed is highest in stoichiometric and slightly rich mixtures. It has also been reported that propane has very similar laminar flame speed in the lean and stoichiometric conditions but lower in the rich conditions than that of butane or butane-propane – mixtures (Lee D et al., 1998). Flame speed is also largely dependant on the flame temperature, which in turn depends on the unburned mixture temperatures.

Homeyer et al. (2002) studied the combustion of an optimised single cylinder engine using both a mixer-type vapour LPG system and an LPLI system. It was noted that the ignition was more advanced for the LPLI MBT – timing compared to vapour mixer-type system. From a heat release analysis it was also evident that the longer burning duration was due to longer flame development time with LPLI, while the rapid burning duration was similar with both systems. This was believed to be due to lower charge temperatures with LPLI. Raina et al. (1998) studied the variation of MBT – timing with varying fuel composition. The fuel used in the single-cylinder engine experiments was a blend of methane and propane, and it was reported that increasing the fraction of propane, the MBT – timing was retarded. In their recent study on the ignition spark characteristics, Abd-Alla et al. (2003) reported on combustion progress in heavy-duty engines operating on petrol and LPG. The LPG system used was a

vapour phase mixer-type system, and the results on the effect of varying spark energy and duration were shown for both fuels using a fixed petrol MBT – timing, while the AFR was maintained at stoichiometric for both fuels. Both the coefficient of variation of IMEP (COV_{IMEP}) and the flame development angle were demonstrated, and showed significant differences in combustion progress between the two fuels. The overall burn duration was significantly higher in the case of petrol resulting in the peak cylinder pressure 2-3 °CA later than that of LPG, which was attributed to the larger flame development angle. Also, the COV_{IMEP} was higher in the petrol case, showing larger variations in IMEP than LPG especially when lower spark energy was used. These results clearly indicate that the mixture in the vicinity of the spark plug was less homogenous in the case of petrol resulting in longer flame kernel development and greater cycle-to-cycle variations.

There is also a significant body of scientific publications on flame propagation characteristics in dedicated lean-burn LPG engines. Although the mixture formation process in lean-burn applications differs from the mixture formation in the application suggested in this study, the investigations on mixture stratification in the combustion chamber and the mixture composition and homogeneity in the vicinity of the spark plug provide useful information on the liquid-phase LPG fuel mixing and the consequent combustion progress. Oh et al (2002) studied the effect of injection timing and the combustion chamber geometry on fuel stratification and combustion by direct flame visualisation in an optical engine and calculated the flame speed from the observed flame area. The results show that injection timing has an effect on initial flame speed due to differences in mixture composition. The flame area was measured for two closed-valve injection cases; an early CVI case (injection 100 °CA BFTDC) and a late CVI case (injection 400 °CA BFTDC). The results show faster flame development in the case of early CVI case. The authors suggest that this behaviour is a result of longer fuel residence time in the manifold and consequently a more homogenous mixture entering the cylinder. In the case of late CVI, some of the fuel does not mix completely with the intake air and the intake air entering the cylinder after the end of the injection causes an poor stratification in the combustion chamber with a rich mixture residing on top of the piston in the bottom part of the chamber while there was a lean mixture in the vicinity of the spark plug. The stratification of the liquid-phase LPG injection system, even with CVI, wsas clearly demonstrated.

Also, a later study by the same authors showed that by further optimising the piston and intake port geometries, a nearly homogeneous charge was achieved with late CVI (Lee Y et al., 2004). The same observation was apparent in the experimental study of Lee Y et al. (1999a and 1999b) concerning lean-burn liquid-phase LPG injection engines. Badr et al. (1998) reported higher lean-misfiring limits for butane-propane – mixtures in comparison with pure propane. The effects of EGR and piston geometry on mixture stratification in lean-burn liquid-phase LPG injection engines have also been studied (Woo et al, 2004; Kim et al, 2002; Chiriac et al, 2004). Effect of fuel stratification on combustion characteristics in liquid injection DISI engines was simulated by Hyun et al (2002).

II.3.5 Exhaust emissions

II.3.5.1Major emission components

Oxides of nitrogen is a term used to describe pollutant emissions which mainly comprise of nitric oxide (NO), but also small amounts of nitrogen dioxide (NO_2). NO emissions cause photochemical smog when it oxidises in the environment to NO_2 and react, in the presence of ultra-violet light, with UHC. Nitrogen oxides develop from the nitrogen and the oxygen contained in the air in the combustion process. The formation of nitrogen oxides greatly increases with the combustion temperature.

Unburned Hydrocarbon UHC emissions form primarily due to incomplete combustion. In addition to contributing to the formation of photochemical smog, the UHC emissions are in some cases known to be carcinogenic. It has been suggested by (Stone, 1999) that UHC emission arise from:

1. Loss of fresh charge to exhaust during valve overlap
2. Liquid fuel which fails to vaporise in the cylinder prior to exhaust valve opening
3. Fuel-air mixture trapped in crevice volumes in the cylinder
4. Incomplete combustion due to inadequate flame propagation

CO is a highly toxic gas, and is essentially a product of incomplete combustion. CO_2 is a non-toxic product of combustion. The concern of CO_2 emissions arises from atmospheric pollution and it is considered as a major greenhouse gas. The most significant pollutant emission benefit of using LPG compared to gasoline is the reduced CO_2 emissions. CO_2 is the only harmful emission, which is a product of ideal (or perfect) reaction and therefore the amount of CO_2 emission is directly proportional to fuel consumption and indirectly proportional to engine efficiency. Also, as shown below in Equation II-III, the CO_2 emissions are directly proportional to the carbon to hydrogen ratio for hydrocarbon fuel. The simplified reaction of hydrocarbon fuel and air can be expressed as follows (Nitrogen, which is present also in air, is neglected since it does not have a contribution to the CO_2 emission formation):

$$C_X H_Y + aO_2 \rightarrow bCO_2 + cH_2O \qquad \textbf{Equation II-III}$$

where X is the number of carbon atoms, Y number of hydrogen atoms, a number of oxygen atoms, b number of carbon dioxide molecules and c number of hydrogen oxide molecules. Balancing the reactants and products gives:

$$b = X \qquad 2c = Y \qquad 2b + c = 2a$$

This simple calculation shows that for propane, the amount of carbon dioxide molecules produced is less than average petrol, which has an average carbon number of approximately 10.

II.3.5.2 Emissions from LPG vehicles

Several studies report comparison of the emissions performance of bi-fuel vehicles operating on LPG and petrol. The most significant research carried out was the "Texas Project", mainly funded by the US Department of Energy (alternative fuels program) and the Texas Governor's Energy Office. The aim of the research was to study the potential of bi-fuel vehicle conversions to reduce emission levels. The research included several different LPG conversion kits and several CNG conversion kits, which were each tested on a research fleet of 86 light-duty vehicles. The results showed that there were significant differences in emissions between the conversion kits, and also between the kit – vehicle combinations (Matthews et al, 1996). This was attributed solely to the operation and efficiency of the engine control systems (Chiu and Matthews, 1996), although every conversion kit used lambda feed-back control.

The only statistically significant emission reduction in alternative fuel operation was in their Ozone Formation Potential (OFP), but also a small CO_2 benefit was evident with LPG conversion kits on average compared to the average petrol (Wu et al., 1996; Wu et al., 1998), while almost all conversions showed higher NO_X emissions during LPG operation than during petrol operation.

Watson and Gowdie (2000) also compared several bi-fuel vehicles for emissions. The vehicles tested in the study were equipped with OEM-fitted LPG systems, which was in contrast to the aftermarket conversions studied at the Texas project. The influence of the fuel composition on LPG emissions was studied in a fleet of 12 bi-fuel vehicles and the results were compared to that of petrol operation. The results showed significant differences in emissions when butane content was increased and also when olefin content (propylene and butylenes) was increased. The highest butane content showed the highest HC emissions and lowest NO_X emissions, while increased olefin content showed the lowest HC and highest NO_X emissions. All LPG fuels emitted less CO_2 and NMHC emissions than petrol, but only the highest butane content fuel showed benefit in NO_X emissions compared to petrol emissions.

A large number of Korean vehicles were emissions tested for HC and CO emissions, with varying mileage, engine size and technology. This large-scale emission testing also included 38 LPG fuelled vehicles, which were aftermarket conversions. The test results showed higher CO and HC emissions for the LPG vehicles when compared with petrol vehicles (Ryu and Song, 2002).

Several studies also account for bi-fuel emission testing of a development engine or the vehicle on an engine or chassis dynamometer. Smith et al. (1997) compared emissions from an engine converted to a mixer-type LPG bi-fuel system. The results showed that the LPG CO emissions were higher than petrol, whilst both the HC and the NO_X emissions were lower for LPG than for petrol. However, this was explained by the simultaneously measured AFR, which was measured from the exhaust gas composition. The measurements indicated that the mixture composition during LPG operation was slightly rich, while during petrol operation the mixture composition was lean from the stoichiometry. In this study, the LPG fuelling was controlled by a standard LPG conversion control unit, which operated from both a base fuelling map

and lambda feed-back control. The petrol fuelling was controlled by the OEM control unit. Both the engine-out and post-catalyst emissions were measured, and the catalytic conversion efficiency during LPG operation was comparable to that of petrol. Stodart et al. (2001) compared bi-fuel LPG vehicle emissions between two vehicles; where one vehicle was converted to an MPI vapour injection LPG system and the other vehicle used an MPI LPLI system. Both systems used a second control unit for optimal LPG fuelling calibration. The LPLI system was also calibrated for optimum spark timing, while the vapour system used the petrol spark timing. The results showed that the HC and CO_2 emissions were lower for both systems when compared to petrol operation. The NO_X emissions were very similar when the vapour injection system emissions were compared with the petrol operation, but the liquid LPG system showed significant NO_X benefit when compared to petrol operation. This effect was evident in the study of Kang et al. (2001a), where significantly lower exhaust temperature was observed with a LPLI system when compared with a mixer type system during measurements in a single cylinder engine.

This advantage in NO_X emissions associated with the liquid injection system over the vapour injection system could be explained by the difference in the mixture formation process. Because the rate of formation of NO_x is exponentially dependant on the adiabatic flame temperature, even a relatively small decrease in flame temperature will produce a significant decrease in NO_x. Additionally, it is well known that the flame temperature is an essentially linear function of reactant temperature, where a unit decrease in reactant temperature results in nearly the same decrease in flame temperature. In vapour mixer-type injection systems the fuel enters the manifold at the same temperature as the intake air and there will be no charge cooling effect due to vaporising fuel.

In the study by Chang et al. (2001) speciated and Total Hydrocarbon (THC) emissions were measured on a vehicle dynamometer using 35 LPG vehicles and 35 petrol vehicles. The results showed that the THC emissions were slightly higher for the LPG vehicles in comparison with the petrol vehicles. However, when the composition of HC emissions was analysed, it was evident that in contrast to petrol vehicles, only lighter hydrocarbons were found in the LPG exhaust gas. Further, when the components were weighed by their Oxygen Forming Potential (OFP), based on the

concept of the Maximum Increment Reactivity (MIR) factor, the authors found that the OFP was approximately 50% that of petrol. A study by Tanaka et al. (2001) suggested that the use of LPG vehicles reduces the *i-*, *n*-pentanes emission components, but increases *i-*, *n*-butanes and propane emission components measured at road sides in various urban areas in Japan. Kim and Bae (2002) compared speciated HC, CO_2 and NO_X emissions from a four-cylinder engine operated by a mixer-type LPG system and a CNG system. The results showed that the main component for LPG HC emissions was propane (60% on a mass basis) and for CNG HC emissions was methane (also 60% on a mass basis). The fraction of propylene in the HC emissions was significantly higher for LPG in comparison with CNG, while the other components showed a similar fraction in HC exhaust emissions for both fuels. There were smaller amounts of fuel components in the exhaust in the case of LPG, which was attributed to the higher exhaust temperatures during LPG combustion, which promotes late-cycle oxidation of components. The NO_X emissions were also significantly higher in the case of LPG, as well as CO_2 emissions, which was expected from the knowledge of lower carbon number of CNG. Kang et al. (2002) compared emissions of a heavy-duty diesel engine converted to spark ignited, liquid injection MPI LPG engine optimised for LPG with the emissions of the base line diesel engine, and found that the NO_X, THC and CO emissions were significantly lower for liquid injection LPG. Lee D et al. (1999b) showed from a post-flame imaging study that NO_X formation of LPG engines can be significantly reduced by using lean-burn technology. Li et al. (2002) compared emissions from a small motorcycle engine converted to an LPG vapour injection system to a baseline petrol engine. The AFR and ignition control was fully optimised for LPG operation. They showed that the all regulated emission components could be reduced by the use of LPG, but noted that the emission benefit was very sensitive to careful engine calibration.

A number of studies attempted to account for particulate emissions from LPG vehicles. Andersson et al. (2001) report on comparative measurements carried out for several diesel vehicles, petrol vehicles (MPI and GDI vehicles) and a Bi-Fuel LPG MPI vapour injection vehicle. The results showed that the particulate mass emissions were lower in the case of LPG when compared to the MPI petrol during steady state driving conditions. During cold start, however, the particulate mass was slightly higher than that of MPI petrol. Similar results were obtained by Aakko and Nylund

(2003), even though the type of LPG vehicle is not specified in the report. The total particulate mass was measured during the European driving cycle in three different ambient temperatures. In the highest temperature, the particulate mass emitted by the LPG vehicle was comparable to the mass emitted by the MPI petrol vehicle, but as the temperature decreased, the LPG vehicle showed higher particulate mass emissions than the petrol MPI vehicle. This study also included a dedicated CNG vehicle, which emitted negligible amount of measured particulates at each ambient temperature. Ristovski et al. (1998) measured particulate emission size distributions and mass concentration from a dedicated LPG mixer type vehicle and compared the results to that from a petrol MPI vehicle. The results showed that both the mean particulate size and mass concentration were higher in the case of the LPG vehicle. In this case, the particulate emissions were sampled during an accelerated simulation mode driving cycle performed on a chassis dynamometer.

The HC emissions of liquid MPI LPG injection systems have also been studied. Sobiesiak et al. (2003) reported very high cold start HC emissions. This was attributed to injector deposits, which lead to injector leakage during cold soak. When the engine was started again, the fuel which had accumulated in the manifold was combusted with the fuel supplied by the injectors. This resulted in longer cranking periods and high HC emissions during cold start. As a solution, the authors proposed the use of additives in the fuel to prevent the fuel deposits formation. Also, the start after a hot soak resulted in very high HC emissions, which was, according to the authors, due to the presence of fuel vapour in the fuel rail, which resulted in longer cranking times and high HC emissions.

II.3.6 Saturation properties

The factors that reduce the margins to the saturation curve (Figure II-II) are, on one hand, the temperature increase in the fuel lines and on the other hand the pressure decrease in the fuel lines. The fuel transport in the supply and return lines can be divided in two sections in terms of heat transfer. The first section includes the fuel tank and the fuel pipes under the vehicle, where the air is at ambient temperature. The second section includes the fuel pipes, which are under the bonnet, and the injectors. Here, the temperature is much higher than ambient due to heat transfer from the

engine, and this especially affects those components, which are in direct contact with the engine head (e.g. injector housings).

In order to avoid the premature vaporisation in the fuel lines, the primary concern is to reduce the heat transfer in the second section described in the previous paragraph, and several methods have been proposed in the literature to achieve this. The formation of bubbles can cause inconsistent injection and poor AFR control. Plastic injector housings are used to reduce the heat transfer (Salomons et al., 1998; Stanglmaier et al., 1998; Andersson et al., 1998). Also, there has been some attention paid to the heating of the tank due to the heat transfer from returning fuel. There are some systems that propose that placing a heat exchanger in the return line or by fitting a separate cooling circuit near the fuel return line would reduce the heat input to the tank (Salomons et al., 1998; Acedo et al., 1998). On the contrary, it has been suggested that by heating the tank above the ambient temperature the fuel could be maintained in its liquid phase in the system (Cipollone and Villante, 2000b). This is based on the idea that as the fuel is transferred through the pipes located under the vehicle, the fuel is cooled due to low ambient temperature around the pipes. Therefore the margins to the saturation curve are increased also in critical points in the system.

The pressure variations in the fuel rail in the LPLI system is caused mainly by two factors. Firstly, as mentioned previously, the pressure in the fuel line varies with varying tank pressure. Secondly, the sequence of operating injectors causes propagation of pressure waves inside the system. Even when using a fuel line damper, the pressure may vary by 20-30 kPa depending on the engine speed and resonance conditions (Cortese et al., 2000). The amplitude of the pressure waves is mitigated by the pressure regulator. The movement of its mobile equipment permits to oppose a variable efflux area to the fuel returning to the tank. The pressure fluctuations induced by the sequence of injectors can produce locally instantaneous pressure values that can go under the local saturation pressure.

The pressure waves caused by the injectors are compensated by the regulator. The regulators used in LPLI systems are valves, which regulate fuel pressure by regulating the fuel flow. Therefore, the higher the return flow rate, the better is the pressure regulator performance. The performance of the pressure regulator could be described

with an example of an extreme situation, where the fuel pump speed is relatively low, and hence producing lower flow rate. In these circumstances it is possible, that the injection flow rates are higher than the pump flow rates (Q_{inj}/Q_{pump} is greater than unity). Consequently, during injection all fuel goes through injectors, and no fuel goes through the pressure regulator, and therefore the fuel return line is completely closed. In this situation the regulator is unable to sustain the pressure in the fuel rail during injection. (Cipollone and Villante, 2000a).

A further aspect is the possible vaporisation in the pressure regulator outlet, which is caused by the pressure drop in the regulator. This could be avoided by adding a fixed flow restriction in the tank inlet. This of course would limit the operation range of the pressure regulator. It is shown that the absence of the pressure regulator results in a significant pressure drop as a consequence of the opening of each injector (Cipollone and Villante, 2000b). The pressure drop is increased by the overlapping of injectors at high engine speeds. To optimise the fuel pump efficiency at a given tank temperatures, a variable speed fuel pump has also been developed (Jaasma, 1999).

When the engine is started, the fuel in the rail must be in a liquid state in order to provide a combustible mixture to the engine. When the engine is turned off after it has achieved the normal operating temperature, heat conduction from the engine components can heat the LPG near the coolant temperature (approximately 90°C). Because the rail pressure normally returns to tank pressure (the saturation pressure at ambient temperature) when the engine is turned off, this heat input will vaporise the LPG in the fuel rail. When restarting the engine, the pressure in the rail increases, but it is insufficient to condense the LPG in the rail. Therefore, the engine cannot be restarted before both the heat and the vapour are removed from the fuel rail by cool liquid LPG. In bi-fuel engines, the engine could always be started using petrol and the LPG pump could be activated simultaneously. The engine could then be switched to LPG as soon as all the LPG in the supply lines is liquid.

Many systems have been developed to overcome this problem. These include a secondary fuel pump to decrease the purge time (Andersson et al., 1998). This was to increase the fuel flow in the system, i.e. increasing the amount of fuel circulated in order to remove the heat to the tank. Also, using lower thermal conductivity material

and lower thermal masses in the fuel rail and injector housing reduces the amount of heat conducted from the engine (Stanglmaier et al., 1998). The same authors suggests that according to a first-law energy balance model, the most important parameters in reducing the hot-start delay are the thermal mass of the fuel rail and the mass flow rate of the fuel (Stanglmaier et al., 1998). This would mean that increasing the boost pressure during hot start actually increases the hot start delay, as the flow rate is significantly decreased, and that the circuit should be used in the opposite way to maximise the flow rate during hot starts. Further more, the authors suggest that decreasing the total volume of fuel between the pump and the regulator decreases the time to purge the system of vapour. This was implemented by locating the pump near to the fuel rail.

III. DEVELOPMENT OF THE SYSTEM ARCHITECTURE

III.1 IDENTIFYING SYSTEM REQUIREMENTS AND DESIGN RESTRICTIONS

The main system requirements are:

1. The system should be universal, which means there is none, or very few, vehicle specific components. Universality means that the same system could be installed as an aftermarket conversion to virtually any petrol vehicle.
2. The injection system should be controlled solely by the original petrol control unit without a need for any separate control unit for LPG operation. This requirement is due to OBD –compatibility.
3. The system should be a liquid injection system to prevent backfire events, to prevent the loss in engine output power associated with the vapour injection systems and reduce NO_X emissions.

This chapter describes in detail, how the above mentioned requirements could be realised in practise.

III.1.1 Fuelling control

To enable the petrol ECU to control the LPG fuelling the LPG injector flow rates need to be adjusted to compensate the different fuel properties. According to stoichiometry, on a volumetric basis approximately 38% more fuel per unit volume of air should be provided in the cylinder when using liquid LPG. Although, the fine adjustment of the fuelling is controlled by the ECU by the feed-back from the EGO sensor and the base fuelling is adjusted with the control unit learning capabilities, these controls have limits, and the limits vary from vehicle to vehicle. Therefore, the LPG injector flow rate should be adjusted so that the LPG injection duration would be as close as possible to the petrol injection duration (Equation III-I to Equation III-III).

$$t_{inj,petrol} = t_{inj,LPG} \qquad \textbf{Equation III-I}$$

$$V_{st,LPG} \approx 1.38 * V_{st,petrol}$$ **Equation III-II**

$$t_{inj} = \frac{V_{st}}{A_{inj}\sqrt{\left(\frac{2}{\rho}\right)\Delta P}}$$ **Equation III-III**

where V_{st} is the volume of the injected fuel required for stoiciometric mixture. This requires that the greater volumetric flow rate across the injectors when using LPG, while the injection duration, t_{inj}, is maintained constant for both fuels. The flow rate could be adjusted by (Equation III-III):

a. adjusting the pressure difference across the injector (ΔP)
b. adjusting orifice area of the injector (A_{inj})

The main consideration in the proposed flow rate control method is that the conversion system should be universal. The aim is to use the same system components for every type of vehicle, which requires that the chosen LPG injector would be able to compensate the injection duration requirement (Equation III-I) for many different petrol injector flow rates. This is because, as well as the actual fuelling requirement, the petrol injector flow rates differ from one engine to another.

The easiest way to adjust the flow rate is to use an adjustable pressure regulator. However, the available pressure range is limited by several factors. The lower limit of the pressure range is limited by the margins to the saturation pressure. The upper limits of the pressure range are limited by both the pumping system capabilities and injector capabilities. Therefore, it is unlikely, that the available pressure adjustment range would be sufficient to compensate the fuelling requirement for every type of vehicle. Therefore, it is anticipated that the LPG injector flow area needs to be adjusted as well.

III.1.2 Fuel rail pressure

Another important consideration in developing the system architecture is to ensure sufficient margins to the saturation pressure and temperature, in order to prevent premature vaporisation in the fuel rail. As discussed in Chapter II, in the existing LPLI systems, this is ensured by maintaining a constant pressure difference between the fuel rail and the fuel tank. However, in the proposed system this method is not possible because of the fuelling control. Firstly, there will not be another control unit to compensate the fuelling due to changing rail pressure and the consequent change in the injector flow rate. Secondly, the pressure will be adjusted to compensate the different volumetric demand of fuelling to be able to use the same injection durations with LPG and petrol. Therefore, the fuel pressure in the LPG line is initially adjusted by the conversion installer to a certain level, and can not be changed afterwards.

This method addresses few potential problems. As mentioned earlier, the margins to the saturation conditions limit the available injection pressure range to adjust the injector flow rates. To prevent the saturation conditions, the fuel rail pressure should be as high as possible. On the other hand, the injector operation is limited by the pressure. As discussed later in this chapter, the injector needle opening and closing is affected by the injection pressure, and there is a definite upper limit for the injection pressure, after which the injector will not open any more. The fuel pumping system sets a limit to the pressure, the higher the boost pressure, the higher the power consumption. Therefore, there is an obvious trade-off which means an unavoidable compromise in fuel pressure adjustment, because in terms of flow rate adjustment, the pressure should be able to be adjusted as low or as high as possible.

III.1.3 Bi-Fuel injection system configuration

Another issue is the actual LPG injector and fuel rail configuration. The petrol injectors are usually installed in the intake manifold, close to the intake valves. In the bi-fuel-systems, the ideal place to install the LPG injectors would obviously be in the vicinity of the petrol injectors. However, particularly in small engines, this could be very difficult as the space available in the intake manifold is very limited. Also, to make it possible to install another fuel rail with injectors directly to the manifold adds another challenge for the requirement of universality; the conventional rigid design of

the fuel rail is not suitable because of varying engine dimensions from vehicle to vehicle.

Another option is to locate the injectors and the fuel rail remotely, and connect the injectors to the manifold with flexible pipes. In this type of configuration a rigid fuel rail could be used.

III.2 SYSTEM DESIGN AND INTEGRATION

III.2.1 Injector

The main operational requirements for the LPG injectors are that the injector is already available (due to cost and time constraints) and that the injector is capable of operating in high pressures (due to flow rate control and margins to the saturation pressure). The approach for selecting injectors was to evaluate performance of several automotive production injectors first in an ASNU injector diagnostic test bench (Figure III-I, on left) and then continue testing with selected injectors in a purpose built high pressure rig (Figure III-I, on right). The method to evaluate the performance of the injectors in the first part of the injector selection was to measure the flow rates of several injectors at different pressures. The ASNU injector test bench is capable of producing an injection pressure up to 10 bar. The tester allows the injection duration and frequency to be programmed. Injectors are driven at this frequency and duration for a time period of 15 seconds, after which the flow rates can be calculated by measuring the volume of injected fuel contained in a measuring tube located below each injector. The high pressure tests were carried out by using the injector control of the ASNU tester to operate the injector in the high pressure rig. The injected test fluid was also gathered in a measuring tube.

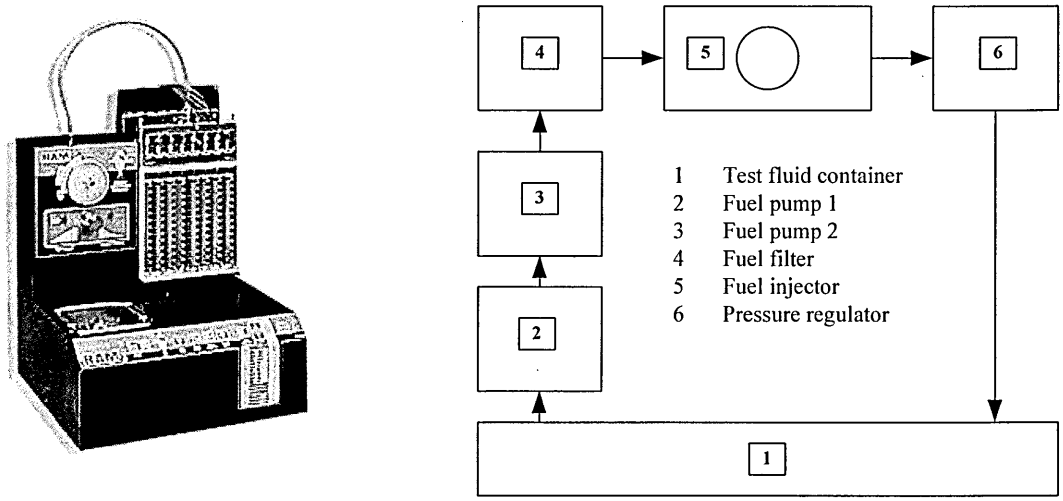

Figure III-I. ASNU Injector test bench (left) and a schematic diagram of the high pressure injector test rig (right).

The criteria for injector performance were determined by the injector flow rate response when injection pressure is increased. Ideally, the flow rate should increase with increasing injection pressure, but in practice, the needle lift characteristics change with the pressure. The best performing injector will show a nearly linear relationship between the flow rate and pressure, indicating that the injector flow rate can be adjusted with injection pressure and the flow rate and injector operation is consistent. The injector performance is illustrated in figures as a dimensionless quantity called flow area index (FAI). The index describes the change in flow area as a function of injection pressure. For a perfect injector, the flow area does not change with pressure, but in practice the rail pressure always affects the needle dynamics, by reduced needle lift distance or increased lift duration. FAI is calculated in reference to the flow rate measured with an injection pressure of 3 bar, because the injectors tested are designed to be used in gasoline multi-point injection engine, where injection pressure typically is 3 bar. Therefore, FAI equals 1 for all the injectors at 3 bar. If the flow area would not change in the entire pressure range, the index would be 1 for every pressure, which would mean that the flow rate would increase linearly with increasing pressure (Equation III-IV).

$$FAI = \frac{c_{inj} A_{inj}}{\left(c_{inj} A_{inj}\right)_{ref}} \qquad \text{Equation III-IV}$$

where *ref* describes a reference value, obtained by measuring the flow rate at injection pressure of 3 bar.

$$c_{inj} A_{inj} = \frac{V}{t_{inj} \sqrt{\left(\frac{2}{\rho}\right) \Delta P}} \qquad \text{Equation III-V}$$

Where V is the volume of injected fuel [m^3], t_{inj} is injection duration [s], A_{inj} is the injector flow area [m^2], c_{inj} is the contraction coefficient of the injector, ρ is the density of fuel [kg/m^3] and ΔP is the pressure difference between the fuel rail and the manifold [Pa]. Two type of injectors were tested. The most common type of petrol fuel injectors are so-called top-feed injectors. The fuel supply for this type of injectors is conducted from the top of the injector (Figure III-II, on left). The major advantage

of using top-feed injectors is that the injector needs to be sealed only from the top, from the connection between the fuel rail and the injector and therefore requires a significantly less complicated fuel rail configuration when compared to side-feed injectors. Another type of injector is the side-feed injector (Figure III-II, on right). This type of injectors the fuel supply is arranged so that the fuel flows through the injectors, when the injector needs to be sealed from both bottom and top of the injectors. This requires more complicated fuel rail configuration, but the continuously flowing fuel through the injectors reduce the heat transfer to the fuel decreasing the risk of vapour lock in the injector.

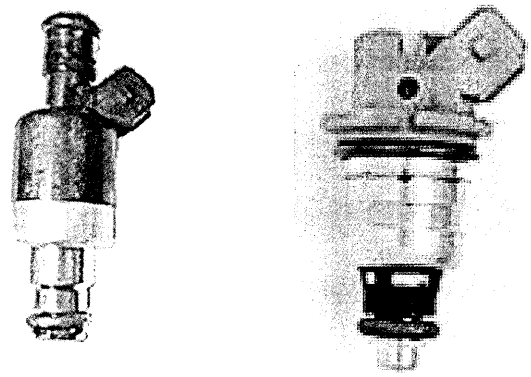

Figure III-II. A typical top-feed injector (left) and bottom-feed injector (right).

Table III-I. The characteristics of injectors used in the flow rate tests.

Manufacturer	Part number	Type	Impedance Ω
Nippon Denso	23250-16160	Top-Feed	15.1
Nippon Denso	195500-3040	Top-Feed	14.6
Rochester	5235136	Top-Feed	14.7
Rochester	17091189	Top-Feed	14.7
Bosch	0280 150203	Top-Feed	15.1
Bosch	0280 150725	Top-Feed	15
Bosch	0280 150702a	Top-Feed	15.1
Bosch	0280 150702b	Top-Feed	15.2
Nippon Denso A	N/A	Top-Feed	14.8
Bosch EV6	N/A	Top-Feed	14.8
Bosch	0280 155609	Side-Feed	14.5
Bosch	0280 155503	Side-Feed	15.4
Siemens Deka A	3362X	Side-Feed	14.8
Nippon Denso B	N/A	Side-Feed	14.7
Siemens Deka B	N/A	Side-Feed	2.1
Nippon Denso C	N/A	Side-Feed	14.6

The characteristics of all tested injectors are listed in Table III-I. Figure III-III shows the results from the injector tests. The injectors were tested at a frequency of 21 Hz, which corresponds to an engine speed of 2500 rev/min. The injectors were divided into two groups, top-feed injectors and side-feed injectors. The injectors were tested with two pulse widths, 3 ms and 12 ms, corresponding to idle pulse width and heavy load, respectively. Injected fuel volume is measured after the tester has completed its cycle.

The results indicate that there is one injector in both groups, which performs clearly better than the others. From the top feed injectors, Bosch *0702b performs the best in terms of change in flow area. From the side feed injectors, the Siemens Deka low impedance injector performed best at shorter injection duration, while the two Bosch side feed injectors performed slightly better across this pressure range. However, the results also show that for those injectors, the injector flow area changes significantly after 8 bar, while the Siemens Deka injector shows more consistent performance across the entire pressure range. This is explained well by the fact, that the Siemens Deka injector was the only low impedance injector tested. Generally, the low impedance injectors have shorter opening time, and because of the lower impedance, the solenoid can dissipate more power than the high impedance injectors, and therefore more mechanical power is provided for lifting the needle.

Two injectors were chosen for high pressure flow rate tests, Bosch *0702b and Siemens Deka B. The reason for choosing two injectors is that it would be ideal to test both side feed and top feed injectors, because of the option to use two types of fuel rails. Also, it is considered that the side-feed injectors have a benefit in lower heat transfer, since there is a constant flow through the injector, which will presumably help to keep the injectors cool and therefore decrease the risk of bubble formation inside the injector and in the fuel rail.

Both of the selected injectors have a plain orifice nozzle with a single orifice hole in the middle of the injector. Though it is appreciated that the shape of the orifice and the number of orifice holes affect greatly on the spray pattern and vaporisation of the fuel, at this stage the injector performance was evaluated only by its performance (flow rate response) in high injection pressures.

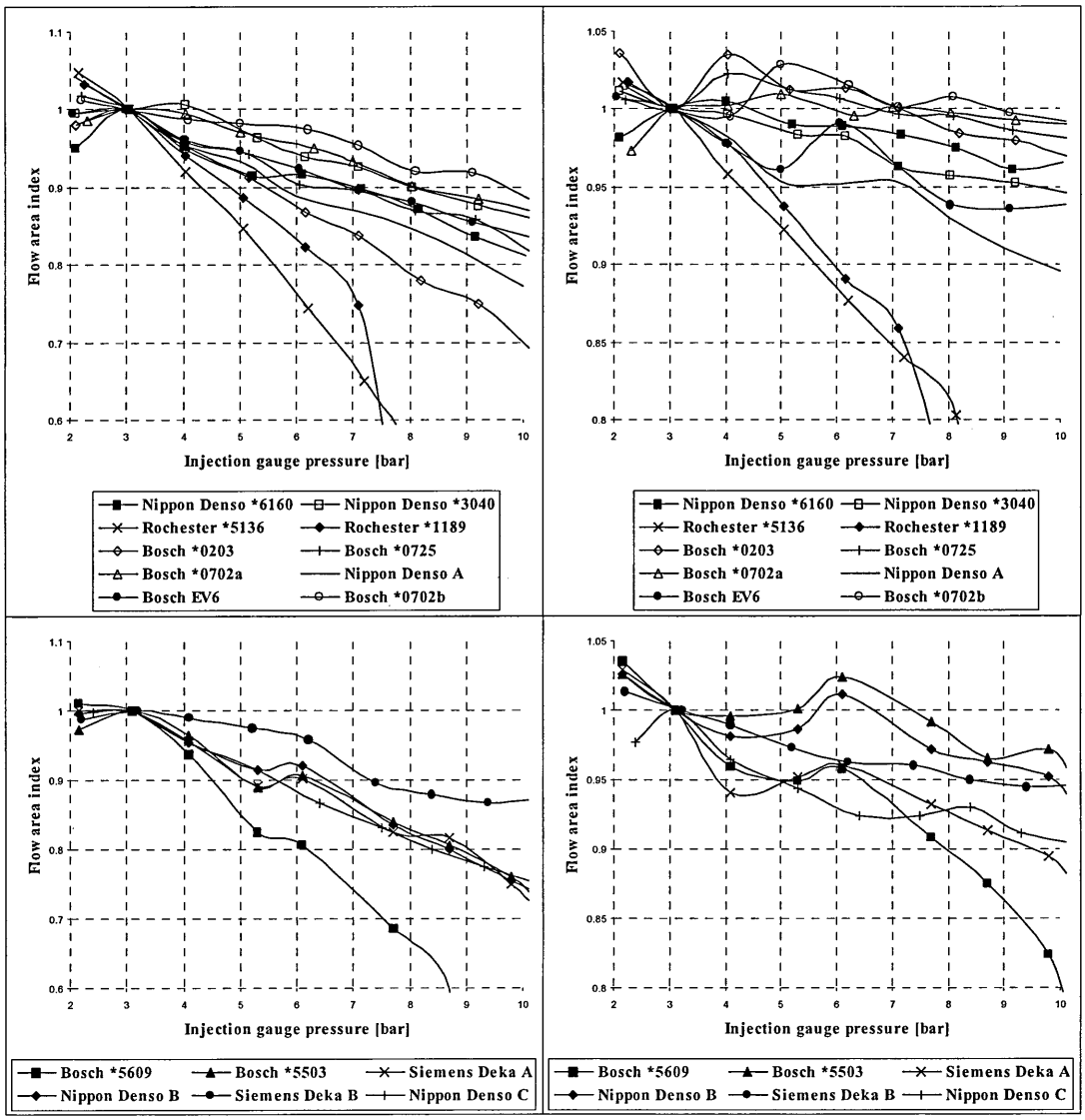

Figure III-III. Injector flow area indices in injection pressure 2-10 bar for top feed injectors (top), side-feed injectors (bottom) with injection duration of 3 ms (left) and 12 ms (right).

On the other hand, the Bosch *0702 is a high impedance injector and Siemens Deka B is a low impedance injector. Most petrol ECUs are designed to drive only high impedance injectors, and are not capable of dissipating the high return current from the low impedance injectors. This means that if a low impedance injector is chose, an additional circuitry is needed to supply the higher current required by the low impedance injector.

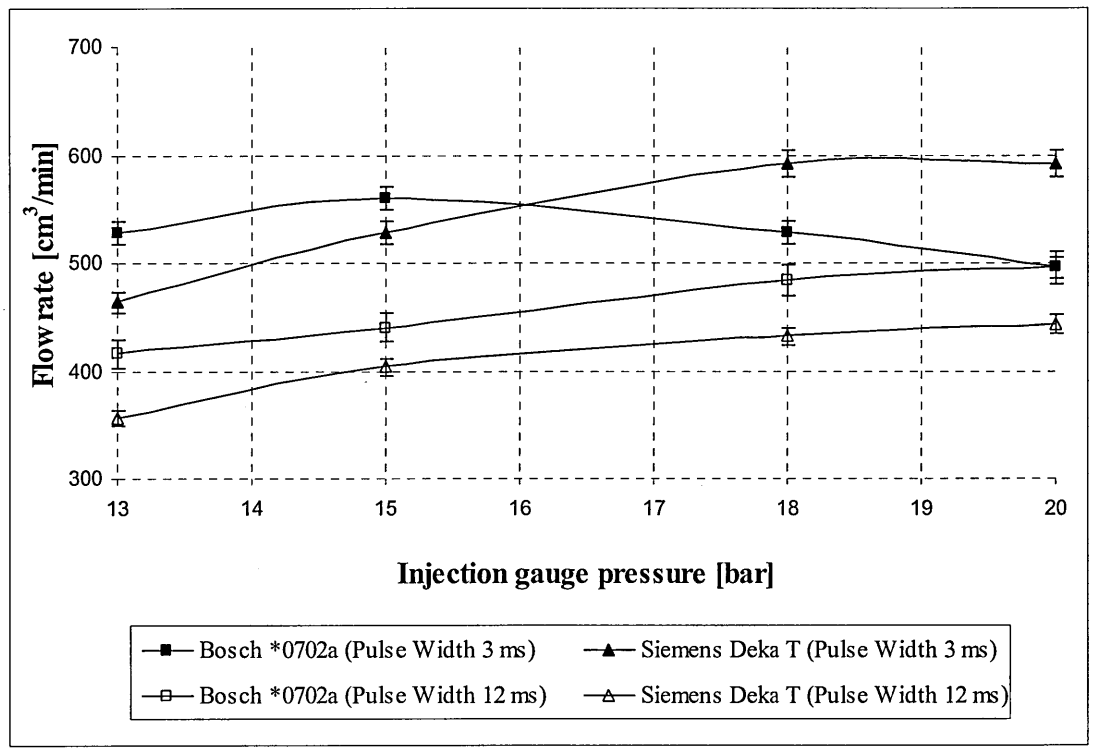

Figure III-IV. Injector flow rates at high pressures.

The results from high pressure injector measurements are plotted in Figure III-IV. The measurements show that both injectors perform reasonably well when injection duration is longer, though for neither of the injectors the increase in the pressure does not cause a big change in flow rate at more than 18 bars. With shorter injection duration, the Siemens Deka injector performs significantly better, showing increasing flow rates with increasing pressures up to 18 bars. The injector provides reasonably good flow even at 20 bars. The Bosch injector, on the contrary, is not performing satisfactorily at pressures of more than 15 bars. The flow rate at 18 bars is significantly lower than at 15 bars, which suggests that the injector is not working consistently. Also, there is no option to adjust the flow rate at pressures more than 15 bars by adjusting the fuel pressure. Therefore it can be concluded that the only satisfactorily performing injector is the Siemens Deka Injector.

Figure III-V shows a comparison of absolute flow rates of the Siemens Deka injector and the Bosch injector. The reference flow rate is the flow rate of the original Bosch EV6 injectors at nominal pressure of 3 bars. The reason for this presentation is to draw a comparison in flow rates between the petrol injectors used in the bi-fuel engine tests described in Chapter V. The comparison gives some rough guidance on fuel

flow compensation needs for the injection timing. The flow rates are corrected for the lower density of LPG.

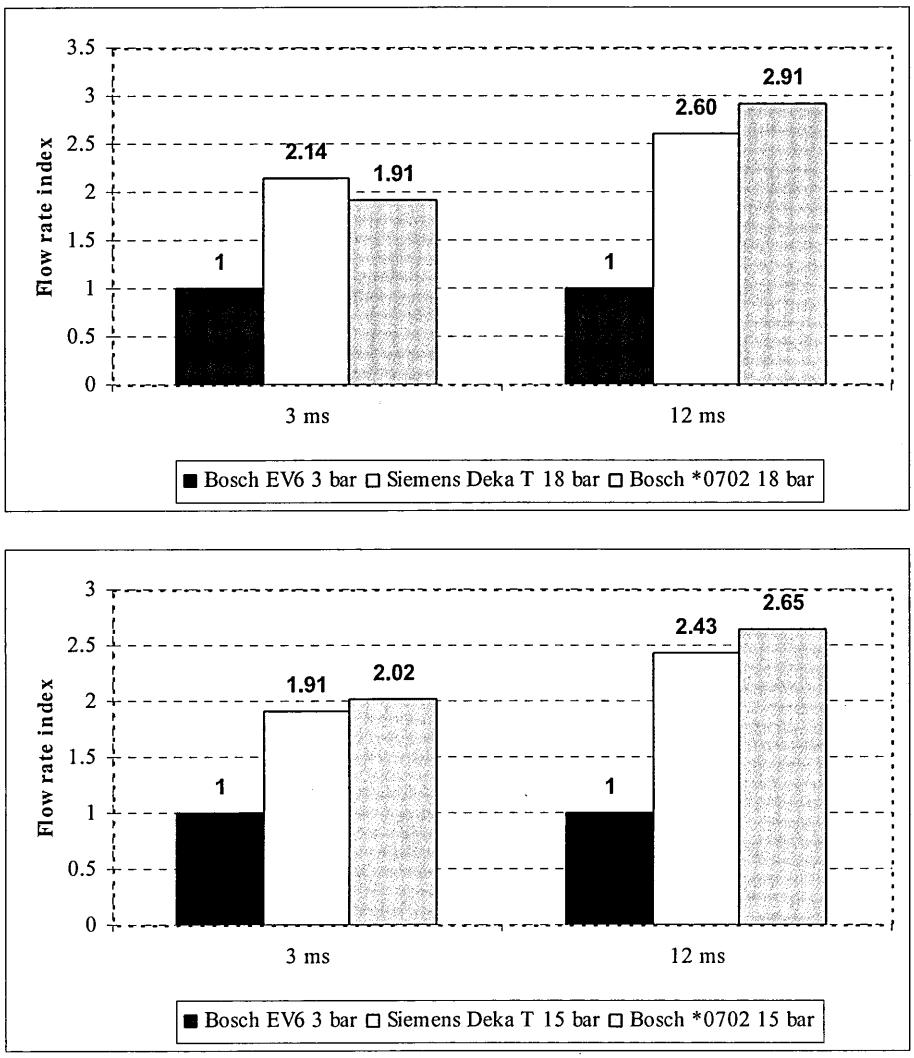

Figure III-V. Siemens Deka and Bosch flow rates at 18 bar injection pressure (top) and at 15 bar injection pressure (bottom) compared to Bosch EV6 flow rates.

The figure shows clearly that even at low injection pressures, injection flow rate is approximately twice as high as for the reference petrol injector. This result stimulated the requirement for another, additional method to compensate the fuelling flow rate. Figure III-VI shows the calculated combined effect of an adjustable injector flow area and injection pressure to injector flow rate. The figure shows that by choosing carefully three to five injector orifice diameters, the flow rate could be adjusted to a wide range of petrol injector flow rates.

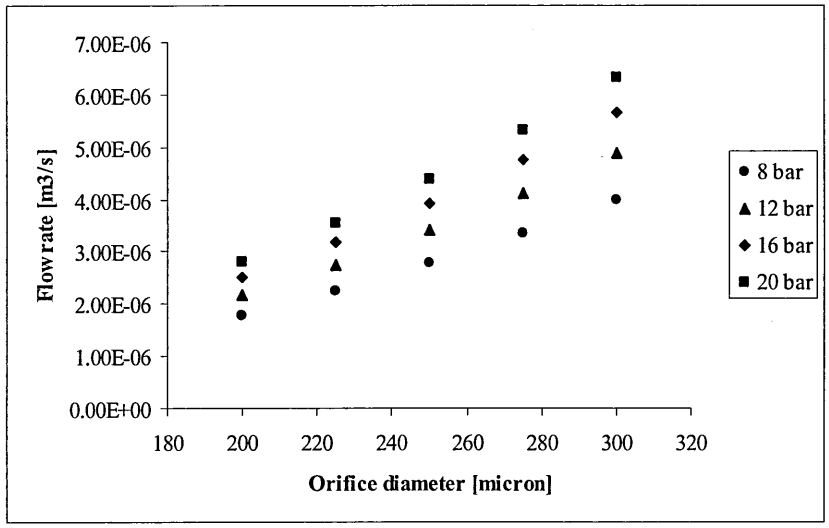

Figure III-VI. The calculated effect of the injector orifice area and injection pressure to the flow rate.

Figure III-VII presents the proposed method to alter injector orifice area by installing an additional reducing hole in the original injector orifice. The small orifice component is held on the original injector hole with a plastic cap. Careful consideration is needed in designing and manufacturing the shape of the component for several reasons. First, the component needs to seal very well between the injector orifice plate and the additional orifice reducing component to avoid leaking and any vaporisation between the two surfaces. Secondly, the shape of the orifice area affects critically to the contraction coefficient of the injector and hence to the injector flow rate.

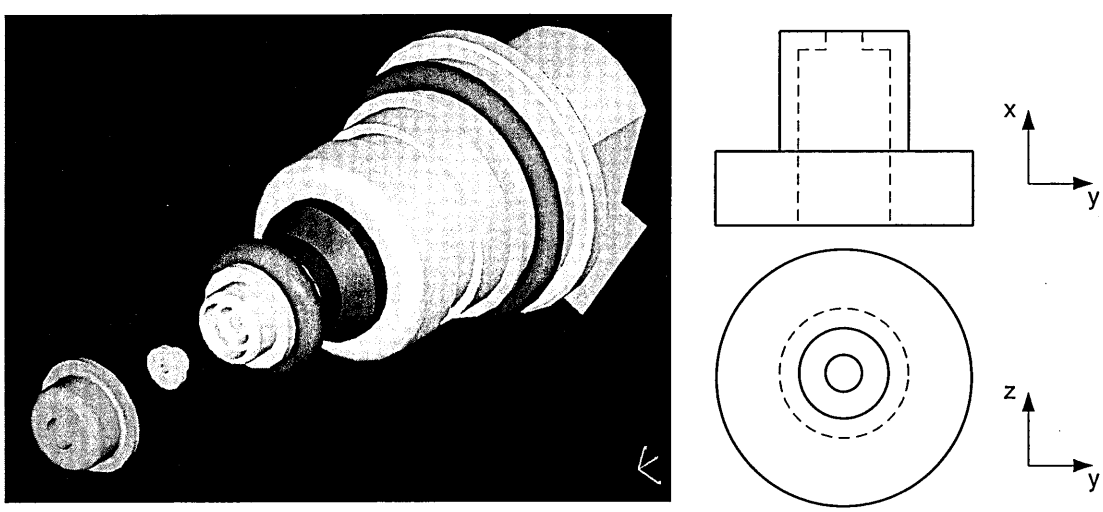

Figure III-VII. Method to adjust the injector orifice area.

The method of using flow restrictors to adjust the injector flow rate involves several challenges. First, the required geometrical accuracy sets very high demands on the quality of the manufacturing process of the restrictors. Within this work the restrictors used were manufactured by spark eroding, and the quality of the manufacturing process was inadequate to meet the high requirements for the geometry. This became crucial in particular in the engine experiments, where the combustion measurements were not possible because the variation in the injector flow rate due to variation between four restrictors. The flow rate depends on the dimensions of the orifice area, the shape of the orifice, the alignment of the restrictor with the original injector orifice. Also spray pattern depends largely on the orifice area shape. These limitations and challenges of using the method are discussed later in Chapters IV and V.

III.2.2 Injector Actuation System

The injectors require an additional driver, because they are low impedance injectors (2.0 ohm) and therefore require more current to open. The vast majority of production vehicle ECUs are designed to drive high impedance injectors, which are typically 14 – 16 ohm. For high impedance injectors, the supply current is typically from 0.65 A to 1 A, depending on the injector impedance and the available battery voltage. For low impedance injectors, the same figure is approximately 3-6 A. The reason for low impedance injectors performing better in high pressure injection application is evident when one considers the mechanical power required to lift the injector needle, the higher the pressure above the needle, the more power required. The mechanical power is converted, along with heat, from electrical power by the injector coil.

The production ECU is not capable of providing the required current for low impedance injectors, which lead to the development of additional injector drivers. The main design specifications involved in the development were following:

a. The original ECU is solely triggering the injectors.
b. The high current will not be able damage the ECU. This is possible because typically the injection signal given by the ECU is an earth-triggered signal,

and therefore the return current from the injector solenoid is dissipated by the ECU.

c. A high constant current to the injector solenoid will be avoided by the usage of peak and hold solenoid driver strategy, where a high peak current is supplied to the injector to enable the needle lift (peak-mode), and then the current is reduced to a level, where the needle is held during the rest of the injection duration (hold-mode). This operation is particularly critical when using liquid LPG; the constant high currents to the solenoid lead to excessive heat transfer to the fuel which contributes to premature vaporisation.

The fundamental diagram of the injector driver circuit is presented in Figure III-VIII. The circuit comprises of two main circuits, the solenoid driver circuit and the isolator circuit. The solenoid driver chip (Texas Instruments DRV102) is a high current power switch with Pulse-Width Modulated (PWM) output. The power switch operates in two phases. The first phase (the beginning of the pulse), the load is supplied a DC current, and after a predetermined time has elapsed, the load is supplied a Pulse-width Modulated (PWM) current (second phase) in a predetermined duty cycle. The oscillator frequency is constant at 24 kHz. The DRV 102 has got an internal current limiter, which does not allow the current to rise above 2.5 – 2.8 A. The injector current measured while actuating the Siemens Deka low impedance injectors with the circuit is demonstrated in Figure III-IX. There are two main adjustable parameters which has an effect on solenoid operation; the DC period duration (adjustable with a capacitor) and the hold current level (adjustable with a resistor).

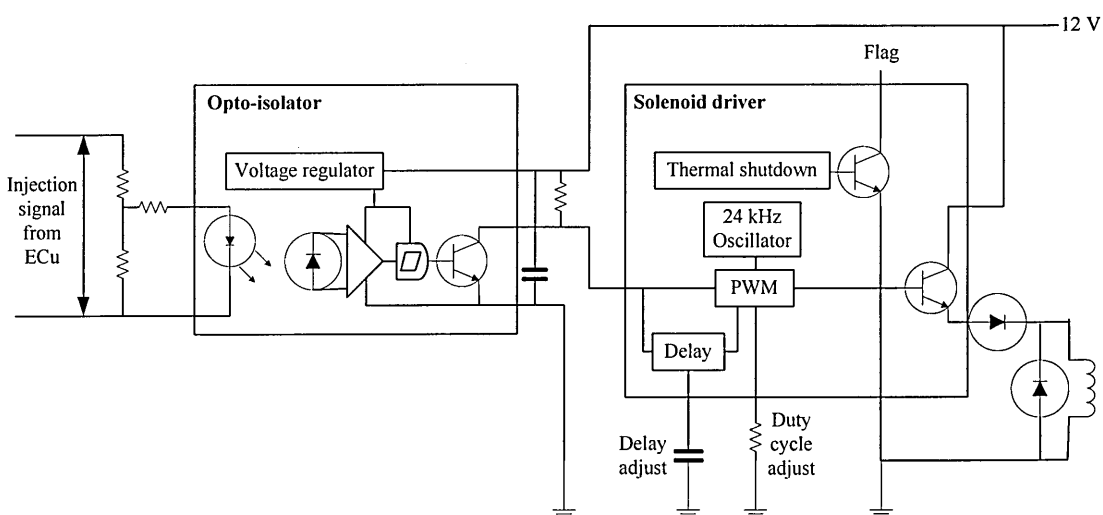

Figure III-VIII. Injector actuator circuit.

The purpose of the opto-isolator circuit is to act as an interface between the original ECU and the driver circuit. The circuit consists of infra-red emitter diode, which is connected to the ECU injector signal. Resistor values in the input side are carefully calculated to achieve the right voltage and current supply for the emitter diode, as these components are sensitive to overload, which results in breakdown. When the injector is switched on by the ECU, there is current flowing through the emitter diode. The infrared radiation is sensed by photodiode sensitive to the same wavelength. The photodiode is coupled with a transistor, and when the photodiode is picking up the radiation from the emitter diode, the transistor is switched off and the current is allowed through the transistor from the power supply to the load. The output in this case is connected to the input of the DRV 102. This circuit prevents the current from flowing back to the original ECU, because the grounds of the ECU signal and DRV 102 output (injector) are not connected, and it is impossible from the opto-isolator to work in the reverse way. Therefore, the ECU signal is isolated in reverse way from the low impedance injector.

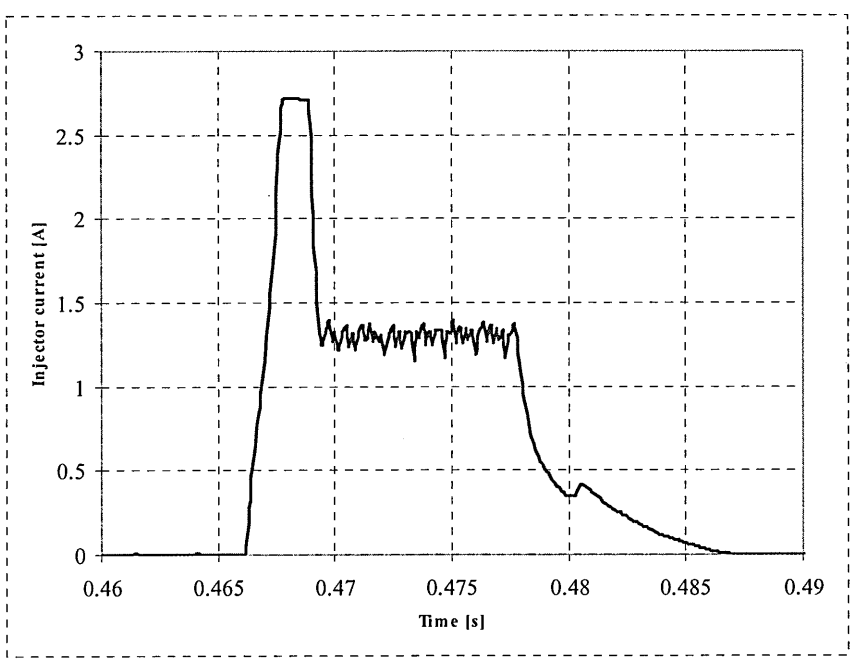

Figure III-IX. Injector current time-history using the peak and hold injector circuit.

III.2.3 Fuel rail system

At this stage it was considered necessary to develop a prototype fuel rail, which would fit in many types of vehicles. The solution was to construct an aluminium case for each injector, and connect the cases, which are called injector pods, to each other with flexible pipes (Figure III-X). This system was customised to accommodate two alternative types of injector configurations; Close-Coupled LPG Injector System (CCLIS) and Pipe-Coupled LPG Injector System (PCLIS). In the CCLIS system, the injector pods are mounted directly in the manifold, while in the PCLIS system, the injector pods are fitted with a flexible pipes. The pipes are then connected to the intake manifold.

The CCLIS configuration does not allow petrol injectors to be fitted in the same point in the manifold. This was purely for economical reasons. The manufacturing of pods, which could accommodate both injectors, was considered to involve unreasonable costs at this stage of the product development. Another point is that, although the remote injector configuration can be done with a simple rigid fuel rail, the remote system used in this work is done by using remotely installed injector pods. This is because the two alternative configurations, CCLIS and PCLIS systems are compared, and it was desirable to keep the flow conditions similar in both cases. Two pipe lengths were used, 200 mm and 400 mm, as well as three different pipe diameters; 1.2 mm, 2 mm and 4 mm. The smallest pipes were made of polyamide, 2 mm diameter pipes were braided pipes with Teflon coating inside and the largest diameter pipes were rubber pipes.

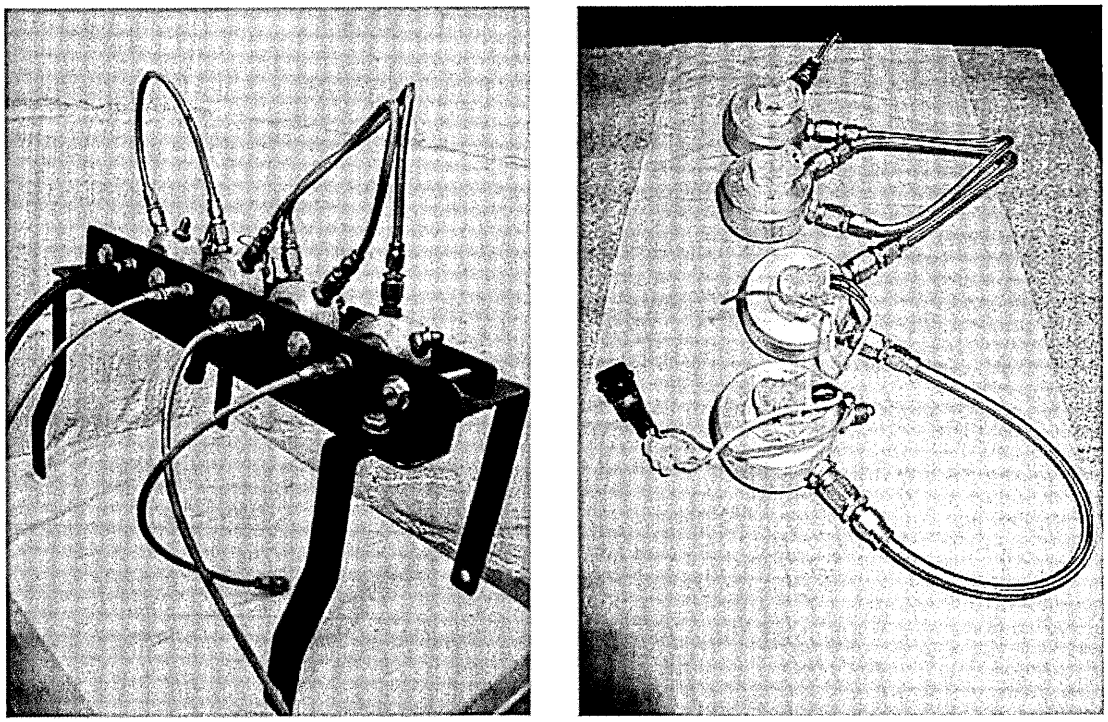

Figure III-X. PCLIS injector configuration (left) and CCLIS injector configuration (right).

III.2.4 Fuel pump system

The pump performance was evaluated by measuring the flow rate, boost pressure and current drawn the from battery simultaneously. By plotting this information, the pump efficiency can be evaluated. The efficiency (η_{pump}) is a ratio of power required from the battery to the power produced, and is obtained by Equation III-VI,

$$\eta_{pump} = \frac{I[A]*U[V]}{\dot{V}\left[\frac{m^3}{s}\right]*p[Pa]}$$

Equation III-VI

where I is current draw, U battery voltage, V flow rate and p fuel pressure. Figure III-XI shows the results for two high-pressure automotive fuel pumps installed in series. The measurements were repeated for 8 different pressures. The flow rate decreases almost linearly with the increasing pressure. The flow rate is important in the propane liquid injection system for two reasons. Firstly, the flow rate has to be high enough to deliver a sufficient amount of fuel through injectors. As there might be two injectors open at the same time at high loads, the flow rate has to be higher than

two times the injector flow rate. Furthermore, the pump flow rate has to be sufficient to compensate the pressure fluctuations in the fuel line which result from the injector opening and closing. Secondly, the flow rate should be as high as possible to minimise the heat transfer from the engine to the fuel. The shorter the residence time in the fuel rail, the less fuel heats up in the neighbourhood of the engine.

Considering the needs of injectors, the flow rate should be 1.2 l/min to deliver sufficient amount of fuel to the engine in the worst case scenario (two injectors open at the same time). A sufficient margin should be then added to maintain the return line open to provide compensation to pressure fluctuations, and minimum flow rate is at least 1.5 l/min, depending on injectors, pressures and pressure regulator characteristics. The results show that sufficient flow rate is available at pressures up to 18 bars, but not higher. This suggests that this pump configuration could only be used up to 18 bar system pressure.

The results also show that current draw from the battery increases linearly with increasing system pressure. If, again, considering the worst case scenario, when the atmospheric temperature is near to zero, or even below, the tank pressure drops to a few bars. In that situation, the boost pressure should be 18 bars, and the corresponding current draw 22 amperes. This is a requirement very difficult to achieve for a 12 Volt car battery, especially when there are often other electrical appliances on at the same time. The power production of the pump assembly is plotted in the same figure. The maximum power production is achieved at a system pressure of 15 bars. The efficiency is highest at approximately 10 bars, but does not drop dramatically until pressure increases up to more than 15 bars. This comparison would suggest that a working pressure of 15 bars would be the optimal solution in the trade off with flow rate, power production, efficiency and current draw.

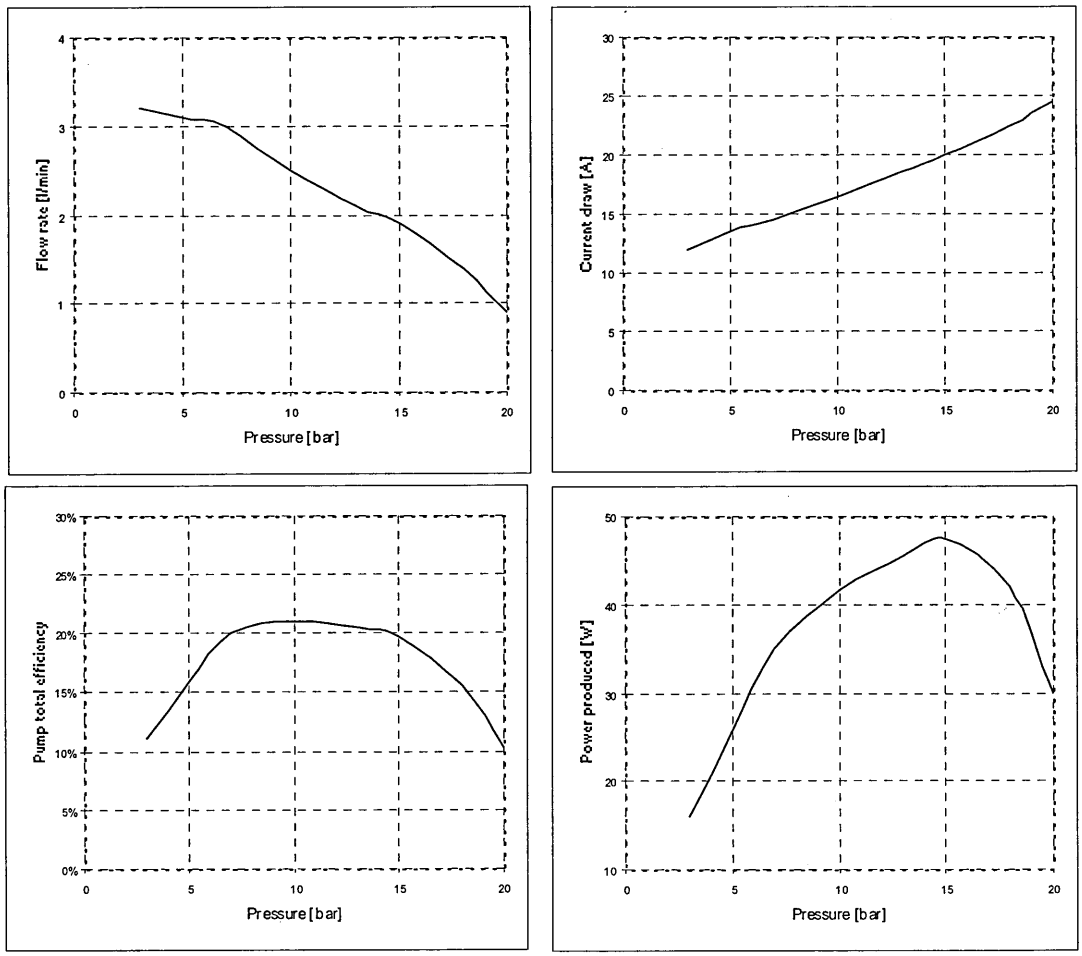

Figure III-XI. Flow rate (top left), current draw (top right), efficiency (bottom left) and power production (bottom right) for pump system with two pumps in series.

III.2.5 Fuel pressure regulator

The performance of a KENMAC KCB pressure regulator was measured by using it in the fuel line as a back pressure regulator. A regulator is needed for two reasons; to compensate the fuel line pressure variations caused by changes in temperature (the liquid and vapour in the tank is in saturation vapour pressure and therefore the pressure changes with changing temperature) and pressure variations due to injector opening and closing. Because the ambient temperature changes at a slow rate, it does not raise an issue with regulator response time.

The magnitude of the pressure drop due to injector opening and closing is critical considering the premature vaporisation. The typical injector duration is 2 – 20 ms. The regulator frequency response becomes an issue, as the regulator element (in this

case a spring) has to be able to respond very fast to the resulting drop in pressure. This response was measured by measuring the pressure in the fuel line simultaneously with the injector current. The test configuration used is described in Figure III-I. The injection pressure was measured with a Keller piezo-resistive pressure sensor and logged simultaneously with the injector current, which was measured with a LEM HEME current probe. The results (Figure III-XII) show that the pressure drops as a result of opening injector, but the drop is not as dramatic as with the needle valve which was used to compare the results.

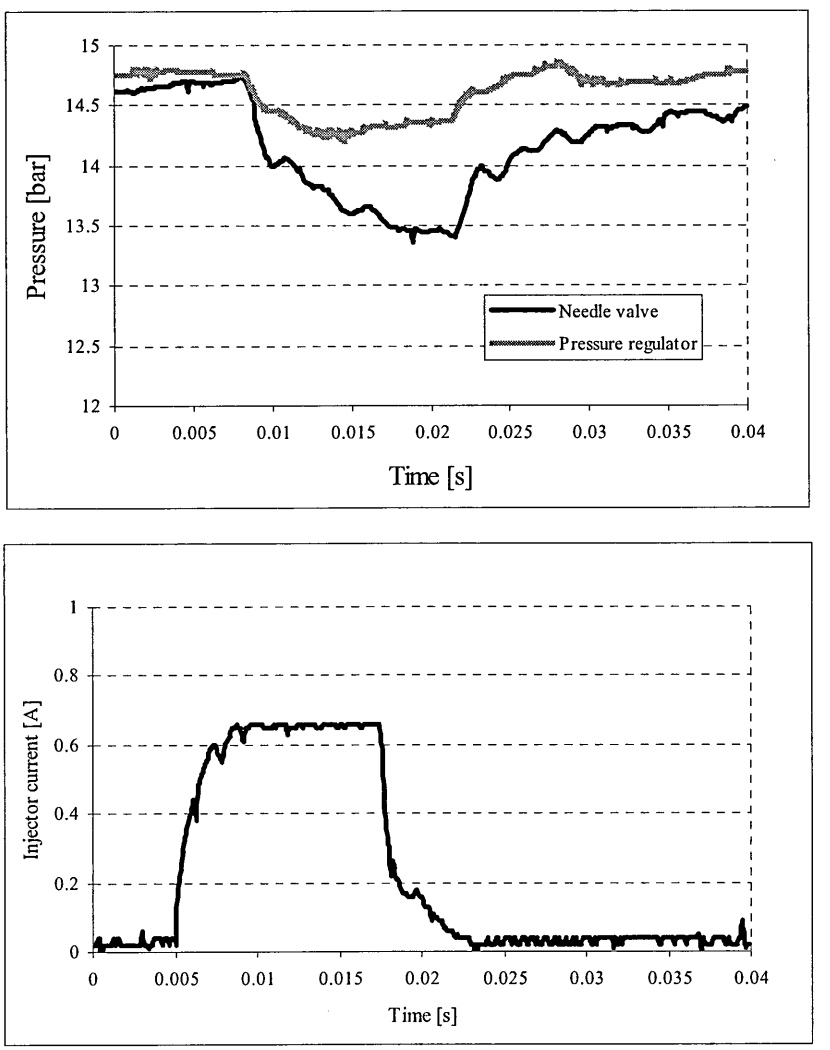

Figure III-XII. Pressure fluctuation in the fuel line (top) and simultaneously measured injector current (bottom).

III.3 DISCUSSION

III.3.1 Premature vaporisation in the fuel rail

Premature vaporisation in the fuel rail is one of the most challenging issues in the LPLI systems. This has been taken into account by using higher injection pressures and flow rates than existing LPLI systems. However, it is not expected that the problem will not occur in spite of the greater margins to the saturation conditions, and therefore another solution is proposed. The approach to tackle the problem in this work is not finding ways to prevent it, but rather how to detect it. There are several methods to reduce the heat transfer to the fuel, but the methods can not be considered as universal, because the heat transfer depends on the individual engine characteristics and operating conditions. This work is described in Chapter VI.

III.3.2 Pipe – Coupled injection system configuration

There are two important issues concerning the use of PCLIS system:

1. The fluid transport time is an important factor from the point of view of mixture control, and it is a problem when using the same injection control for both petrol and LPG. The fuel metering occurs away from the manifold in the case of the PCLIS system. The fluid travels through the coupling pipe to the manifold, where the mixing with the intake air takes place. The injection timing is optimised for petrol injection, when the fuel is injected directly to the manifold. Therefore, in PCLIS system, the fuel injected may not reach the cylinder during the same cycle, long travelling times may result in longer feed-back control respond times and inaccurate fuelling control during transients.
2. Because the fuel is metered away from the manifold, the fuel starts vaporising in the pipes, and the vaporisation enthalpy would be taken from the pipe walls, rather than from the intake air, which is expected to cause a reduction in engine power.

Predicting the transport time and vaporisation rate through the pipes is extremely complicated due to a variety of factors affecting them. Firstly, the transport time

depends largely on the vaporisation rate; the liquid fuel travels through the pipes at# significantly slower than vapour. Also, pressure varies significantly in the pipes due to pulsating injectors, and this obviously depends on the injection pressure and injection duration. Vaporisation depends also on the temperature of the pipe systems. Further, the travelling time, pressure fluctuations in the pipe and vaporisation depend on the length and the diameter of the pipe. Due to this complexity, it was decided to measure the fuel travelling time and the state of the fuel using optical methods. This is described in Chapter IV. Also, the effect of vaporisation in the pipes on the mixture formation and consequently the combustion and engine performance is measured in the experiments in a bi-fuel engine, which is described in Chapter V.

III.3.3 Injection pressure

It is taken into consideration, that in a petrol injection system the injection pressure is maintained constant by referencing the fuel rail pressure to the manifold pressure. This is obviously not the case in the system described in this chapter. The fuel rail pressure is maintained constant, which means that the injection pressure varies slightly because of varying manifold pressure. However, in this work, this effect is neglected because the injection pressure is relatively high (18-20 bar) compared to the changes in the manifold pressure (0.5-0.7 bar), and it is assumed that the consequent slight change in the injection pressure is compensated by the lambda feed-back control and the learning capability of the ECU.

IV. LPG SPRAY IMAGING

IV.1 ABSTRACT

In order to study the characteristics of two alternative bi-fuel injector configurations, a schlieren imaging method was employed to visualise density gradients in the fuel spray. The objective was to compare the performance of the two systems, and also to study the response of Pipe-Coupled Liquid Injection System (PCLIS) parameters on the fuel spray, such as injector flow rate, coupling pipe diameter, injection frequency and injection pressure.

It was noticed that the Close-Coupled Liquid Injection System (CCLIS) had significantly higher fuel density in the mixing area when compared with the PCLIS system, which indicates that CCLIS system will perform considerably better than PCLIS system in the mixture formation mechanics, charge cooling effect, and in engine emission control point of view. Another important observation was that the fuel continues emerging from the pipes throughout the entire cycle with the PCLIS configuration.

The PCLIS system showed unacceptable performance when using very small diameter pipes due to long fluid travelling times and high cycle-to-cycle variation, which was particularly evident in high injection frequency. However, from the point of view of mixture formation and intake charge cooling the smallest diameter pipes performed best, indicating lower rate of vaporisation in the pipe. Also it was noticed that higher flow rate injectors showed higher density gradient at the pipe exit when compared to lower flow rate injectors. The cycle-to-cycle variation was also higher with low flow rate injectors. Injection pressure had very little effect on system response.

As a conclusion, CCLIS system is the most attractive system to use in liquid LPG engines, while PCLIS system shows undesirable characteristics from an engine control point of view. However, PCLIS system has potential, as long as the system limitations are well understood. The system performs better with larger diameter pipes and higher flow rate injector, when injection durations are short.

IV.2 INTRODUCTION

IV.2.1 Mixture preparation process in CCLIS and PCLIS

The objective of this study is to investigate spray characteristics of two alternative injector configurations for bi-fuel LPG engines. In Close-Coupled Liquid Injection Systems (CCLIS) the fuel injectors are mounted directly on the manifold, as conventional petrol MPI configurations. In Pipe-Coupled Liquid Injection System (PCLIS) the injectors are mounted remotely, and connected to the manifold with pipes. As the fuel metering occurs away from the manifold, the LPG fuel starts also to vaporise before entering the manifold and consequently the air-fuel mixture preparation differs from the CCLIS. As in the CCLIS the most interesting aspects in terms of mixture preparation are spray geometry and vaporisation, in the PCLIS case the emphasis of the analysis is on fuel concentration on pipe exit, fluid travelling time through the pipe and cycle to cycle variations when injectors are pulsed in typical engine injection frequency. The most important factors affecting the characteristics mentioned above are considered fuel injector flow rate, mass or volume of injected fuel, injection frequency, pipe diameter and length and injection pressure. The most suitable method to analyse these characteristics in both CCLIS and PCLIS cases was considered spray imaging, which would provide both spatial and temporal information on fuel spray structure.

IV.2.2 Fuel spray imaging methods

The most popular fuel injector spray measurement techniques are based on the monochromatic laser light sheet. The major advantage of these techniques is the opportunity to obtain quantitative information on a fuel spray with high temporal and spatial resolution.

The Mie scattering technique is based on light – surface interaction, and the Mie scattering response is proportional to the total surface area of scattered particles. The technique is widely used to measure spray pattern and spray penetration. LIF (Laser Induced Fluorescence) technique is used to measure fuel vapour distribution, spray penetration or fuel vaporisation. The technique is based on wavelength conversion (red-shift) of a LIF active molecule and the signal intensity scales with the droplet

volume (when the dye concentration is low), or mass. Because fuel spray measurements are generally carried out using LIF-inactive mono-component fuel, such as iso-octane, a tracer component is added to the fuel to provide the fluorescence emission of the spray. The fluorescence tracer is chosen to closely represent the saturation properties of the fuel. Laser Sheet Dropsizing (LSD) is a method combining Mie and LIF imaging; acquiring simultaneous Mie and LIF signal, provide information on mean droplet sizes (Jermy and Greenhalgh, 2000).

Several studies show the successful application of LIF imaging to mixture formation analysis of liquid phase injection LPG sprays. Lee S-W et al. (2002) carried out investigations on stratified charge mixture formation in a high pressure and temperature constant volume chamber using LIF imaging to measure the gas-phase LPG and Mie scattering to measure the liquid LPG droplets. Since LPG itself is not fluorescent, LPG was mixed with diethyl methylamine (DEMA), which has a low boiling point and strong fluorescence intensity. The same authors used high-speed videography (9000 fps) with copper vapour laser sheet illumination to image liquid phase LPG in a constant volume chamber (Lee S-W et al., 2001). Oh et al. (2003) applied LIF to characterise LPG fuel spray and stratification in lean-burn single cylinder optical engine. Acetone was used as the fluorescing dopant, which was chosen for its strong fluorescence signal and is less sensitive to oxygen quenching, though its boiling point is significantly higher than that of LPG.

Schlieren and shadowgraph techniques are also used to image fuel spray systems. Rather than using structured monochromatic light, the image, or shadowgram is formed using a white light source for illumination, though a laser can be used for schlieren in some cases. The techniques are based on observing density or refractive index gradients in inhomogeneous media. While a schlieren image displays the light deflection angle caused by a refractive index gradient, a shadowgraph displays the ray obscuration resulting from the scattering and refraction. Schlieren imaging is most often used to observe mild gradients or for quantitative evaluation, whilst shadowgraph responds best to strong gradients and is used to measure spray penetration.

Schlieren and shadowgraphy methods have been popular methods for decades to study air-fuel mixture concentrations, spray geometry, vaporisation and mixture formation processes. Namazian et al. (1980) used schlieren imaging to visualise in-cylinder density fields of propane fuelled optical engine to analyse mixture formation, in-cylinder motion and combustion. Lee S-W et al. (2003) applied combined schlieren imaging and shadowgraphy to analyse LPG spray penetration and vaporisation in a high temperature and pressure constant volume chamber. Shadowgraphs of an impinging spray displayed the liquid spray while the more sensitive schlieren images revealed the smaller density gradients in vapour phase areas of the spray. Oguma et al. (2003) studied LPG and diesel spray vaporisation, spray tip penetration and spray area in a constant volume chamber using direct parallel-light shadowgraphy and high speed video camera. Imaging comparison of vaporisation characteristics and spray geometry with different fuel composition was demonstrated, showing higher light deflection for higher boiling point fuel compositions, indicating higher vaporisation rates for lower boiling point composition fuels. Numerous studies demonstrate the application of schlieren imaging in analysing mixture formation and fuel jet behaviour in natural gas engines (Gimbres et al., 1999; Boyan and Furuyama, 1998; Ouelette and Hill, 1992). Paulsen and Valland (1996) used schlieren imaging to obtain quantitative information on diesel engine in-cylinder flow field fuel concentration by calculating the local light refraction based on the data extracted from schlieren images. The schlieren technique has also recently been used to measure spray geometry and vaporisation in GDI engines (Ortmann et al., 2001) and to visualize piston-film evaporation (Alger et al., 2001).

Global Rainbow Thermometry (GRT) is an imaging technique recently applied to measure droplet size and surface temperature of droplets. The technique is based on deriving the droplet characteristics from the structure of so-called Airy-fringes formed by monochromatic light interfering with spherical droplets (van Beeck et al., 2001; Yildiz et al., 2002). The technique was successfully applied to flashing propane sprays by Knubben and van der Geld (2001) to measure both mean droplet size and droplet temperature.

For this study, all the above mentioned techniques were considered as possible spray imaging methods. Combined LIF and Mie would provide quantitative data on droplet

sizes and liquid-vapour distribution, but the selection of suitable dopant would be challenging considering the low boiling point of propane. The dopant should have similar saturation properties to propane to achieve co-evaporation. The saturation characteristics of the fluorescing material would be critical in the case of PCLIS in particular. GRT would be ideal to measure vaporisation and heat transfer from the propane spray, but again, in the case of PCLIS there would possibly not be enough spherical liquid droplets emerging from coupling pipes. The schlieren method was therefore considered most suitable for measurement of both phases, though quantitative data would be limited. The method is also fairly economical, as no laser light source is required.

IV.3 MATERIALS AND METHODS

IV.3.1 Schlieren theory

Schlieren and shadowgraph techniques have been successfully used for decades for visualising inhomogeneous transparent media. Refractive index gradients resulting from temperature difference or pressure difference in high speed compressible flows or mixing dissimilar materials cause light rays to refract from the initial paths and consequently redistributing the image illumination. This refraction is essentially a result of a change in speed of light. Refractive index (n) is defined by:

$$n = \frac{c_0}{c} \qquad \textbf{Equation IV-I}$$

where c is the speed of light and c_0 is the speed of light in a vacuum. For gases, simple relationship between refractive index and density can be drawn using:

$$n - 1 = k\rho \qquad \textbf{Equation IV-II}$$

where k is Gladstone coefficient and ρ density. Further, the relationship between density and temperature and pressure can be obtained using the ideal gas law. Density versus refractive index relationships also exist for liquids and solids, but are more complicated to calculate and are mainly a function of temperature, viscosity and concentration. Refractivity is also stronger for liquids, for example for air in atmospheric temperature $n-1$ is 0.0002766 as for water $n-1$ is three magnitudes higher (see Table IV-I).

Table IV-I. Refractive indices of some common gases and liquids

Substance	Chemical formula	Temperature [°C]	Phase	Wavelength [nm]	Refractive Index	
Air	Standard air	15	gas	580	1.0002766	1
Water	H_2O	20	liquid	575	1.33336	1
Water Vapour	H_2O	0	gas	589	1.000254	2
Nitrogen	N_2	15	gas	546	1.0002835	1
Methane	CH_4	25	gas	589	1.000444	1
Methanol	CH_4O	20	liquid	589	1.3288	1
Acetone	C_3H_6O	20	liquid	589	1.3588	1
Heptane	C_7H_{16}	20	liquid	589	1.3878	1
Ethanol	C_2H_6O	20	liquid	589	1.3611	1

1 CRC Handbook of Optical Materials

2 Kaye: Tables of physical and Chemical Properties

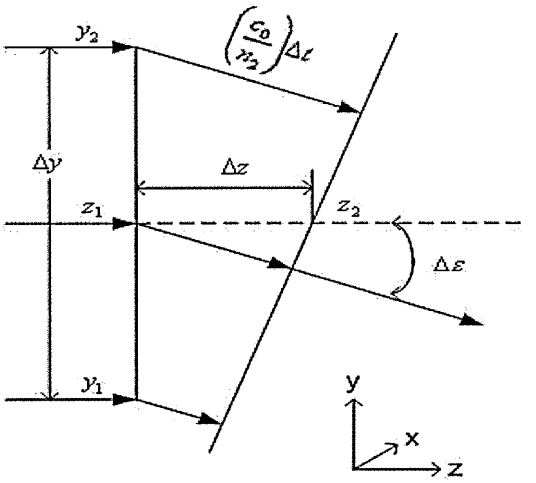

Figure IV-I. Elemental diagram of light refraction by refractive index gradient. (Adapted from Settles, 2001).

The mathematical basis of a schlieren image is described in Figure IV-I. The entire derivation is described in Equation IV-III – Equation IV-VIII. From the figure and Equation IV-I the angle of deflection ($\Delta\varepsilon$) can be expressed as:

$$\Delta\varepsilon = \frac{\left(\frac{c_0}{n_2}\right) - \left(\frac{c_0}{n_1}\right)}{\Delta y}\Delta t \qquad \textbf{Equation IV-III}$$

by expressing Δt in terms of Δy and c (local speed of light), and combining these expressions and simplifying the terms

$$\Delta\varepsilon = \frac{n}{n_1 n_2}\frac{(n_1 - n_2)}{\Delta y}\Delta z \qquad \textbf{Equation IV-IV}$$

Letting all the finite differences approach zero and simplifying expression $n/n_1 n_2$ to $1/n$, we obtain

$$\frac{d\varepsilon}{dz} = \frac{1}{n}\frac{dn}{dy} \qquad \textbf{Equation IV-V}$$

Since $\Delta\varepsilon$ is a very small angle, it approximately equals to dy/dz (small-angle approximation). Rewriting the equation yields to expression of the ray curvature

$$\frac{\partial^2 y}{\partial z^2} = \frac{1}{n}\frac{\partial n}{\partial y} \qquad \textbf{Equation IV-VI}$$

For a 2-axis system, similar expression can obviously be written for x-axis. Integrating once

$$\varepsilon_y = \frac{1}{n}\int\frac{\partial n}{\partial y}\partial z$$ **Equation IV-VII**

For two-dimensional schlieren medium of extent L along the optical axis and describing surrounding medium n_0

$$\varepsilon_y = \frac{L}{n_0}\frac{\partial n}{\partial y}$$ **Equation IV-VIII**

From this expression, it is clearly shown that gradient $\partial n/\partial y$ causes the deflection. However, it is notable that in most cases the light has deflected more than once passing through an inhomogeneous media, and therefore the deflection angle derived from the visual effect does not provide explicit information on various deflections the light has passed and consequently, does not provide information on various refractive index gradients along the optical path.

IV.3.2 Optical system

The experimental system used in measurements is described in Figure IV-II. The optical system used is the so called z-type schlieren system, which is one of the most often used schlieren systems (Settles, 2001). The expression derives from the three-beam configuration, which is created using two oppositely-tilted, symmetrical on-axis parabolic concave mirrors. A parallel beam was created between the two parabolas where the measurement area lies. A diverging illuminator beam was created by a point source (EGNG Machine Vision strobe with 3-4 μs pulse width), and the opposite converging analyser beam was focused by a lens on the image plane to form an image of the test region. A knife edge was placed vertically on the focus of the second parabola. The purpose of the knife-edge is to cut off the deflected rays caused by the horizontal gradient, and instead of contributing to the image illumination as a phase difference, these deflected rays cause a magnitude difference in image illumination for the corresponding image point. For this study, a very small cut-off was used to optimise the image sensitivity both in liquid and vapour phases. Increasing the cut-off would increase the sensitivity to smaller gradients, but reduce the sharpness on the liquid spray edges. The image was refocused with a lens onto the

sensor of a CCD camera (LaVision Spraymaster3) and acquired and saved on a computer. The chamber was purged after each set of images and the background images were taken before and after purging.

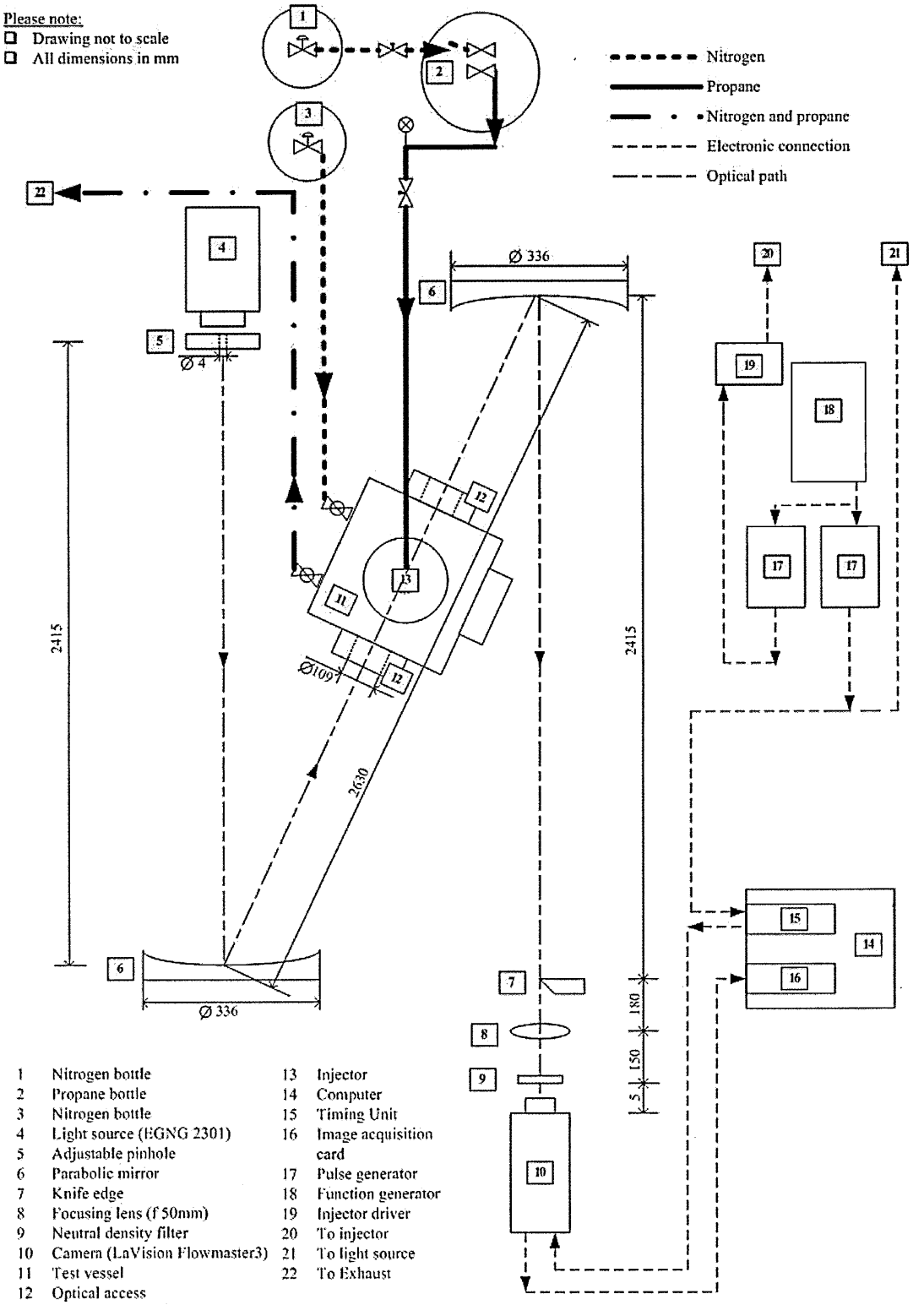

Figure IV-II. Schematic diagram of the optical system

IV.4 RESULTS

IV.4.1 Parametric study of CCLIS

To study the spray geometry of CCLIS injectors, the injector is mounted directly on the top of the pressure chamber. The windows of the chamber allow visualisation of the spray 3 mm below the injector tip, the entire diameter of the spray measurement area being the diameter of the window, 109 mm.

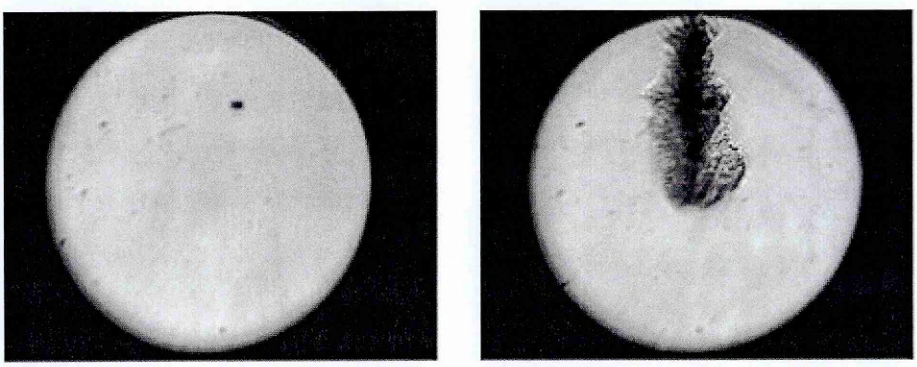

Figure IV-III. Raw schlieren images with no spray (left) and with LPG spray (right)

Figure IV-III shows the raw images of the measurement without spray and with spray. First, images were background compensated by subtracting the spray image from the background image, and consequently the image of spray is inverted having high intensity in the high refractive index gradient region and equivalently zero intensity count in the region where light rays pass the measurement region without experiencing deflections. Therefore, the image intensity count scales with the density gradient, such that the higher intensity count corresponds to higher density gradient and vice versa.

An image array is referred as K, which is an array of elements x (intensity count) of size s (number of pixels) $K = x[s]$. For each injection stage, 40 images were acquired, referred as count $j=40$, and average image, or array, $\overline{K}$ calculated (see Equation IV-IX). Root mean square image (RMS_K) describing the magnitude of intensity variation of 40 images in each image array element (rms_s) is calculated (Equation IV-X). RMS_K is an array ($RMS_K = rms[s]$). Further, fluctuation intensity (FI_K), which normalises the rms array with the average intensity array, is also calculated (Equation IV-XI).

$$\overline{K} = \frac{1}{N_j}\sum_{i=1}^{N_j} K_i$$ **Equation IV-IX**

$$rms_s = \sqrt{\frac{1}{N_j}\sum_{i=1}^{N_j}\left(x_{s_i} - \overline{x}_s\right)^2}\ ,\ \overline{x}_s = \frac{1}{N_j}\sum_{i=1}^{N_j} x_{s_i}$$ **Equation IV-X**

$$FI_K = \frac{RMS_K}{\overline{K}}$$ **Equation IV-XI**

Figure IV-IV shows the results of the processing described above at two stages of injection. Soon after the start of the injection (2 ms ASOI) the rms variation shows high counts (red) in the periphery of the spray, the maximum counts being at the tip of the spray, while in the core of the spray the magnitude of the variation is almost absent (blue).

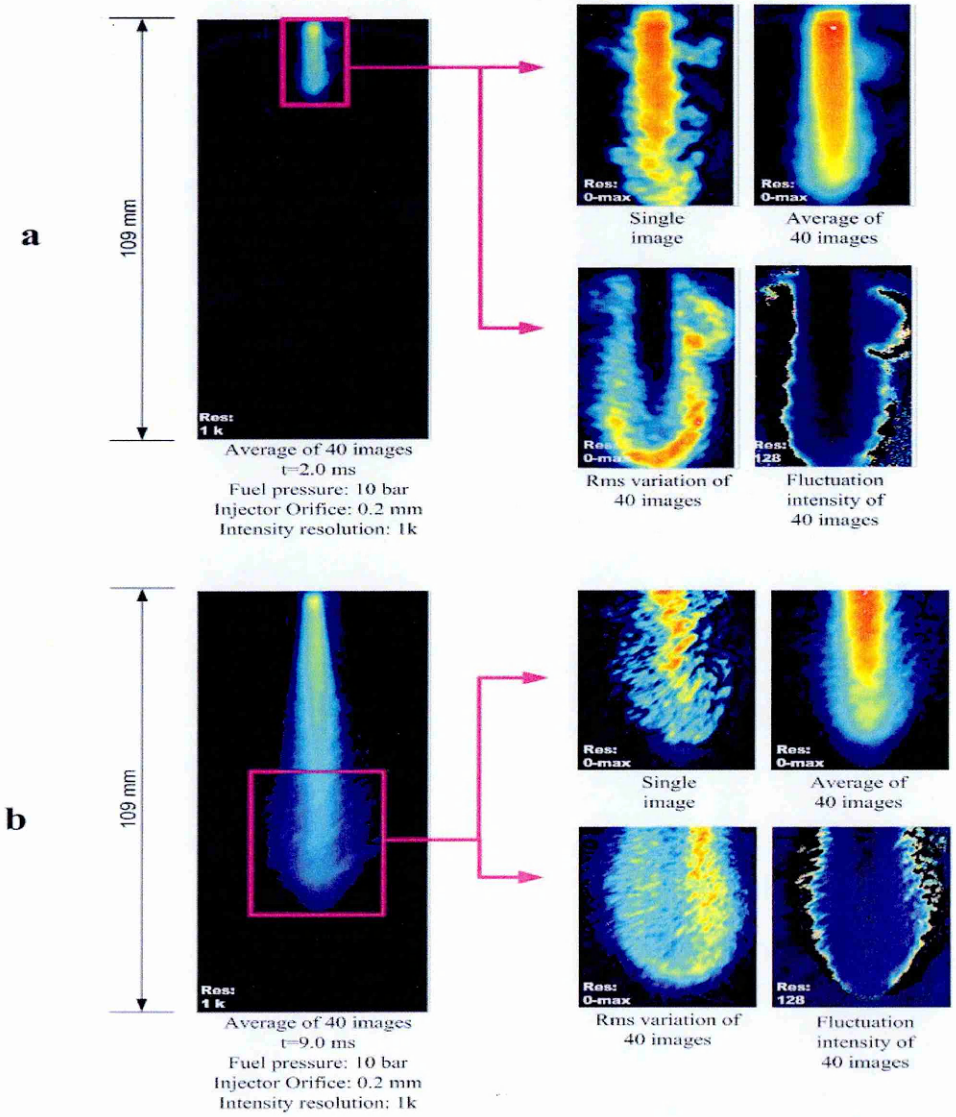

Figure IV-IV. Processed images of LPG spray during early injection (a) and late injection (b)

As described earlier in this chapter, in a schlieren image the image intensity scales with the refractive index gradient through the measurement region. In the case of fuel spray measurements, the intensity does not only scale with the gradients in the fuel spray composition, but also with the temperature and pressure gradients through the measurement region. Another important factor affecting the image intensity is that the sensitivity of the intensity response depends on the magnitude of the knife-edge cut-off, the larger cut-off having more sensitivity to smaller gradients. Due to these arbitraries it is very difficult to calibrate the schlieren image to show quantitative measures on the spray density gradients.

During the measurements presented in this chapter, the knife-edge cut-off was kept the same throughout the entire experiment. The calibration of the image intensity to spray density gradient -relationship is not carried out, and therefore the quantitative data on the density gradient is not obtained. However, since the knife-edge position is not changed during the measurements, qualitative data on the spray geometry is obtained from the images in order to compare different injector configurations.

Also, because the intensity and refractive index gradient scales with the temperature and pressure gradients as well as the fuel spray density, the main emphasis in this work is on the spray geometry, the analysis of image-to-image variation and the fuel travelling times (in the case of PCLIS). However, some references are made in the discussion on the image intensity to fuel spray concentration –relationship, but it is emphasized that the image intensity also includes arbitrary factors due to temperature and pressure changes through the measurement region contributing to the image intensity. Considering this limitation of the technique, as well as the fact that the sensitivity of the optical system (knife-edge cut-off) is kept constant throughout the measurements, the discussion is limited to comparison of different injector configurations.

Considering these above mentioned limitations, the images presented in Figure IV-IV suggests that both in the single and average intensity images the highest density gradient are in the core of the spray. Also, it is evident that in the later injection case (9 ms ASOI) the rms variation is more uniform, showing a higher magnitude of variation in the centre of the spray when compared to the rms variation in the early

density gradient in the tip of the spray. Figure IV-IV suggests that during the early part of the injection, there is more consistent liquid jet region (no variation) in the core of the spray, while at the edges the liquid jet breaks up and high number of small droplets and vapour results in high magnitude of variation in images. The variation at the edges of the spray is also an indication of presence of turbulent eddies. In the early part of the injection the spray tip is accelerating, while in the late part of the injection the tip is more static, which contributes to the high variation in the spray tip in the early part of the injection. In the case of late injection, the variation, and therefore fraction of vapour in the spray is higher and larger turbulent eddies have formed.

The spray properties of three different injectors with different flow areas were measured, each at three different injection pressures. The injection duration was corrected for each injector and the injection pressure was compensated for varying flow rate in order to maintain the injected mass of fuel to be the same for each injector – pressure combination. The test sequence, injector characteristics, and the injection duration correction are described in Table IV-II.

Table IV-II. CCLS injector parameters

nr	Orifice diameter [µm]	Orifice shape	Injection pressure [bar]	Injection duration [ms]
1	500	a	20	2.2
			15	2.5
			10	3.1
2	250	b	20	4.8
			15	5.5
			10	6.7
3	200	c	20	7.2
			15	8.3
			10	10.1

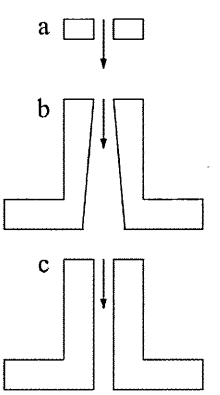

Figure IV-V to Figure IV-VII show the average intensities ($\overline{K}$) and rms variations (RMS_K) for each injector – pressure combination for 9 time steps during injection. All the average rms images are shown with the same intensity resolution. The first time-step refers to time elapsed from the start of the injection pulse.

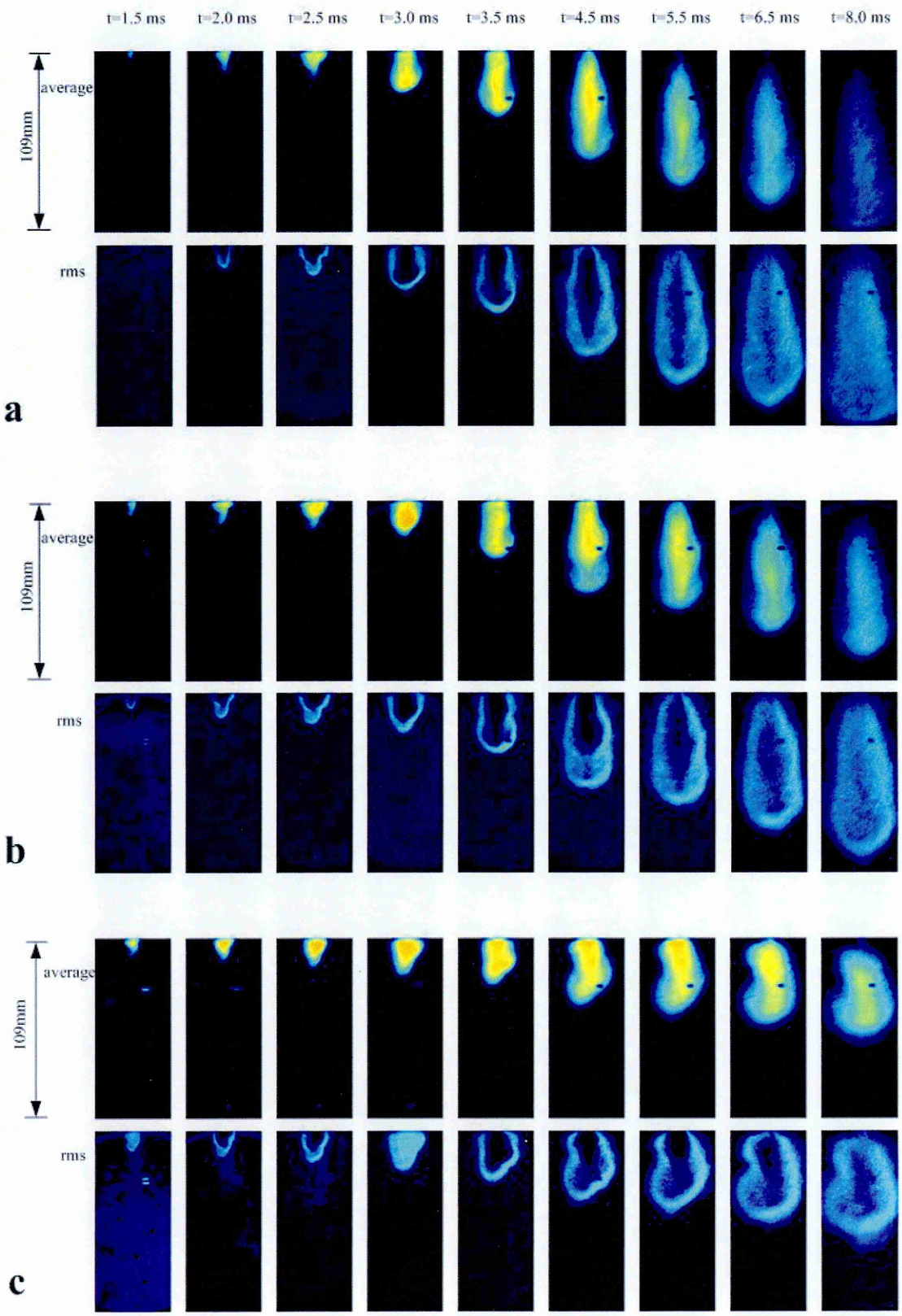

Figure IV-V. LPG spray of injector nr 1 in with injection pressure of 20 bar (a), 15 bar (b) and 10 bar (c)

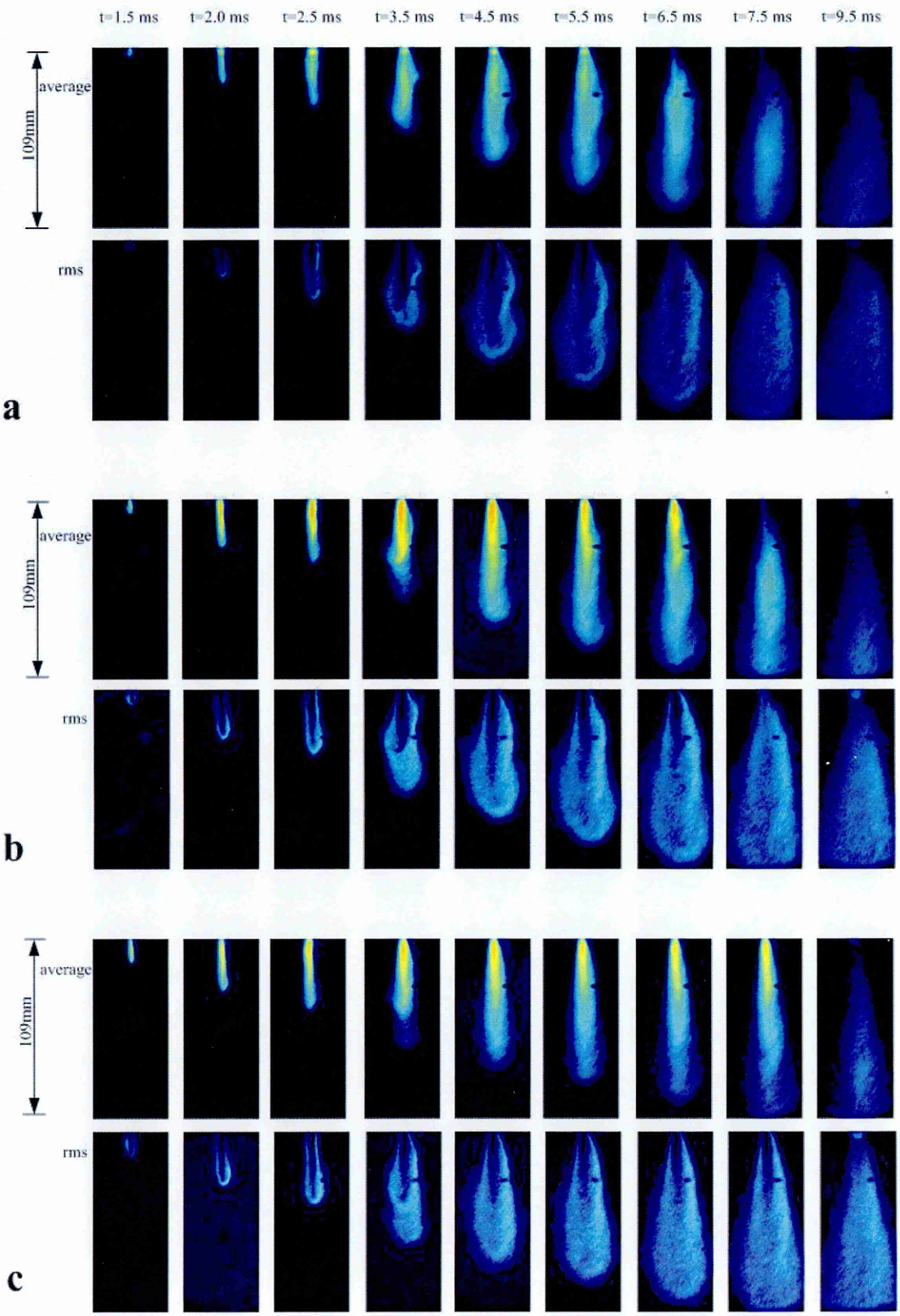

Figure IV-VI. LPG spray of injector nr 2 in with injection pressure of 20 bar (a), 15 bar (b) and 10 bar (c)

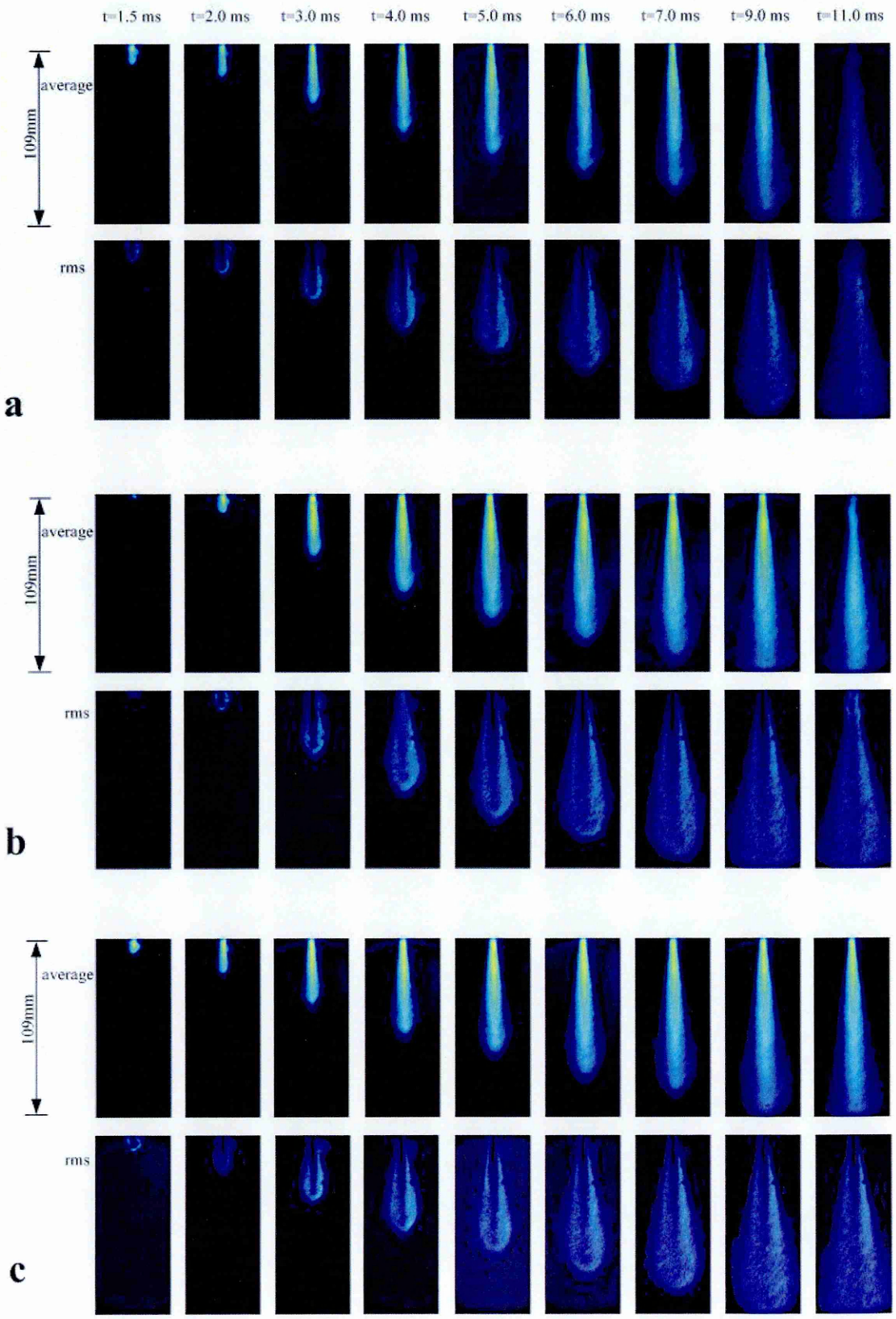

Figure IV-VII. LPG spray of injector nr 3 in with injection pressure of 20 bar (a), 15 bar (b) and 10 bar (c)

This indicates that the injector coil charging takes approximately 1.3 ms. Please note that the term ASOI used in the discussion later refers to the time elapsed after the start of the injection pulse, and not to the start of mechanical opening of the injector. Also, the interval between the time-steps varies between injectors due to varying injection duration. Images show consistent spray behaviour. In the case of highest flow rate injector (Figure IV-V), the spray velocity is higher at higher injection pressures. While the spray penetration depth is higher at higher injection pressures, the spray is wider in lower injection pressures. The image sequence for a 20 bar injection pressure shows the change in rms variation geometry during injection. The injector closes at approximately 4.0 ms. Prior to this, the rms images show strong variation at the edges of the spray, and no variation in the core of the spray. After injector closing, the rms value through the spray becomes gradually more uniform as the image average intensity decreases. In the last image of the sequence, 4 ms after the injector has closed, both the average intensity and rms images show nearly uniform counts throughout the spray area indicating a high proportion of vapour phase fuel.

Figure IV-VI shows images of spray through smaller and different shape of injector orifice. The first observation is the uneven structure of the spray, which is a clear indication of an unsymmetrical conicity of the orifice. Injection pressure does not have as strong an influence on spray penetration and structure as it has in the case of larger injector orifice area. The images representing rms variation through the spray suggest that the proportion of vapour, and the degree of turbulence, is significantly higher than in larger orifice injectors. The spray is narrower, but the area of high rms variation is wider and though the area of no rms variation is present, it is clearly narrower than the high variation area. This indicates that the fuel vaporises faster and the degree of turbulence is higher, as a result of the smaller injector orifice diameter.

This spray behaviour is even more evident in the images taken of the spray through injectors with the smallest orifice area. The spray is a narrow jet with a wide mixing zone at the tip of the spray. Rms variation is not very strong near to the injector tip, and the narrow low variation zone penetrates only approximately 40 mm. The spray penetration does not show significant variation between different injectors. Image intensity in the centre of the sprays tends to be higher in lower injection pressures

especially in the case of two larger orifice injectors, which could be explained by the wider liquid spray zone resulting in stronger light refraction.

IV.4.2 Parametric study of PCLIS

As mentioned earlier in this chapter, the mixing dynamics is rather different in the pipe-coupled LPG injection system due to fuel vaporisation, injector pulsation and consequent pressure fluctuation in the pipe and fluid travelling time. Using the same optical measurement system, the injectors were now mounted on a separate rail above the pressure chamber and connected with a pipe to the top of the chamber. To study the complicated fluid transport mechanism, the injectors were pulsed at a frequency typical to a SI engine, and images were acquired during the entire cycle. The effect of several parameters (injector orifice diameter, injection frequency, injection pressure and pipe diameter were investigated. Detailed injector system configurations are shown in Table IV-III.

Table IV-III. PCLS injection parameters

nr	Orifice diameter [μm]	Orifice shape	Injection frequency [Hz]	Injection pressure [bar]	Injection duration [ms]	Pipe diameter [mm]	Config nr
1	500	a	15	20	2.2	1.2	1
						2	2
						4	3
				15	2.5	1.2	4
						2	5
						4	6
				10	3.1	1.2	7
						2	8
						4	9
			25	15	2.5	1.2	10
						2	11
						4	12
2	250	b	15	15	5.5	1.2	13
						2	14
3	200	c	15	20	7.2	1.2	15
						2	16
				15	8.3	1.2	17
						2	18
				10	10.1	1.2	19
						2	20
			25	15	8.3	1.2	21
						2	22

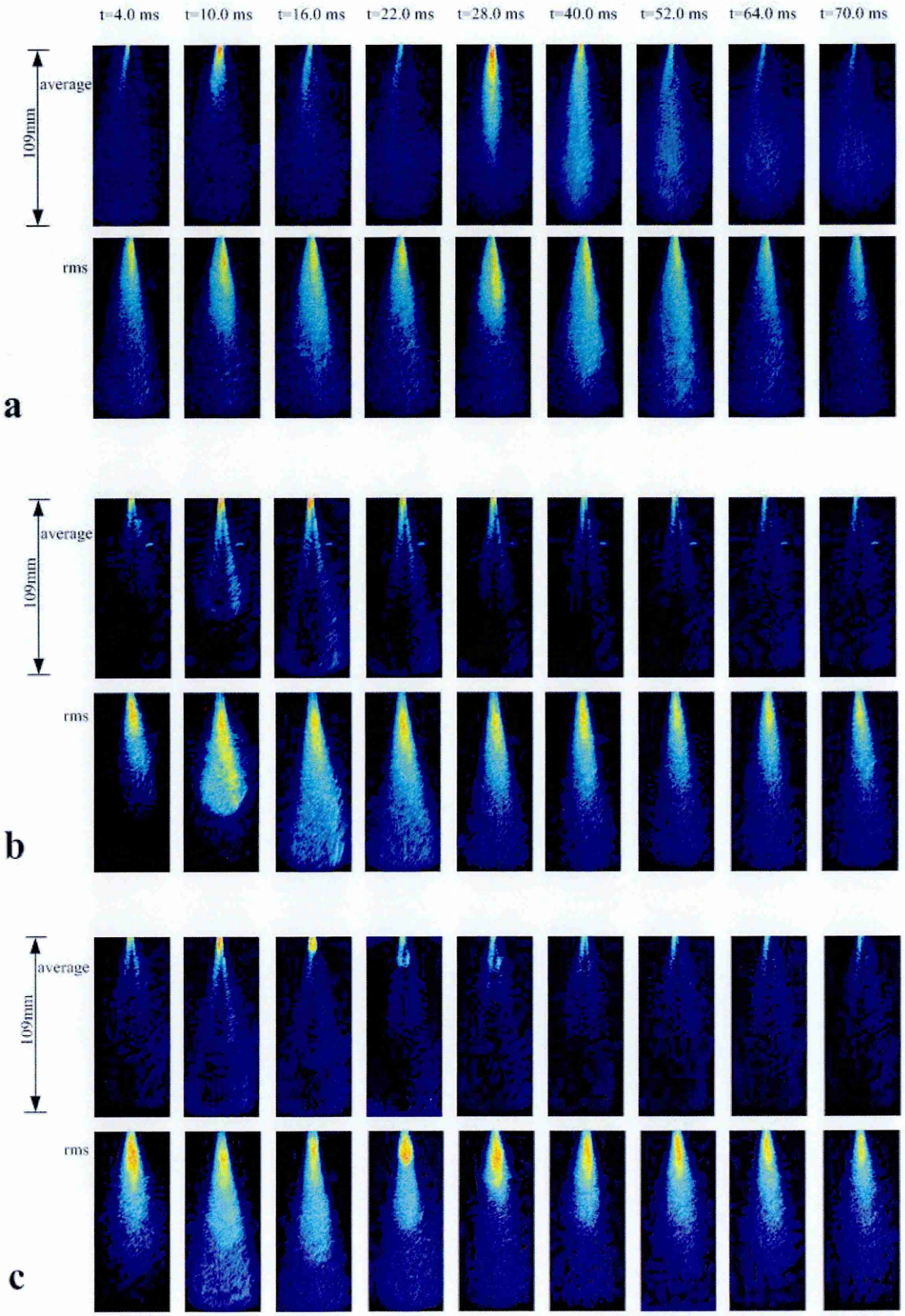

Figure IV-VIII. LPG spray of injector nr 1 with injection pressure of 15 bar and with pipe diameter 1.2mm (a), 2mm (b) and 4mm (c)

The images of the fuel spray using three different pipe diameters (injector 1 with injection pressure 15 bar and frequency of 15 Hz) are shown in Figure IV-VIII. The average images show significant differences in both spray pattern and intensity between the three pipe diameters, the larger diameter pipes having a hollow spray. The rms image does not indicate similar tendencies to the CCLIS case. The magnitude of variation is high through the spray, only in 2 mm and 4 mm pipe cases when the image intensity is high, there is a clear area of very low rms variation, which indicates the presence of liquid fuel and a low level of turbulence. Irregular temporal variations of the images indicate inconsistent flow transport properties in the pipe, which might be a result of small temporal variations in pipe temperatures or propagation of pressure waves, which consequently affects significantly to fuel vaporisation, density and velocity in the pipe.

Figure IV-X shows 20 consecutive background compensated images taken at the pipe-exit in two cases. The images were taken at the last time-step of the cycle, which in this case was 6 ms before the start of next injection. The images on the right have been taken with smallest pipe diameter, and they show higher cycle-to-cycle variation than the images on the left, take with largest pipe diameter. Considering engine operation, the end of the cycle variation is the most critical since it indicates that there is varying amount of fuel reaching the cylinder each cycle due to continuous, but varying density flow through the pipes. Another important observation is the apparent fuel flow at the pipe exit through the entire cycle. Even though in each pipe diameter there is a high intensity period in the early part of the cycle, the fuel flow continues until the new cycle starts. The irregular flow and the fuel continuously emerging from the pipe result in having less control over the AFR and mixing, though how significant this is, depends on the magnitude of the variation.

As a result of these observations the image processing method was further refined to measure the intensity and variation between 40 consequent images. A small area in the image, shown in Figure IV-IX, in the region of the pipe exit was extracted. The new image array was defined as $M = x[e]$, where e refers to the size of the array. An average intensity (Equation IV-XII) of the background-compensated image M was calculated ($\bar{x}_M$). This value was averaged through 40 images (Equation IV-XIII) to

obtain $\bar{x}_j$. The rms variation of the average intensity through 40 images (rms_j) was calculated (Equation IV-XIV). Equation IV-XV defines the maximum intensity $\bar{x}_M{}^{max}$, minimum intensity $\bar{x}_M{}^{min}$ can be obtained similarly.

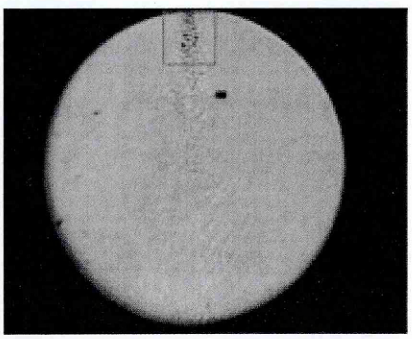

Figure IV-IX. Spray area at the pipe exit used in calculations

$$\bar{x}_M = \frac{1}{N_e}\sum_{i=1}^{N_e} x_i \qquad \textbf{Equation IV-XII}$$

$$\bar{x}_j = \frac{1}{N_j}\sum_{i=1}^{N_j} \bar{x}_{M_i} \qquad \textbf{Equation IV-XIII}$$

$$rms_j = \sqrt{\frac{1}{N_j}\sum_{i=1}^{N_j}\left(\bar{x}_{M_i} - \bar{x}_j\right)^2} \qquad \textbf{Equation IV-XIV}$$

$$\bar{x}_M{}^{max} = \max\left\{\bar{x}_{M_1} \ldots \bar{x}_{M_{Nj}}\right\} \qquad \textbf{Equation IV-XV}$$

Figure IV-XI to Figure IV-XVII represent the results of average intensity and variation calculations for each injector system configuration. The bar chart on the left shows $\bar{x}_j$ (black bar), $\bar{x}_M{}^{max}$ (grey bar) and $\bar{x}_M{}^{min}$ (white bar) for each time step over one complete cycle. The bar chart on the right shows the rms_j value for each time step. It should be noted that the intensity counts on the y-axis of the charts are presented purely for comparison purposes, because they do not contain easily interpretable information on quantitative measure of fuel density. However, it is assumed here that the fuel emerging from the pipes is both liquid and vapour and the image intensity is proportional to the fuel spray concentration, even though it is appreciated that the image intensity depends also on the level of turbulence and temperature variations.

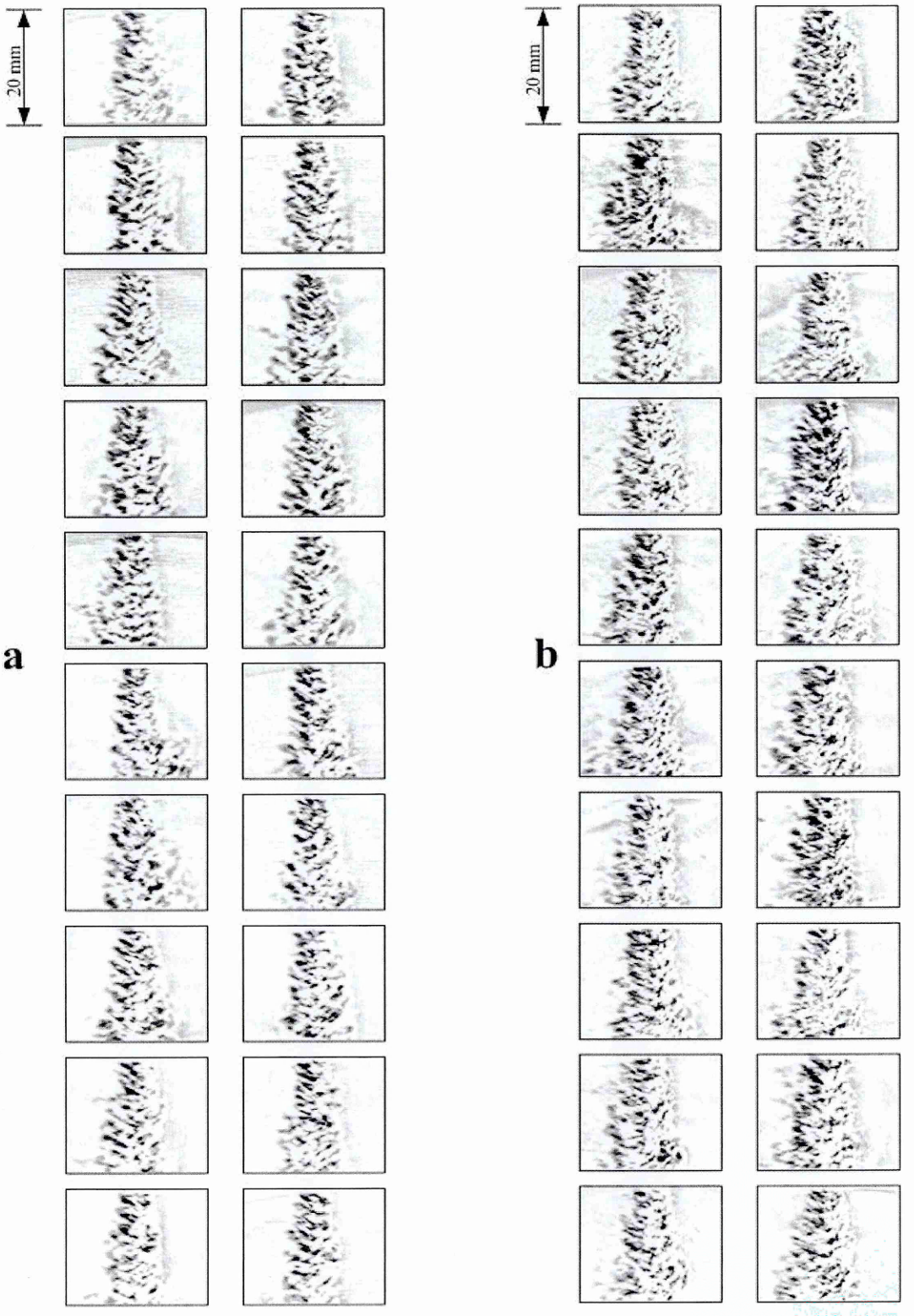

Figure IV-X. Fluctuation in image intensities with pipe diameter of 4mm (a) and 1.2mm (b). Images 6 ms before start of next injection.

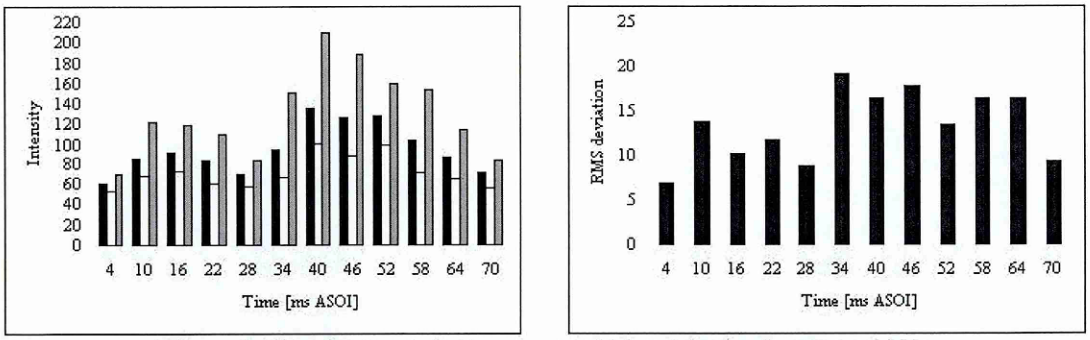

Injector: 3, Pipe: 1.2 mm, Injection pressure: 10 bar, Injection frequency: 15 Hz

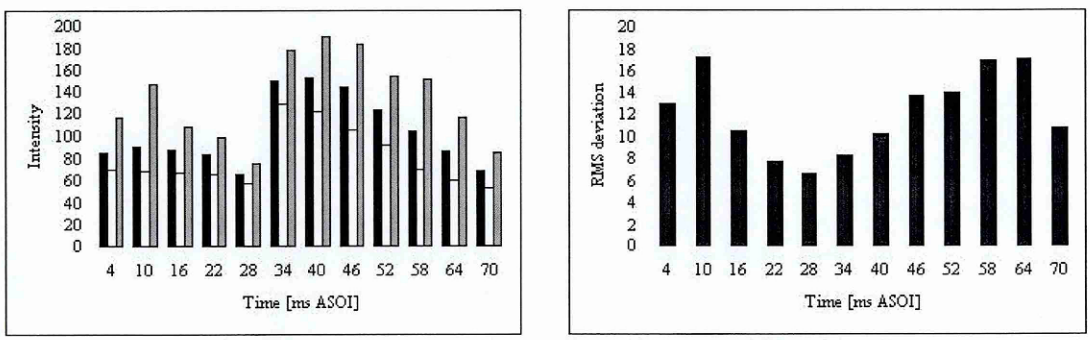

Injector: 3, Pipe: 1.2 mm, Injection pressure: 15 bar, Injection frequency: 15 Hz

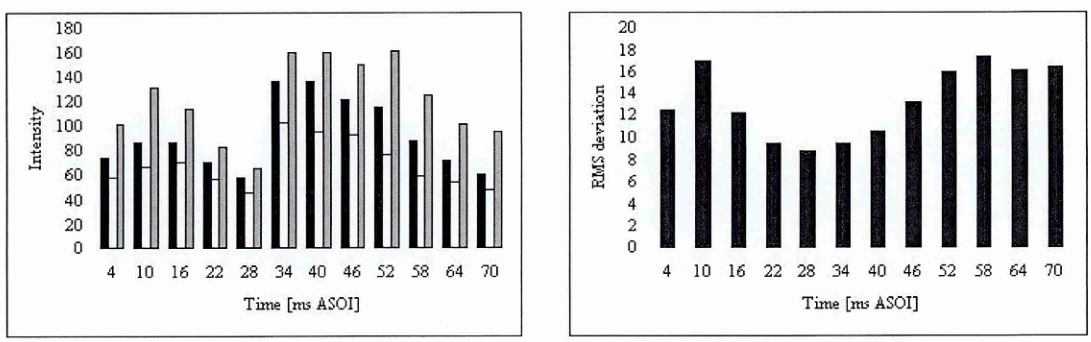

Injector: 3, Pipe: 1.2 mm, Injection pressure: 20 bar, Injection frequency: 15 Hz

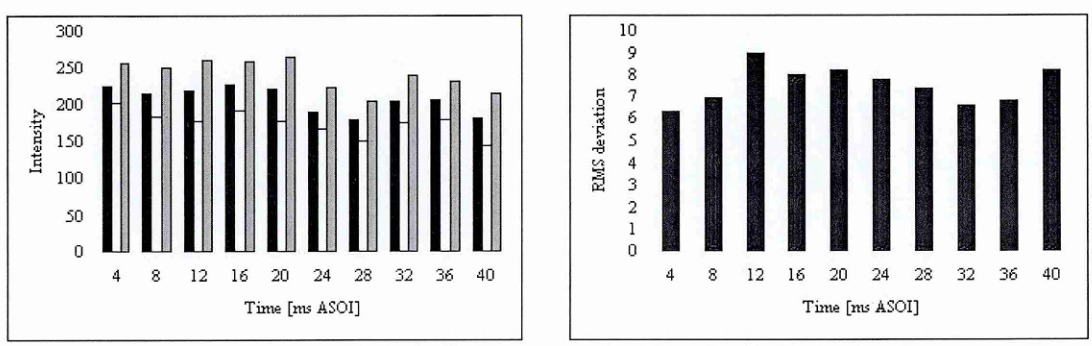

Injector: 3, Pipe: 1.2 mm, Injection pressure: 15 bar, Injection frequency: 25 Hz

Figure IV-XI. Average ($\bar{x}_j$), minimum ($\bar{x}_M^{\min}$) and maximum ($\bar{x}_M^{\max}$) intensity at the pipe exit on the left and rms deviation (rms_j) on the right. Injector 3, Pipe 1.2 mm.

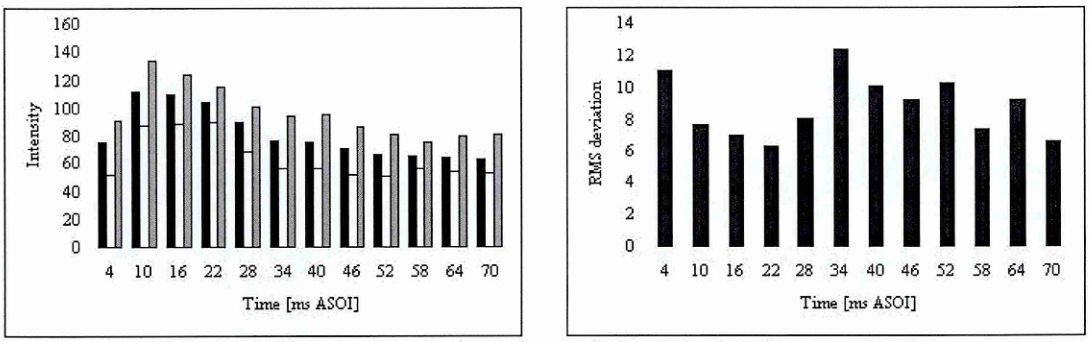

Injector: 3, Pipe: 2 mm, Injection pressure: 10 bar, Injection frequency: 15 Hz

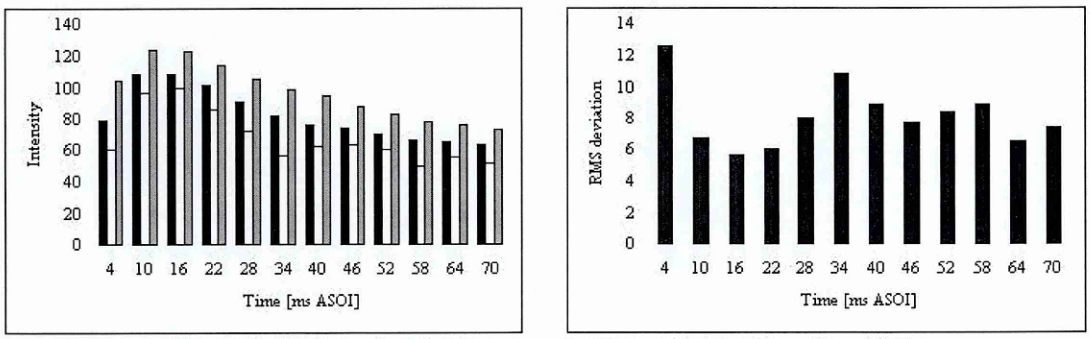

Injector: 3, Pipe: 2 mm, Injection pressure: 15 bar, Injection frequency: 15 Hz

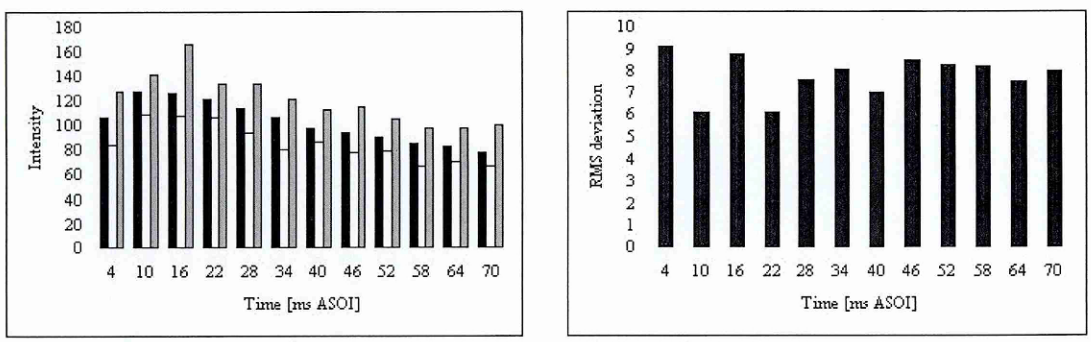

Injector: 3, Pipe: 2 mm, Injection pressure: 20 bar, Injection frequency: 15 Hz

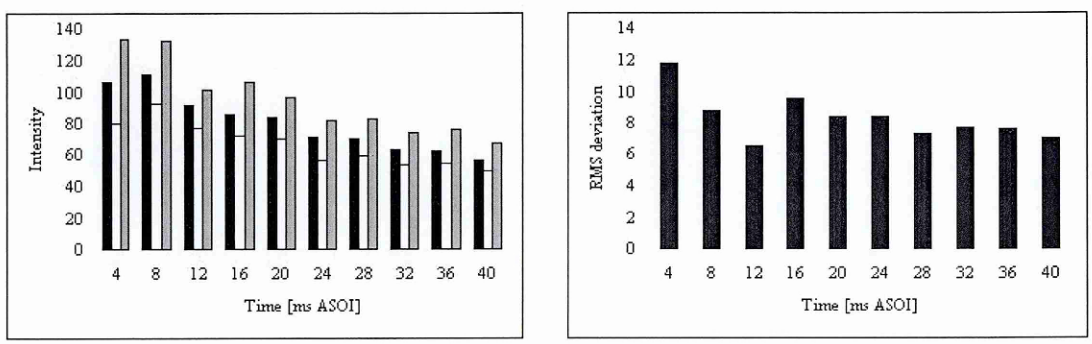

Injector: 3, Pipe: 2 mm, Injection pressure: 15 bar, Injection frequency: 25 Hz

Figure IV-XII. Average ($\bar{x}_j$), minimum ($\bar{x}_M^{\min}$) and maximum ($\bar{x}_M^{\max}$) intensity at the pipe exit on the left and rms deviation (rms_j) on the right. Injector 3, Pipe 2 mm.

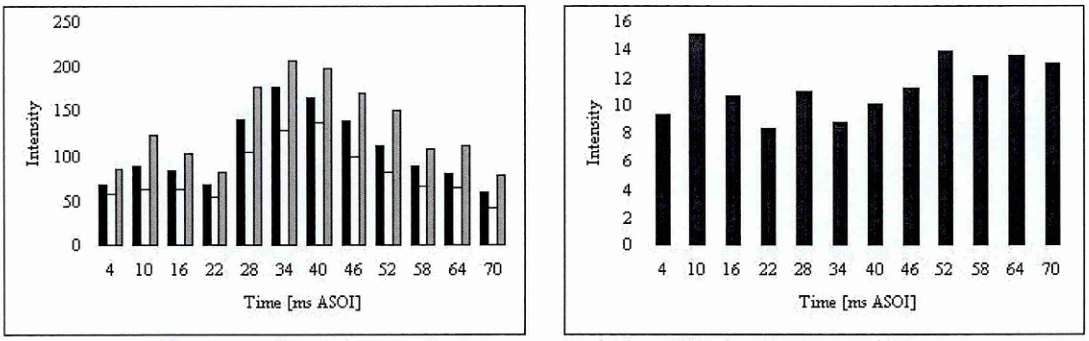

Injector: 2, Pipe: 1.2 mm, Injection pressure: 15 bar, Injection frequency: 15 Hz

Figure IV-XIII. Average ($\bar{x}_j$), minimum ($\bar{x}_M^{\min}$) and maximum ($\bar{x}_M^{\max}$) intensity at the pipe exit on the left and rms deviation (rms_j) on the right. Injector 2, Pipe 1.2 mm.

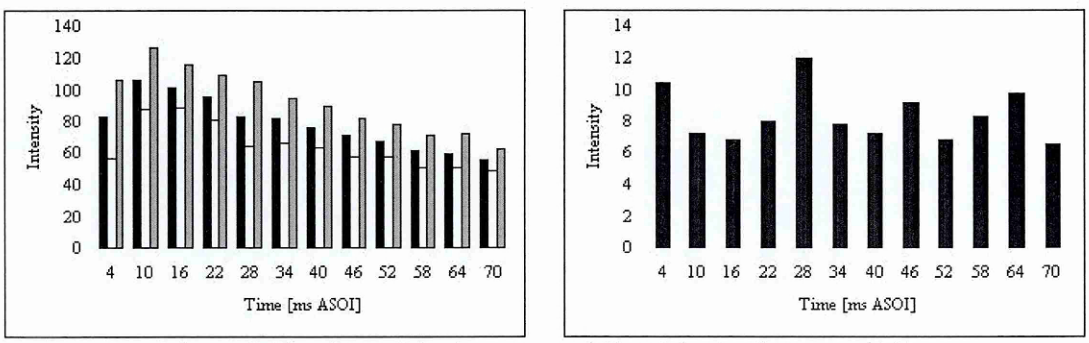

Injector: 2, Pipe: 2 mm, Injection pressure: 15 bar, Injection frequency: 15 Hz

Figure IV-XIV. Average ($\bar{x}_j$), minimum ($\bar{x}_M^{\min}$) and maximum ($\bar{x}_M^{\max}$) intensity at the pipe exit on the left and rms deviation (rms_j) on the right. Injector 3, Pipe 2 mm.

The data shows clearly that for all injector system configurations there are temporal variations in fuel concentration through the injection period. It is evident that in all cases fuel flow entering the measurement region is in two phases; strong variations in image illumination intensity suggest presence of fuel of varying concentration. Plots indicate that in the case of the smallest diameter pipe the concentration of fuel entering the chamber is higher than in the case of 2 and 4 mm pipes. Also, highest density fuel exits the pipe later in the injection period. Further, this behaviour is consistently independent of injection pressure or injector flow area. Therefore, it is assumed that the length of the travelling time is dominated be the vaporisation; the expanding vapour expels the liquid slugs in the pipe. It is also noted that the pipe length would obviously have an effect on the travelling time.

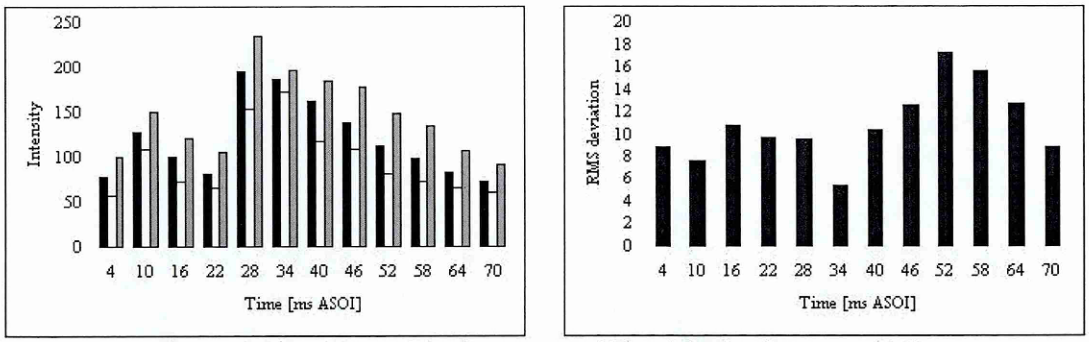

Injector: 1, Pipe: 1.2 mm, Injection pressure: 10 bar, Injection frequency: 15 Hz

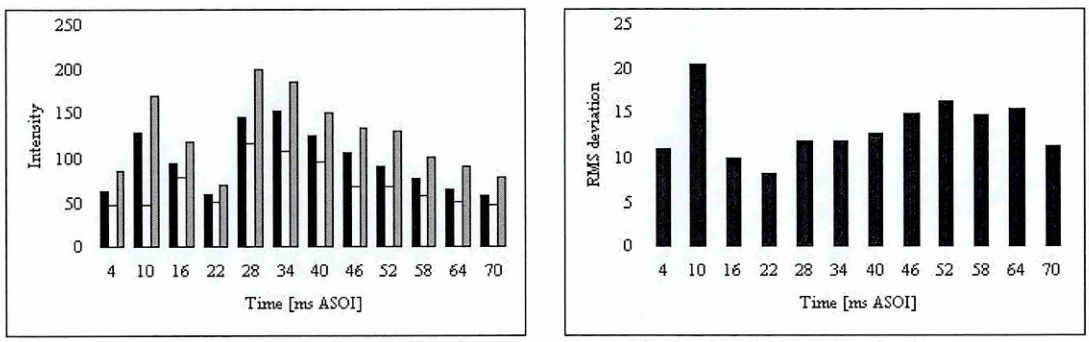

Injector: 1, Pipe: 1.2 mm, Injection pressure: 15 bar, Injection frequency: 15 Hz

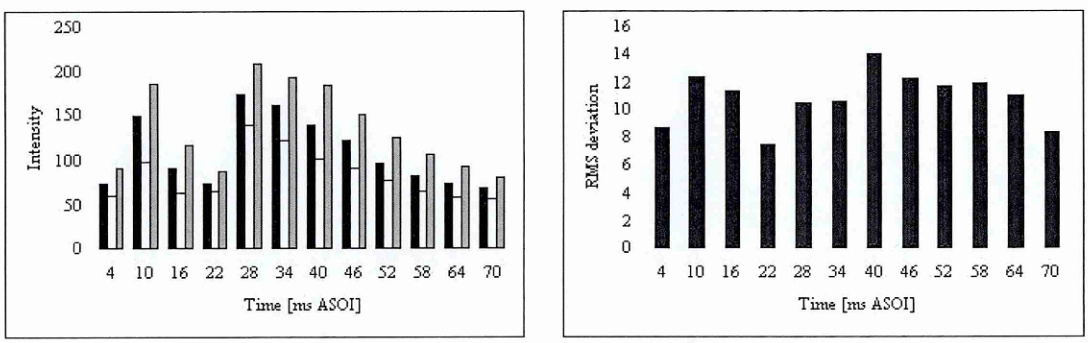

Injector: 1, Pipe: 1.2 mm, Injection pressure: 20 bar, Injection frequency: 15 Hz

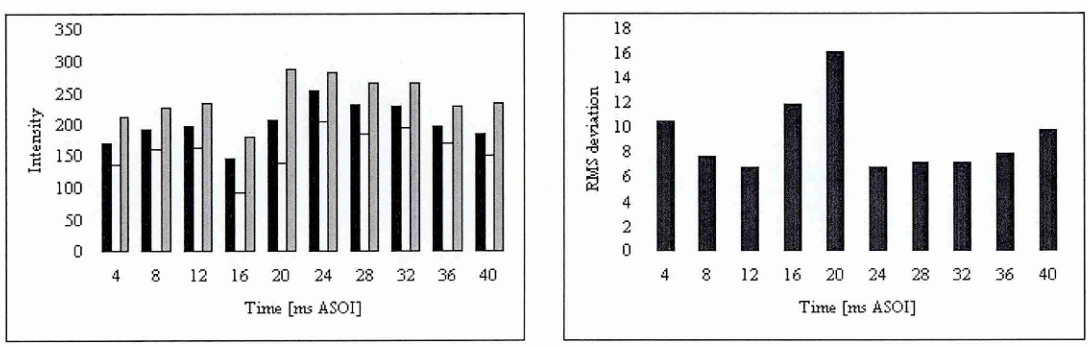

Injector: 1, Pipe: 1.2 mm, Injection pressure: 15 bar, Injection frequency: 25 Hz

Figure IV-XV. Average ($\bar{x}_j$), minimum ($\bar{x}_M^{\min}$) and maximum ($\bar{x}_M^{\max}$) intensity at the pipe exit on the left and rms deviation (rms_j) on the right. Injector 1, Pipe 1.2 mm.

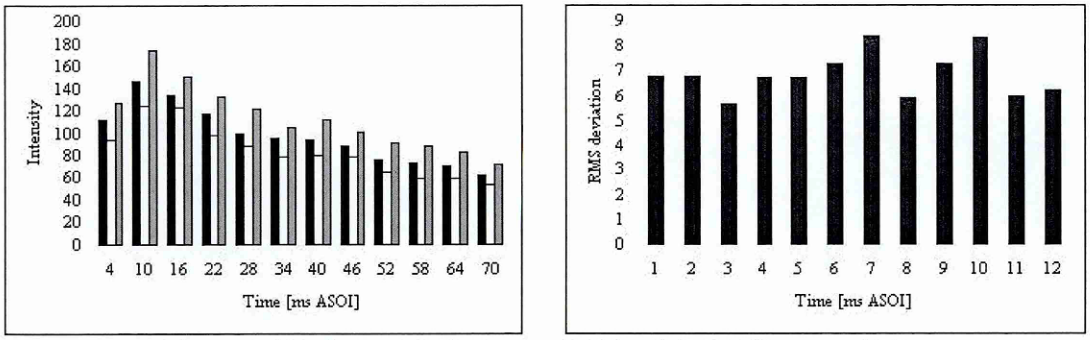

Injector: 1, Pipe: 2 mm, Injection pressure: 10 bar, Injection frequency: 15 Hz

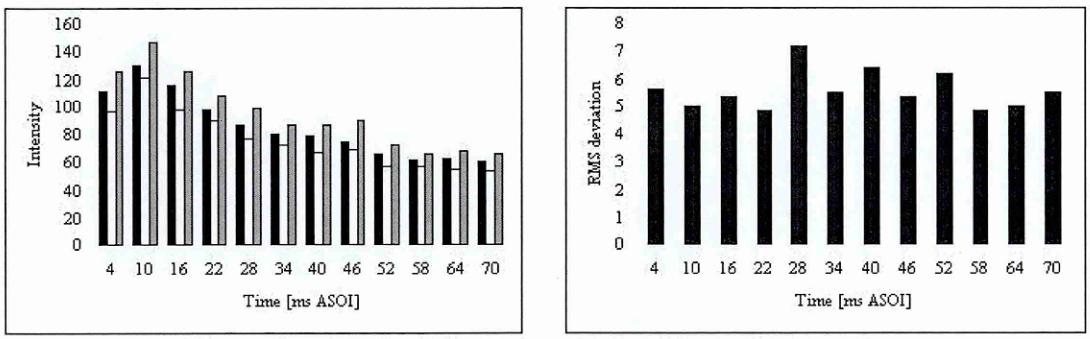

Injector: 1, Pipe: 2 mm, Injection pressure: 15 bar, Injection frequency: 15 Hz

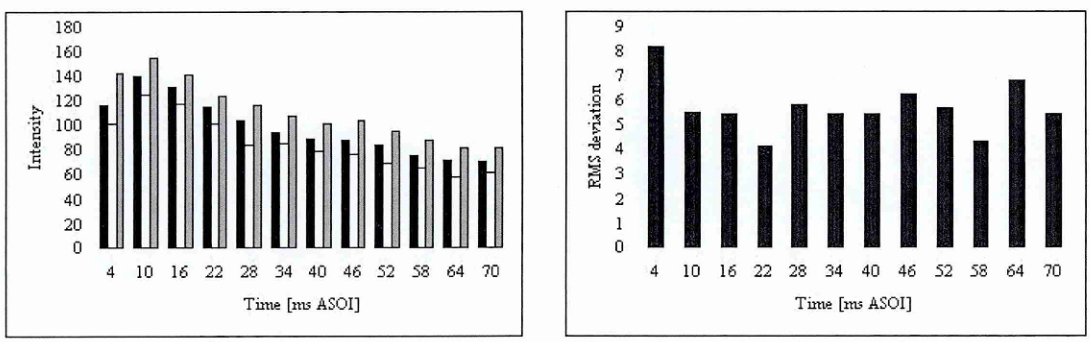

Injector: 1, Pipe: 2 mm, Injection pressure: 20 bar, Injection frequency: 15 Hz

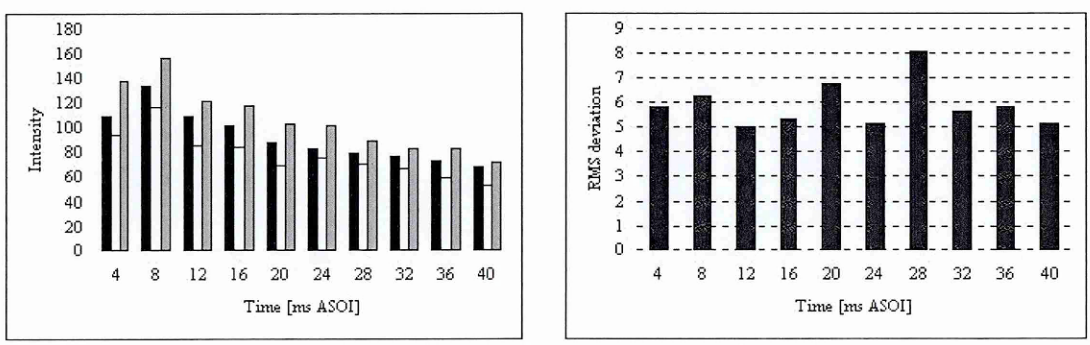

Injector: 1, Pipe: 2 mm, Injection pressure: 15 bar, Injection frequency: 25 Hz

Figure IV-XVI. Average ($\bar{x}_j$), minimum ($\bar{x}_M^{\min}$) and maximum ($\bar{x}_M^{\max}$) intensity at the pipe exit on the left and rms deviation (rms_j) on the right. Injector 1, Pipe 2 mm.

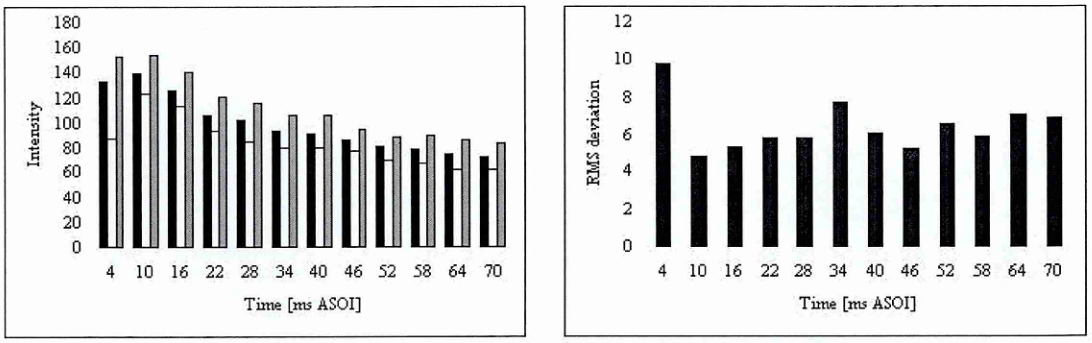

Injector: 1, Pipe: 4 mm, Injection pressure: 10 bar, Injection frequency: 15 Hz

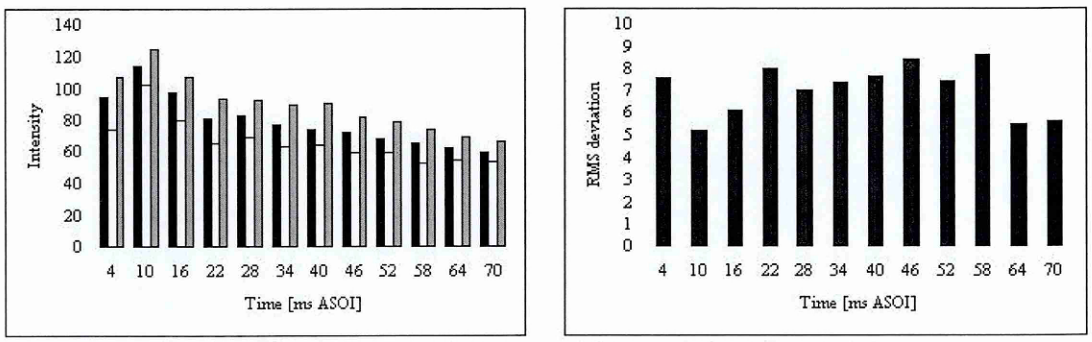

Injector: 1, Pipe: 4 mm, Injection pressure: 15 bar, Injection frequency: 15 Hz

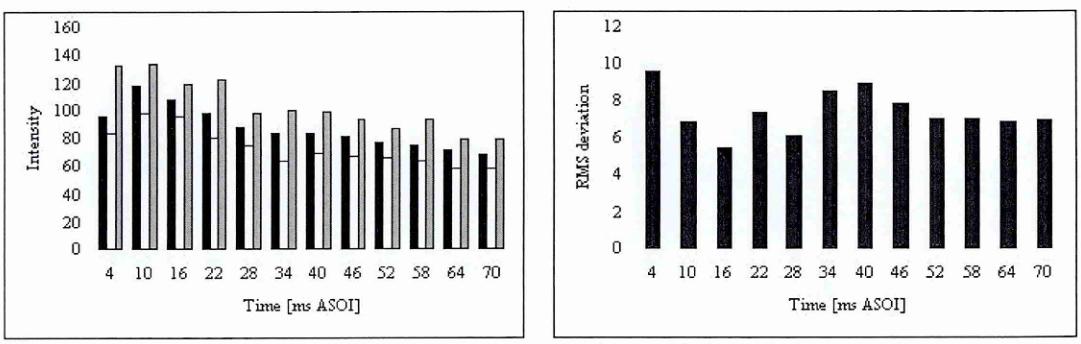

Injector: 1, Pipe: 4 mm, Injection pressure: 20 bar, Injection frequency: 15 Hz

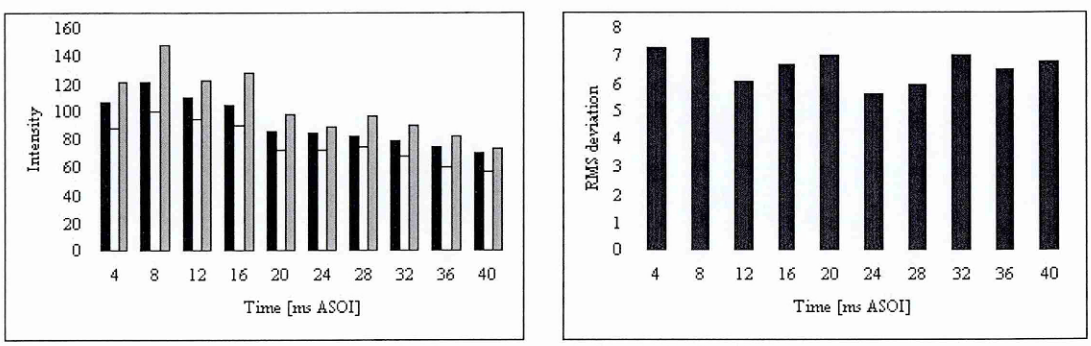

Injector: 1, Pipe: 4 mm, Injection pressure: 15 bar, Injection frequency: 25 Hz

Figure IV-XVII. Average ($\bar{x}_j$), minimum ($\bar{x}_M^{\min}$) and maximum ($\bar{x}_M^{\max}$) intensity at the pipe exit on the left and rms deviation (rms_j) on the right. Injector 1, Pipe 4 mm.

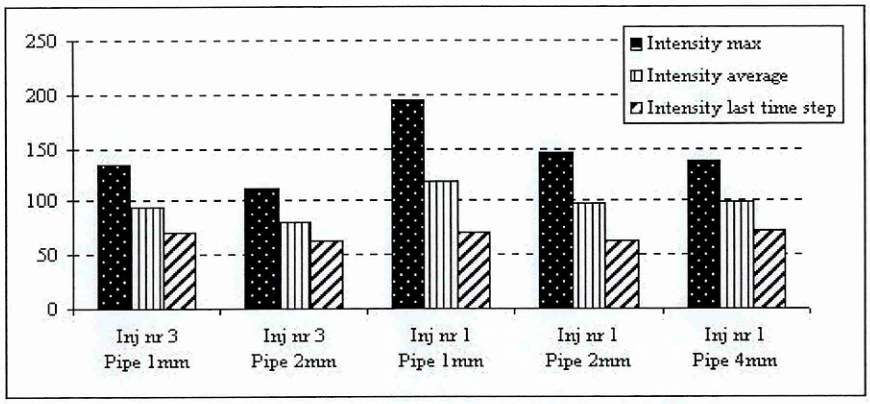

Injection pressure: 10 bar, injection frequency: 15 Hz

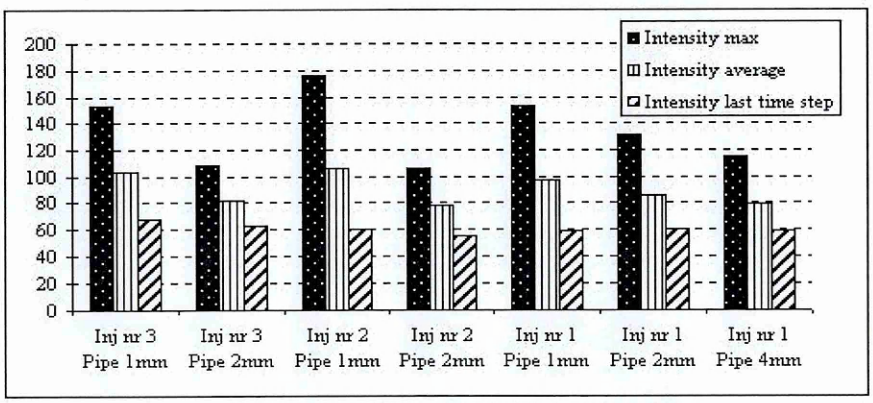

Injection pressure: 15 bar, injection frequency: 15 Hz

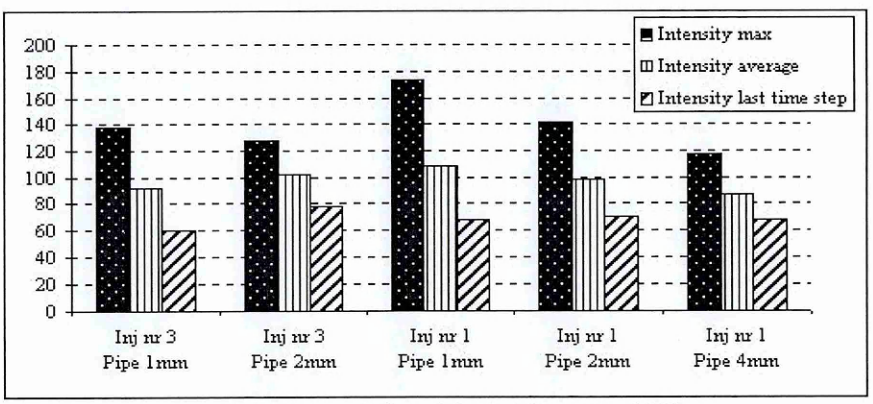

Injection pressure: 20 bar, injection frequency: 15 Hz

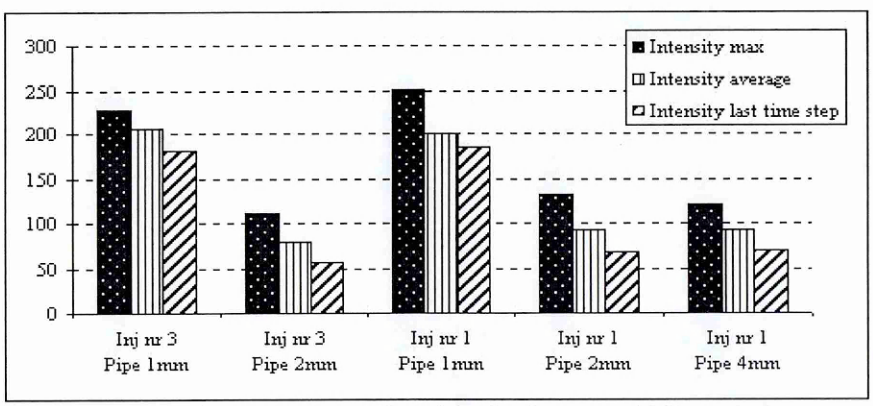

Injection pressure: 15 bar, injection frequency: 25 Hz

Figure IV-XVIII. Summary of cycle-average intensities ($\bar{x}_t$, $\bar{x}_j^{t=10/12}$ and $\bar{x}_j^{\max}$) at pipe exit

These observations suggest that the fuel travelling through the smaller diameter pipes vaporises less on its way than the fuel travelling through larger diameter pipes. A larger proportion of fuel is liquid and fuel velocity is consequently lower resulting in longer fluid travelling times. Increasing injector flow rate by increasing the injector orifice area results in shorter travelling time, though intensities are also higher for higher flow rate injectors. Variation is stronger in smaller pipes, especially in higher frequency. For larger diameter pipes increasing frequency does not seem to have much effect, neither does injection pressure.

The information on the average intensity through the entire injection cycle is presented for each injection pressure in Figure IV-XVIII. Each time step is referred as $t = 10$ (injector frequency 25 Hz) or $t = 12$ (injector frequency 15 Hz). The mathematical expression for total average intensity during the injection period ($\bar{x}_t$) is presented in Equation IV-XVI. Average intensity at last time step ($\bar{x}_j^{t=10/12}$, Equation IV-XVII) and maximum average intensity during injection cycle ($\bar{x}_j^{\max}$, Equation IV-XVIII) are also shown in the figure for each injector system configuration.

$$\bar{x}_t = \frac{1}{N_t}\sum_{i=1}^{N_t}\bar{x}_{j_i} \qquad \textbf{Equation IV-XVI}$$

$$\bar{x}_j^{\,t=10/12} = \bar{x}_{j_{t=10/12}} \qquad \textbf{Equation IV-XVII}$$

$$\bar{x}_j^{\,\max} = \max\left\{\bar{x}_{j_1} \ldots \bar{x}_{j_{N_t}}\right\} \qquad \textbf{Equation IV-XVIII}$$

The cycle-averaged intensity calculations show similar evidence of fuel flow characteristics to Figure IV-XI - Figure IV-XVII. The smaller the pipe diameter the higher is the maximum, and also the average image intensity. Also, the higher the injector flow rate, the higher the maximum liquid fuel concentration, though there does not seem to be a significant difference in cycle average intensity. In higher injection frequency the flow through the smallest diameter pipes indicates high liquid fuel concentration through entire cycle, and the intensity in the last time-step is significantly higher than larger diameter pipes.

The summary of the variation for each pipe diameter is shown in Figure IV-XIX. Variation is expressed in terms of rms average through entire cycle on x-axis in the figures above, maximum rms value encountered during the cycle on left and rms

variation on the last time-step before the start of next injection, $t = 70ms$ ASOI or $t = 40ms$ ASOI on right. The expressions for these values are presented in Equations IV-XIX – IV-XXI). The plots below show the corresponding values of minimum and maximum intensities (Equations IV-XXII – IV-XXIV).

Similarly, Figure IV-XX shows the magnitude of the intensity variation, but plotted for each injector. The plots are presented only for pipe diameter 2 mm and 4 mm, since the results in Figure IV-XIX indicated that the cycle-to-cycle variation for the smallest pipe diameter was unacceptably high, and the figures would not give a clear indication of variation being a function of the injector flow rate.

$$\overline{rms_t} = \frac{1}{N_t}\sum_{i=1}^{N_t} rms_{j_i}$$ **Equation IV-XIX**

$$rms^{\max} = \max\left\{rms_{j_1} \ldots rms_{j_{N_t}}\right\}$$ **Equation IV-XX**

$$rms^{t=10/12} = rms_{j_{t=10/12}}$$ **Equation IV-XXI**

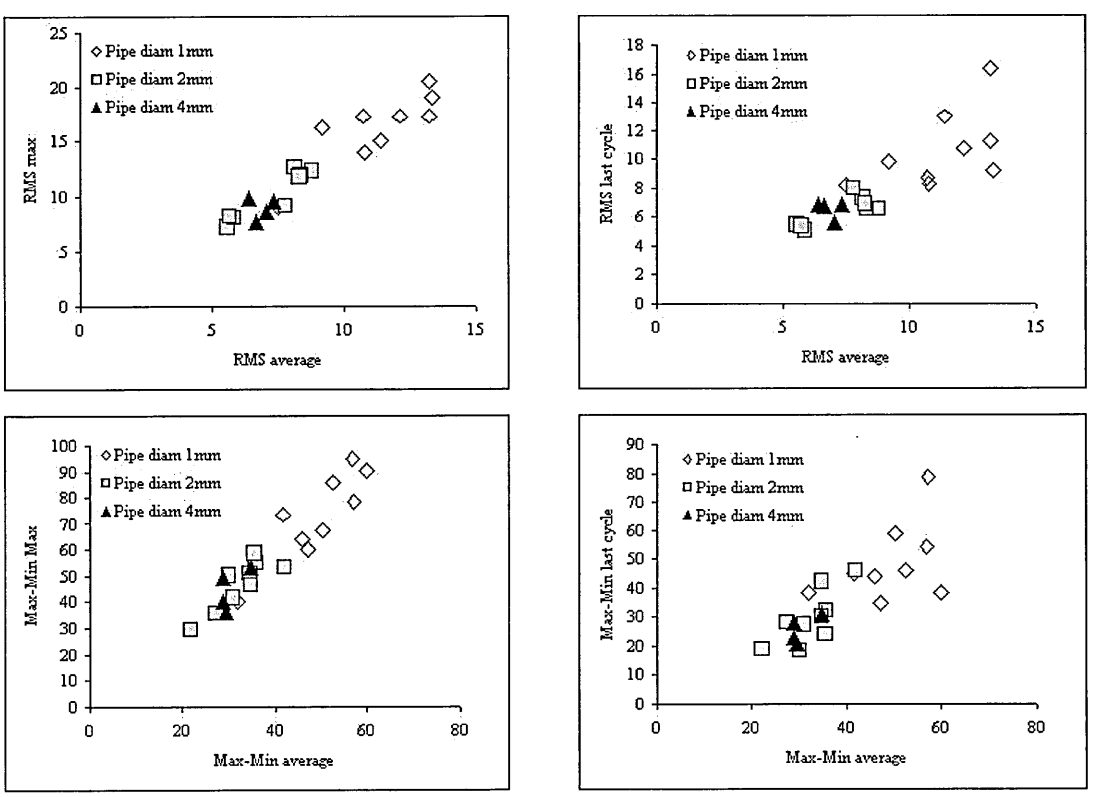

Figure IV-XIX. Summary of intensity fluctuation at pipe exit for each pipe diameter

$$(\max-\min)^{\max} = \max\left\{(\bar{x}_M{}^{\max} - \bar{x}_M{}^{\min})_1 \ldots (\bar{x}_M{}^{\max} - \bar{x}_M{}^{\min})_{N_t}\right\} \qquad \textbf{Equation IV-XXII}$$

$$\overline{(\max-\min)}_t = \frac{1}{N_t}\sum_{i=1}^{N_t}(\bar{x}_M{}^{\max} - \bar{x}_M{}^{\min})_i \qquad \textbf{Equation IV-XXIII}$$

$$(\max-\min)^{t=10/12} = (\bar{x}_M{}^{\max} - \bar{x}_M{}^{\min})_{t=10/12} \qquad \textbf{Equation IV-XXIV}$$

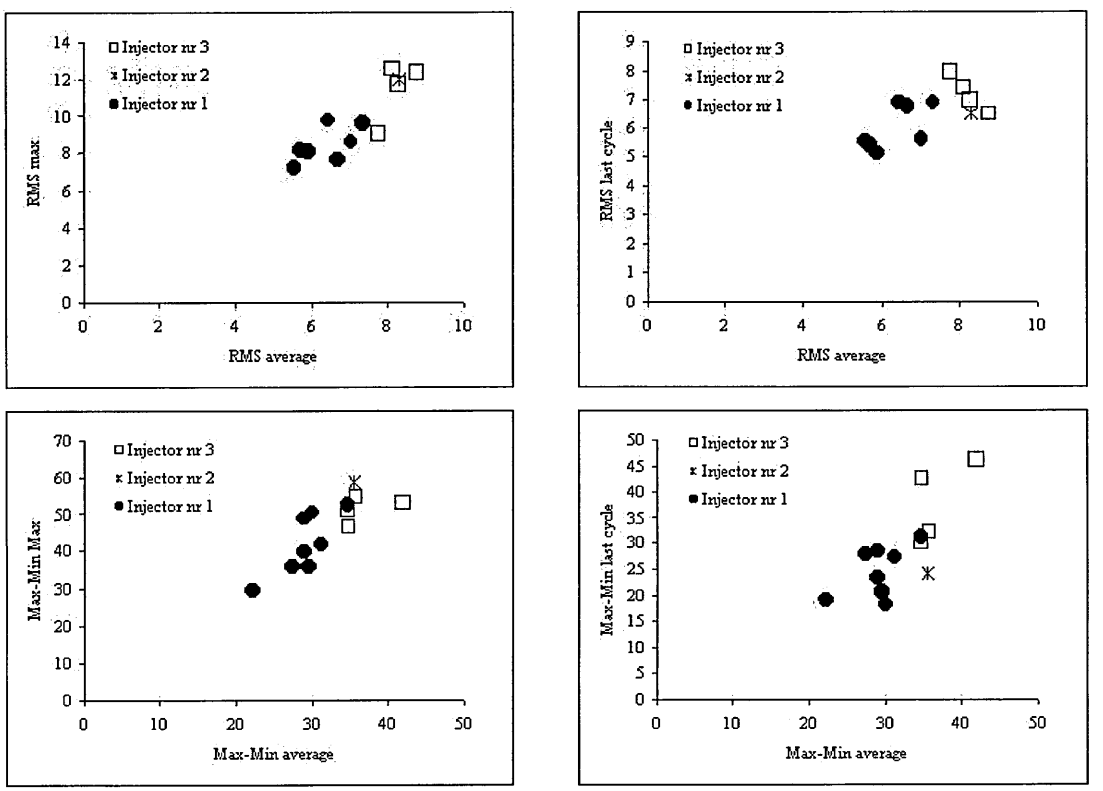

Figure IV-XX. Summary of intensity fluctuation at pipe exit for each injector

As mentioned earlier, the magnitude of intensity variation is clearly highest when the fuel is introduced to the measurement area through the smallest pipes. However, similar tendency is not evident for the larger pipes; the variation does not seem very different between pipes of diameter 2 mm and 4 mm (Figure IV-XIX). In order to understand the significant factors causing variations in the larger diameter sizes, the corresponding values were plotted for each injector orifice diameter, ignoring the smallest diameter pipe measurements (Figure IV-XX). The results show a clear tendency again, the smaller orifice diameter and hence lower flow rate injectors have higher rms and max-min variations.

IV.5 DISCUSSION

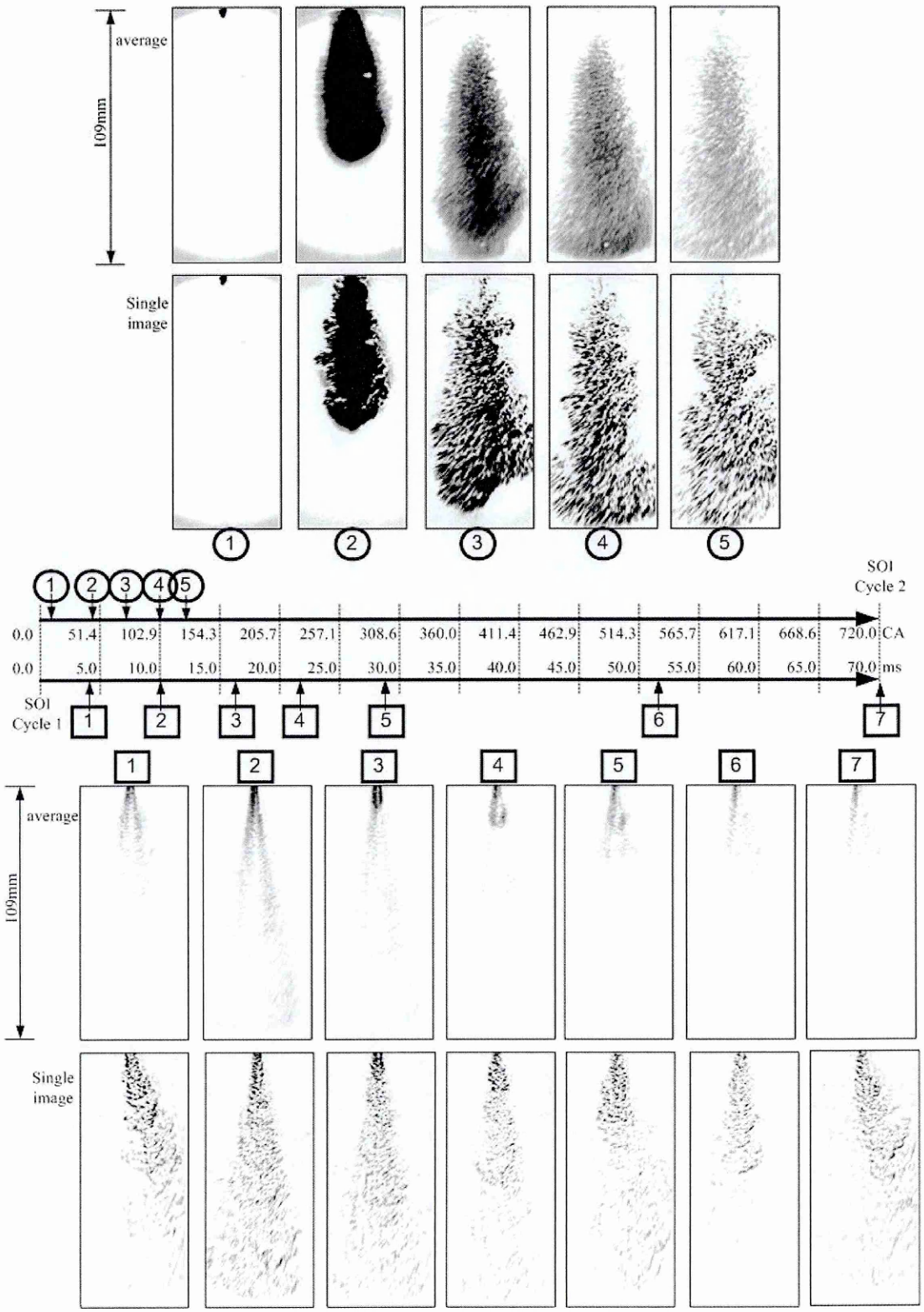

Figure IV-XXI. Comparison of CCLIS and PCLIS.

Figure IV-XXI illustrates the difference between CCLIS and PCLIS injection methods. Here, the images of fuel spray in both configurations are scaled to the same intensity resolution and comparative measures on the fuel concentration are obtained, even though it is emphasized here that the comparison includes an assumption that the arbitraries in image intensity due to the temperature and pressure variations are negligible. The fuel spray in the CCLIS spray (the image sequence above) and PCLIS (below) are also related to the injection timing representing a full 4-stroke engine cycle with sequential injection system. In this type of injection system, the fuel is injected to the inlet of each cylinder once in two engine cycles, or once in every 720° CA. Hence, the bar in the middle represents a full injection cycle. For reference, time in ms is also shown (corresponding engine speed of 1700 rpm).

Comparing mixture formation and fuel metering between the two fuel injection systems, two major observations are made. In CCLIS case, fuel enters the manifold in a few milliseconds, or a few degrees of CA, as in the case of PCLIS, the fuel continues entering the manifold the entire cycle, until the next injection. Also, partly as a consequence of the previous, the fuel enters the mixing volume (manifold) at higher density than in the case of PCLIS. These measures are significant for two reasons. First, the formation fuel-air mixture entering the cylinder has different mechanisms if the mixing takes place while both substances are in gaseous state, rather than mixing which occurs when one substance is vaporising. For this study, the stage of phase change is also significant considering the charge cooling effect. Secondly, there is a significant difference between the two injection processes on mixture control. In sequential MPI engines, the control of engine performance and pollutant emissions relies on fast and accurate fuel metering system. Considering this process, there is a significant advantage on introducing the fuel in the manifold in a relatively short period of time in order to assure that the fuel enters the engine cylinder in the same engine cycle. Clearly, in the case of PCLIS, accurate fuelling control becomes complicated because, even though the desired amount of fuel would enter the manifold inside one engine cycle, the feed-back from the oxygen sensor would not have an immediate effect on fuel metering. Also, fuel arriving in cylinder the cycle after it is injected leads to poor transient response. This, of course, becomes even more crucial in the presence of strong cycle-to-cycle variations, when the actual time of injection has an important effect on engine operation.

Also, the mixture concentration and uniformity depends on the mixing mechanism in the manifold. From the results presented in this it is expected that the charge in the cylinder might be more uniform with PCLIS, because of the continuous fuel flow. This however largely depends on the injection timing. With the CCLIS configuration, if enough time is allowed, the fuel fully evaporates in the manifold before entering the cylinder, which enhances the mixing (but reduces the charge cooling effect). The evaporation does not mean that the fuel vapour would be uniformly distributed with the intake air in the case of CCLIS, and is more likely in the case of PCLIS due to continuous fuel flow to the manifold and therefore the mixing is "spread" through the entire cycle (although there might be some temporal variations in the fuel density during the engine cycle). Another significant effect of continuous fuel flow entering the manifold is the possibility of backfires.

For the PCLIS, the three most important system responses affecting engine performance and pollutant emission formation are considered to be following:

1. Fuel concentration at the pipe exit
2. Fuel transport time through the pipe
3. Fuel concentration cycle-to-cycle variation

Since the image intensity scales with the density gradient, a comparative measure of liquid fuel concentration and hence the fuel density at the pipe exit can be obtained from the images. Fuel density entering the manifold is important particularly when considering the fuel air-mixing phenomena. In MPI SI engines, a homogeneous mixture is desirable in order to achieve complete combustion. Depending on the injection timing, and the phasing of the higher density fuel relative to intake valve phasing, the charge might be slightly stratified in the cylinder. This would be the case if the high density fuel would exit the pipe while the intake valve is open, but this is considered to have a very minor effect because of the minor variations in the fuel density. Taking advantage of the charge cooling effect requires vaporisation to occur in the intake manifold rather than in the coupling pipes, when the latent heat of vaporisation is obtained from the coupling pipe walls, and not the intake air.

Therefore, considering mixture formation, it is desirable to maintain as high a proportion as possible of liquid to the point where fuel enters the manifold.

The results of image intensity measurements show first of all that there is, in all injector system configurations, both phases of fuel present at the pipe exit, which is suggested by the intensity variation. Higher liquid-to-vapour proportion exists in the case of smallest coupling pipe, though this resulted in unacceptable long travelling time. In general, reducing pipe diameter resulted in higher liquid-to-vapour –ratio and also increasing the injector orifice diameter (increasing injector flow rate) resulted in higher peak image intensity suggesting that less fuel vaporises during transport through the pipe.

The fuel transport time is an important factor in bi-fuel engine fuel metering process and too long transport time results in undesirable response in mixture formation and combustion. The importance of transport time is particularly important in three engine running conditions; during engine transients (accelerations and decelerations), engine warm-up and high engine speeds and loads. During transient engine operations both injection duration and injection timing change rapidly to meet the changing fuel demand. The duration that the injector is open affects the fuel delivery primarily the pressure fluctuation in the pipe changes and consequently the pipe flow characteristics. This change in injector duty cycle is changed further when the engine speed (injection frequency) changes simultaneously. Fuel injection timing is adjusted also in most sequential MPI engines and timing is usually optimised for each engine speed and load range.

The measurements of the PCLIS injection system show significant variation in fuel transport times, the smallest pipe diameter coupling having the longest travelling times. This becomes more evident in the case of higher injector frequency, when there is no clear temporal structure to the fuel flow delivering almost constant fuel concentration through the cycle. Transport time is also clearly related to the fuel concentration as the smallest diameter pipe also has highest density fuel flow. Therefore, with the PCLIS, it is desirable to achieve a fuel flow with considerable rate of vaporisation in order to reduce the transport time. Also, the magnitude of the pressure fluctuations in the pipe depends on the pipe diameter, this is particularly

important in the case of low injector duty cycles. The injector orifice diameter did not seem to have much effect on flow transport time in terms of high and low density parts of the flow. Fuel injector duty cycle is also an important factor of the fuel transport time; and therefore it would have been appropriate to study the effect of increasing/decreasing duty cycle as well.

The importance of cycle-to-cycle variation is related to the importance of fuel transport time. In addition to these predicted variables due to engine operating conditions and engine management system behaviour, there was significant image-to-image variation in image intensity in laboratory conditions as well. The fuel density variation is particularly important in the case of the PCLIS injection cycle where both magnitude of density and variation are high. If this phase coincides with IVC, the variation makes a great difference in fuel metering from cycle-to-cycle. Also, if variation still exists in the fuel density at the end of the injection period, just before the start of the next injection, it is an indication that some high-density fuel might arrive to the manifold during the next cycle, regardless of both injection timing and whether it occurs at the same time than IVC.

The variation was measured from 40 consecutive images. The conditions in the measurement facility were kept constant; the fuel pressure, ambient temperature and pressure were constant and injector duration and frequency were constant for each injector configuration. Again, the smallest diameter pipes demonstrated highest variation, while the larger pipes also had high variation in the part of the fuel flow where also the intensity was high. It was evident that also lower flow rate injectors had higher variation when compared with higher flow rate injectors, which is explained simply by longer injector durations. At higher frequency, the variation was particularly large for the small diameter pipes, where high liquid concentration was high throughout the entire cycle.

IV.6 CONCLUSIONS

A summary of the findings:

1. The fuel spray density is higher with CCLIS configuration than in the PCLIS system, and CCLIS had shorter delivery time when compared to PCLIS. With PCLIS configuration the fuel starts vaporising in the pipe, but during the injection period, there is a phase where there is more liquid fuel present at the pipe exit. The CCLIS configuration is expected to have a stronger intake air cooling, while the PCLIS is expected to have more uniform charge concentration due to continuous fuel flow.

2. The fuel flow at the pipe exit in PCLIS case continues through the entire injection period, which is undesirable for engine emission control. There is also a high magnitude of cycle-to-cycle variation in fuel density, which is detrimental in engine operation point of view.

3. The smallest pipe diameter had highest fuel density, highest variation and lowest fuel transport time, and therefore showed unacceptable performance. The variation was higher for smaller injector orifice sizes, which makes it more attractive to use higher flow rate injectors. Fuel pressure had little effect on the fuel transport time and it was assumed that the fuel flow was dominated by the pressure caused by the vaporisation. Injection frequency had an effect only in the case of smallest diameter pipes, when the fuel transport time was lowest.

4. Higher flow rate injectors and smaller diameter pipes had higher peak fuel density, which is expected to have an effect on intake charge cooling and therefore engine performance.

5. The spray structure was different with the two configurations. The spray penetration and cone angle were both larger with CCLIS.

V. ENGINE EXPERIMENTS

V.1 ABSTRACT

Engine experiments are employed to demonstrate the novel bi-fuel liquid LPG injection system and the novel bi-fuel engine control concept. The measurements were carried out to understand and evaluate the limitations on engine performance due to the use of the same control unit for both petrol and LPG, and also to understand the effect of alternative LPG injection system configurations. Therefore, the engine performance is measured for both petrol and LPG engine operation, and also for different alternative LPG injection system configurations.

The measurements were carried out on a small 4-cylinder engine connected to a dynamometer and controlled with a programmable engine control unit. The measurements were carried out using the same engine control parameters for each fuel and injection system configuration. In addition to the measured engine torque, the cylinder pressure and the cylinder pressure phasing was also measured in order to apply the commonly employed analysis for mass fraction burned and rate of heat release.

The results showed that when using fixed ignition timing the engine torque, when operating on LPG CCLIS system, was comparable to the petrol operation torque, though 1 – 2% lower than that of petrol. The engine torque was 3% lower when using a PCLIS injection system with 200 mm long and 2 mm diameter coupling pipes when compared to CCLIS system. The torque produced was further reduced by 1 – 2% when using larger diameter and longer coupling pipes. These differences were explained by both the different magnitude of peak cylinder pressure, and also a difference in the peak pressure timing and phasing of the heat release. These differences were assumed to be a result of both the greater charge mass when using CCLIS system and the different mixture formation process between PCLIS and CCLIS systems. The effect of charge cooling was also evident when the measured in-cylinder temperatures of non-combusting cycles were compared. The CCLIS and petrol operation showed significantly lower charge temperatures than PCLIS.

V.2 INTRODUCTION

The primary objectives of the work described in this chapter are to demonstrate the operation of the newly developed LPG liquid injection system and the control concept on a 4-cylinder engine using a dynamometer and to investigate the effect of spark timing on the engine performance using two different fuels, petrol and LPG, and further, two different LPG injection systems, Close-Coupled Liquid Injection system (CCLIS) and Pipe-Coupled Liquid Injection system (PCLIS). Also, the effect of charge cooling associated with the two LPG systems is investigated in order to understand the advantage of increasing the engine efficiency by using different injection methods (CCLIS and PCLIS).

V.2.1 Engine performance parameters

The major operating variables considered to affect the petrol-optimised bi-fuel engine performance, efficiency and emissions are the following (although other important variables exist, such as the level of EGR and turbulent intensity, but these variables are not the subject of this study and therefore omitted here):

1. Ignition timing
2. Mixture quality
3. Mixture composition

As explained in Chapter II, the optimum timing for the ignition is called Maximum Brake Torque (MBT) – timing. It depends on the engine speed and load, and obviously on the combustion duration. Ignition timing also affects the burnt and unburnt mixture temperatures, and hence the NO_X emission formation, engine knocking and exhaust gas temperatures. Exhaust gas temperatures have an effect on HC emissions, since higher exhaust temperatures promote oxidation during the expansion and exhaust strokes reducing the HC emissions. Also, the engine thermal efficiency reduces with increasing exhaust temperatures.

In SI engines, the mixture is essentially pre-mixed forming a homogeneous mixture of fuel and air entering the cylinder prior to the compression stroke. In the cylinder, the

fresh charge mixes with residual exhaust gases. In the actual engine cycle, especially in MPI engines, the fuel is not necessarily completely vaporised prior to the spark ignition and the mixing is therefore not complete. Also, the residual gases are not completely mixed with the fresh charge. Non-uniformities in the in-cylinder mixture affect the combustion process, and are especially critical in the vicinity of the spark plug during the early part of the flame development.

Mixture composition in this context includes the properties of the fuel, density of the mixture (mass of the cylinder charge), as well as the equivalence ratio (φ). The first item in this list relates to the properties of different fuels, like the heating value and the stoichiometric AFR of the fuel, which together determine the energy density of the composition. As mentioned in Chapter I, the energy density of a stoichiometric mixture of LPG and a stoichiometric mixture of petrol are very similar. The amount of fuel chemical energy obviously has an effect on the magnitude of heat release in the cylinder following combustion. Increasing the intake charge density also increases the mass of chemical energy in the cylinder and therefore also has an effect on the energy density. The fuel equivalence ratio affects the engine performance; the maximum mean effective pressure on petrol operation is achieved with a slightly rich mixture (φ = 1.0 – 1.1). However, as discussed previously, the equivalence ratio is in most cases adjusted to be very close to 1 in order to achieve lowest engine emissions.

V.2.2 Combustion analysis

A widely used method to characterise combustion the progress is to determine the mass fraction burned curve or the related heat release curve. Mass fraction burned (x_b) describes the ratio of the mass of the mixture in the cylinder burnt at any instant during the combustion process to the total mass of the combustible mixture in the cylinder. Mass fraction burned profile is typically an S-shape curve (Figure V-I) and it is most often used in analysing the combustion process in energy release aspect. Rate of heat release ($dm_b/d\theta$) describes the rate of combustion relative to crank angle.

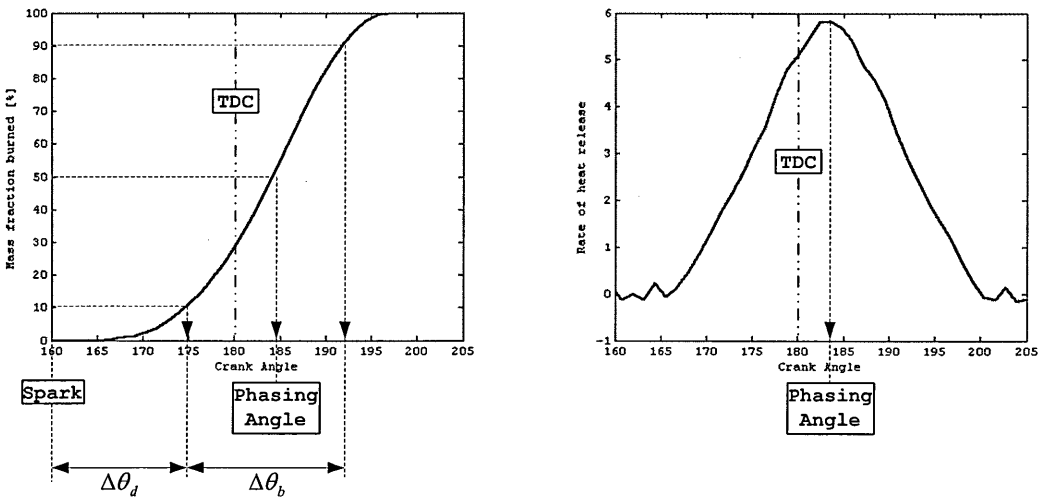

Figure V-I. Mass fraction burned (left) and rate of heat release (right) profiles.

The most commonly used definitions for mass fraction burned profile are (Heywood, 1988):

1. Flame development angle ($\Delta\theta_d$). This is the crank angle interval between the spark event and the time when a small but significant amount of fuel is burned (usually 10%), also referred to as ignition delay.
2. Rapid burning angle ($\Delta\theta_b$). The crank angle interval when the bulk of the fuel is burned and the bulk of the chemical energy released. This is typically 10% - 90% of the mass fraction burned curve.
3. Overall burning angle ($\Delta\theta_o$). The duration of overall burning process, which is the sum of $\Delta\theta_d$ and $\Delta\theta_b$.

Another useful measure obtained from the mass fraction burned curve that is related to the definition of MBT – timing is the angle of maximum rate of heat release, often referred as combustion phasing angle and usually coincides with the 50% mass fraction burned angle. For most SI engine applications, the phasing angle for MBT timing is between 5-10 °CA ATDC. This angle is the steepest point in the mass fraction burned curve, and obviously the highest point of the rate of heat release curve.

Most usually, x_b is determined using the measured cylinder pressure – time history; several methods with varying level of accuracy and complexity has been used in the

calculations. The computationally simplest method was introduced by Rassweiler and Withrow (1938) and it is still widely used in cylinder pressure analysis (Shayler et al., 1990; Brunt and Emtage, 1997; Daniels, 1998; Brunt et al., 1998). The method is based on the simple assumption that the normalised pressure rise due to combustion equals the mass fraction burned, i.e. the rise in the cylinder pressure due to combustion is proportional to the fuel burned (Equations V-I to V-IV). The total measured cylinder pressure is assumed to be a sum of the pressure change due to combustion (Δp_c) and pressure change due to cylinder volume change (Δp_v) resulted from the piston motion. In the absence of combustion, Δp_v is assumed to follow the polytropic relation.

$$\Delta p = \Delta p_c + \Delta p_v \qquad \textbf{Equation V-I}$$

$$p_i V_i^n = p_j V_j^n \qquad \textbf{Equation V-II}$$

$$\Delta p_v = p_j - p_i = p_i \left[\left(\frac{V_i}{V_j} \right)^n - 1 \right] \qquad \textbf{Equation V-III}$$

$$\frac{m_{b(i)}}{m_{b(total)}} = \frac{\sum_0^i \Delta p_c}{\sum_0^N \Delta p_c} \qquad \textbf{Equation V-IV}$$

where V is the volume, n is the polytropic index, m is the mass and the subscription b and c refer to burned and combustion, respectively. This method obviously includes several assumptions and simplifications:

1. Time-varying heat transfer to the cylinder walls is neglected. This simplification results in major overestimation of the actual burn rate towards the end of combustion, when the cylinder temperature is high resulting in high heat transfer rate to the cylinder walls.
2. The equation assumes that the pressure change due to cylinder volume change and heat transfer to the cylinder walls can be represented by a polytropic process, and hence the effect of heat transfer to the combustion chamber walls is limited to the selection of the value for the polytropic index n. In the basic model described above, both the compression and expansion strokes are treated as polytropic processes in which pV^n = constant. Typically the value of n used in the

calculations is experimentally determined from measured value prior to the ignition event (Stone and Green-Armytage, 1987).

3. The model assumes that the ratio of specific heat capacities of the gases (γ) remains constant. In the actual cycle, the specific heat capacities change due to both temperature and composition.
4. The model assumes that the normalised pressure rise due to combustion is directly proportional to the mass fraction burned. This simplification leads to the assumption that combustion occurs in constant volume and also that the mixture chemistry remains constant during combustion. In the actual combustion process both the total number of species and the dissociation vary during the combustion process.
5. The model does not take into account the flow in and out of the piston crevices, nor does it consider piston blow-by.
6. The model assumes that the combustion is complete and in its basic form described above does not include the combustion inefficiency; in actual engines some of the fuel does not burn during the engine cycle.

Another approach to calculate the heat release is based on the first law of thermodynamics (Gatowski et al., 1984; Chun and Heywood, 1987; Eriksson, 1998). Some of these computationally more complex models treat the combustion chamber contents as a single zone and are often referred as single-zone models. Equation V-5 shows the computation for the chemical energy, i.e. gross heat release using the energy conservation equation combined with the ideal gas law for the cylinder contents for each crank angle increment.

$$\frac{dQ_{ch}}{d\theta} = \frac{\gamma}{\gamma - 1} p \frac{dV}{d\theta} + \frac{\gamma}{\gamma - 1} V \frac{dp}{d\theta} + \frac{dQ_{ht}}{d\theta} \qquad \textbf{Equation V-V}$$

where Q is the energy, γ is the ratio of specific heat capacities of the gases, θ is the crank angle and the subscriptions *ch* and *ht* refer to chemical and heat transfer, respectively. The first term on the right hand side of the equation represents the change in the internal energy and the second term is piston work. The third term is the convective heat transfer from the cylinder contents to the cylinder walls. Often the formulation also includes a mass flux term, for an MPI SI engine, a single mass flux

term is due to the flow into and out of the crevices. The formulation shows a few significant advantages compared to the Rassweiler-Withrow model. First, the model takes into account the heat transfer to the cylinder walls and mass flux across the system boundary. The convective heat transfer is usually calculated using well-known heat transfer models reported by Eichelberg (1939), Annand (1963) or Woschni (1967). Secondly, the model allows for the change of γ to be included into the formulation, where γ is most often considered to be a linear function of temperature. When compared with the Rassweiler-Withrow model, it is also notable that if the convective heat transfer is substituted from the Equation V-V, the heat release calculated will essentially be similar to those calculated by the Rassweiler-Withrow model. This gross heat release is also often called the *apparent* heat release. Furthermore, the model assumes complete combustion.

Other models take into account two zones contributing to the combustion process; unburned and burned mixture zones (Egnell, 1998; Guezennec and Hamama, 1999). These models are therefore called two-zone models and are significantly more complicated than the two models described above. The two-zone models use similar formulation based on the first law of thermodynamics (energy conservation) and the ideal gas law with heat transfer models, but provide more accurate results as the temperature, heat transfer and the thermodynamic properties (γ) can be solved separately for each zone giving more accurate information on the state, concentration and composition of the cylinder contents. Also, these models take into account the combustion efficiency by using information on measured exhaust gas composition in the calculations.

All the above described methods to calculate x_b as a function of crank angle include errors due to the measurement of cylinder pressure and crank angle, and the accuracy of the mass fraction burned and heat release analysis depend largely on the accuracy of the measurement system and calibration. These errors typically include incorrect absolute pressure referencing, thermal shock, measurement errors from the pressure transducer, amplifier system calibration errors, and incorrect or inaccurate crank angle phasing. According to the simulation carried out by Brunt et al. (1998) the effect of these errors on the mass fraction burned analysis is of order of 0.5% - 3.0%.

For this study, the Rassweiler-Withrow method was chosen for its simplicity and demonstrated accuracy (Stone and Green-Armytage, 1987). The model therefore demonstrates explicitly the net heat release of the combustion process. This major simplification is considered reasonable since, as stated earlier in this chapter, the main objective of this study is to compare different fuel injection systems, while all the other engine conditions remain constant.

V.2.3 Cylinder temperature measurements

The cylinder temperatures of non-combusting cycles were measured in order to understand the effect of fuel injection and vaporisation on the intake charge temperature and density. Several methods have been recently used to measure in-cylinder temperatures of combusting cycles. Contact methods involve the use of a contact probe inserted into the cylinder. Recent applications include cylinder wall temperature measurements using thin-film thermocouples (Emi et al., 2002). Rakopoulos and Mavropoulos (2000) used thin-wire thermocouples to measure in-cylinder heat-flux in DI diesel engines. Optical, non-contact methods to measure cylinder temperatures include Moire deflectometry (Li et al., 1999), LIF (Schiessl and Maas, 2003), Laser Interferometry (Kawahara et al., 2001) and Coherent Anti-Stokes Raman Spectroscopy (CARS) (Bood et al., 1997). The non-contact methods have several advantages over the contact methods, mainly because they are non-intrusive (the in-cylinder flow-field is not affected by the contact probe) and because they are not affected by thermal inertia of the contact probe and therefore offer significantly better temporal resolution. However, these methods are often too complicated, time-consuming and costly because optical access is required, as well as sophisticated optical measurement systems or a fuel dopant. Therefore, for this study, a simple contact method was chosen, as the purpose of the measurements was strictly to compare the different fuel – air mixing processes and their effect on the charge temperature, and not to obtain quantitative charge temperature data.

In this study, the cylinder temperature is measured by inserting a fine wire thermocouple in the cylinder in the place of a spark plug. The engine was therefore run only with three combusting cylinders. The temperature data was taken both with the injector disabled and enabled; the resulting difference in mean temperature is

assumed to be a result of intake air cooling caused by vaporising fuel. The method includes several errors due to complex heat transfer processes in the engine cylinder. Firstly, the cylinder temperature is very difficult to adjust to the same initial value between measurements. Secondly, the thermal inertia of the thermocouples is relatively large, which leads to extensive response time. However, the method is considered to be valid for comparisons between different injector configurations, if these restrictions and limitations have been taken into account and the qualitative nature of the data obtained is appreciated.

V.3 MATERIALS AND METHODS

V.3.1 Experimental facility

The test engine used in the measurements was a small light-duty Nissan engine (Table V-I) connected to a Froude eddy current dynamometer. The engine and all its appliances were standard OEM equipment.

Table V-I. The research engine specification.

Specification		
Swept volume	997.7	cc
Cylinders	4.0	
Valves	16 V DOHC	
Bore	71.0	mm
Stroke	63.0	mm
Compression ratio	9.8:1	

Figure V-II shows the experimental setup used in the engine experiments. The engine is equipped with two separate injection systems. The petrol injection system is the OEM petrol injection system with the standard fuel pump, the fuel filter, the fuel rail, fuel injectors and the intake manifold referenced pressure regulator.

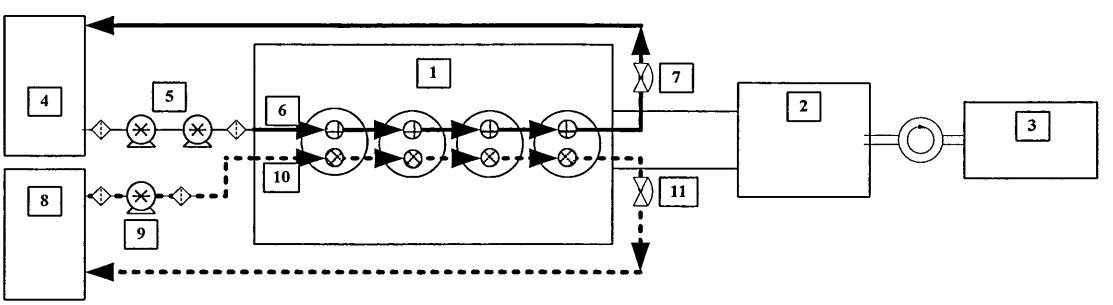

1 Engine (Nissan 998 cc CG10DE MY 2002)
2 Engine dynamometer (Froude eddy current)
3 Engine dynamometer controller
4 LPG tank
5 LPG twin pumps Bosch
6 LPG fuel injectors (Siemens Deka II)
7 LPG back pressure regulator (Kenmac KCB)
8 Petrol tank
9 Petrol fuel pump (Bosch)
10 Petrol fuel injectors (Nissan/Bosch EV6)
11 Petrol fuel pressure regulator (Nissan/Bosch)

Petrol fuel line and injector
LPG fuel line and injector

Figure V-II. A schematic diagram of the experimental setup.

The LPG injection system consists of two fuel pumps installed in series, a magnetic fuel filter upstream of the pumps, a coalescing filter downstream of the pumps, a fuel

rail, Siemens Deka II injectors and a Kenmac back pressure regulator. With the type of pressure regulator and fuel pump system, the fuel injection pressure was adjustable from 8 bar to 23 bar. Two different fuel rail mounting systems were used; for the CCLIS system the fuel injectors were mounted on the manifold in the place of the petrol injectors and for the PCLIS system the injectors were mounted above the engine head attached to a purpose-made fuel rail frame (Figure V-III). Only the PCLIS mounting system allowed the petrol injectors to be mounted in the manifold with the LPG injection system.

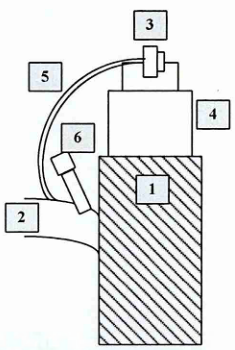

1 Engine block
2 Intake manifold
3 LPG injector and fuel rail
4 Fuel rail frame
5 Coupling pipe
6 Petrol injector and fuel rail

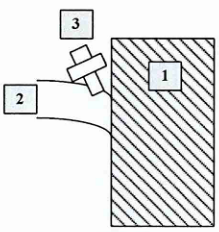

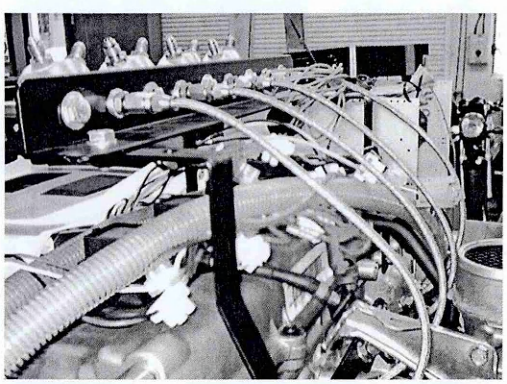

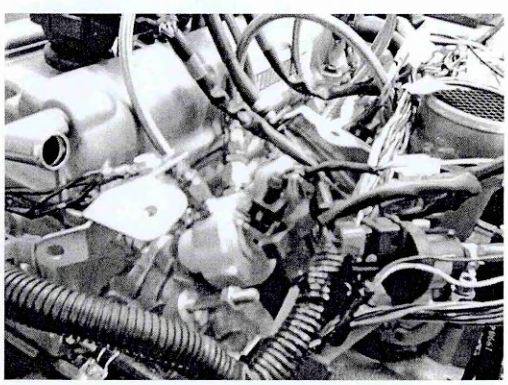

PCLIS CCLIS

Figure V-III. A schematic diagram and a photograph of PCLIS and CCLIS systems installed in the test engine.

The LPG injection system also includes the circuitry for the LPG injector actuation, which is described in detail in Chapter III. The actuator switching is controlled solely by the injection signals from the ECU.

V.3.2 Engine control system and mapping

The test engine was controlled using a Magneti Marelli MR600 programmable control unit. The engine fuelling was calibrated using a wide band Lambda sensor and the air-fuel ratio was adjusted to stoichiometric in the entire load and speed range. Ignition timing was adjusted to MBT – timing by measuring the brake torque during the calibration process, except in the engine speed range of <2000 rpm, where the ignition timing is knock limited. Figure V-IV shows a part of the petrol injection timing ignition timing maps. The engine was calibrated for the entire load range, idle to wide open throttle (WOT), but for image quality purposes only the range at which the measurements were carried out is demonstrated in the figure.

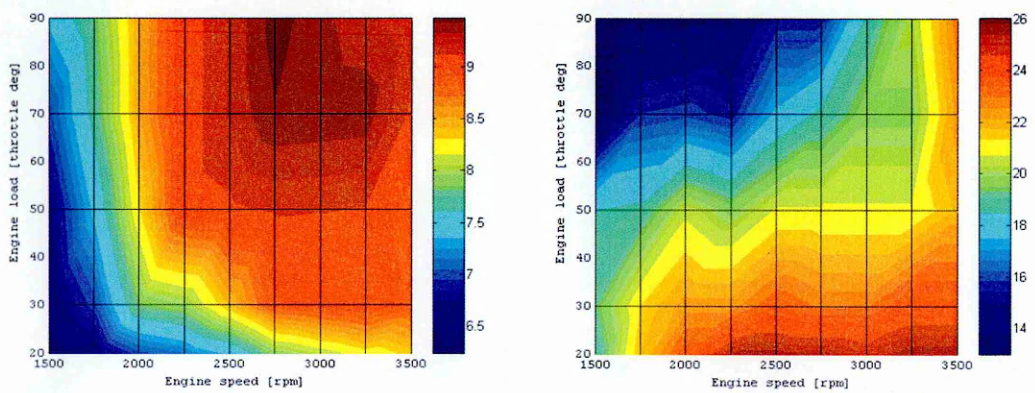

Figure V-IV. Petrol fuel injection map (milliseconds) on the left and ignition timing map in degrees of CA BTDC on the right.

Figure V-V shows the corresponding stoichiometric fuelling map for the CCLIS LPG operation with a fuel pressure of 15 bar using standard Siemens Deka II injectors. The map indicates a significant difference in injection duration between the LPG map and the petrol map. This was expected from the fuel injector flow rate measurements described in Chapter III. However, for the following practical reasons, the injector flow rate was not hydro-mechanically adjusted for these engine measurements.

a) The fuel injection pressure was intended to be kept high enough to avoid any premature vaporisation and consequent bubble formation, which would have a detrimental effect on the fuel metering.
b) The fuel flow rate adjustment by using additional flow restrictors (see Chapter III) was not applied for this study for practical reasons. Manufacturing the flow restrictor elements using economical methods, like spark eroding,

resulted in too high variation in manufacturing quality and consequently too high variation in injector flow rates. For this study, the control over the AFR for all 4 cylinders is considered to be very critical and since the AFR of individual cylinders could not be monitored, the AFR is controlled by changing the injection duration.

It is assumed that even though the purpose of the study is to demonstrate the operation of a bi-fuel engine controlled by a single control unit, which essentially means that no parameters in the ECU would be changed, the issue of using different flow rate injectors is an engineering issue rather than fundamental problem. In a commercial product development situation this would be solved through the involvement of a component supplier and a significantly greater investment of resources, which was not possible in this project. Therefore, it is assumed that the results presented in this chapter would be the same if the LPG fuel metering had been achieved by using petrol injection timing and altering the fuel injector flow rate.

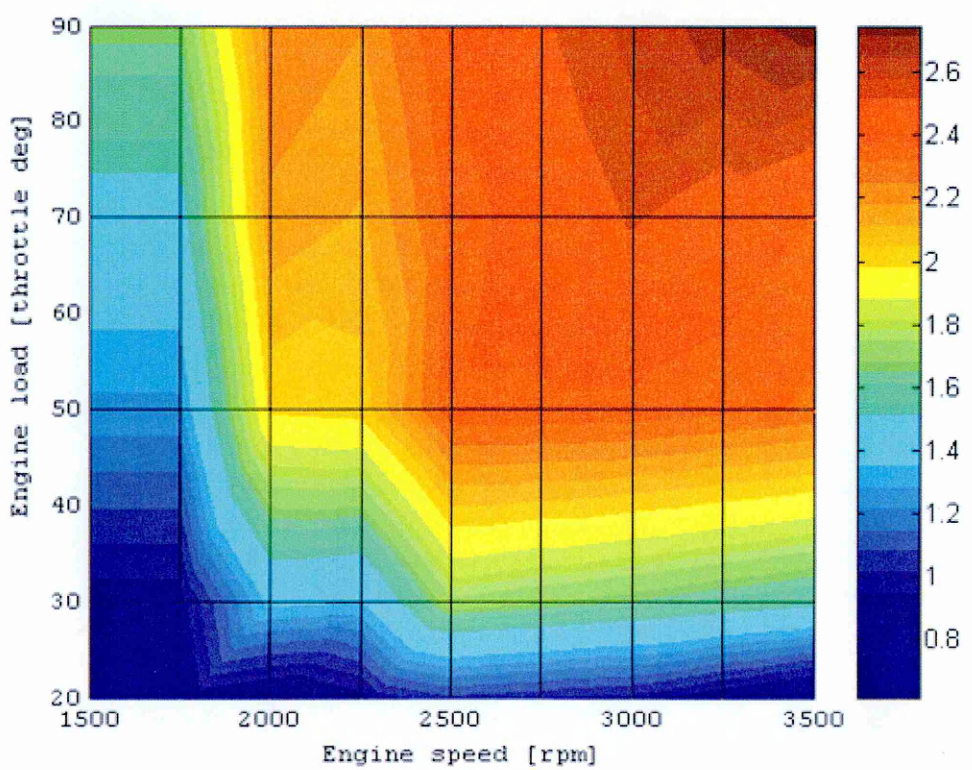

Figure V-V. Fuel injection map for CCLIS LPG system at an injection pressure of 15 bar.

V.3.3 Data acquisition and measurement system

The data acquisition card used in the measurements was a National Instruments DAQ-6026 PCMCIA card used with a laptop computer and a National Instruments LabVIEW data acquisition and signal processing software. The signals were acquired by the system via SCB-68 connector block, except for the cylinder temperature measurements, where a SCB-2345 carrier block and TC01 modules were used for the thermocouple signals and FT01 modules for the analogue voltage signals.

Table V-II shows the details of the sensors used in the measurements. All the signals were acquired simultaneously using hardware controlled sampling. The sampling rate used in the measurements was 20kS/s, which was considered adequate for the type of signals sampled. The most critical sensor in terms of accuracy used in the measurement was the crank position sensor, of which resolution was lower than commonly used in the cylinder pressure measurements. However, the resolution was improved by acquiring the raw signal and calculating the crank position using waveform functions, rather than conventionally triggering the pressure signal acquisition from the crank position signal.

Table V-II. Engine testing sensor data.

Physical measure	Sensor Manufacturer	Sensor Model	Sensor Type
Cylinder pressure	Kistler	6117BFD17	Piezoelectric
	Kistler	5011	Charge amplifier
Cylinder temperature	Omega	K-type (13μm)	Thermocouple
Manifold pressure	Bosch		Piezoresistive
Engine Torque	Test Automation/Froude		
Engine speed	Bosch (Nissan)	60-2	Inductive
Crank position	Bosch (Nissan)	60-2	Inductive
Cam position	Bosch (Nissan)		Hall-effect
Engine load (throttle position)	Bosch (Nissan)		Potentiometric
Injector current	LEM HEME	PR20	
Exhaust oxygen (rich/lean)	Bosch (Nissan)		Switch
Exhaust oxygen (A/F ratio)	Bosch	LSM 11	Wide-band
	Motec	PLM	Analysing unit
Fuel pressure	Keller	PA-22M	Pizoresistive

V.4 RESULTS

V.4.1 Preliminary engine torque measurements

The engine torque for both petrol operation and CCLIS LPG operation was measured over the entire load and speed range. The fuel injection was calibrated for each fuel as explained in the previous section, but the ignition timing was fixed to the petrol MBT timing, and all the other engine control parameters were the same during the petrol and LPG operation. The injection timing used was a late CVI.

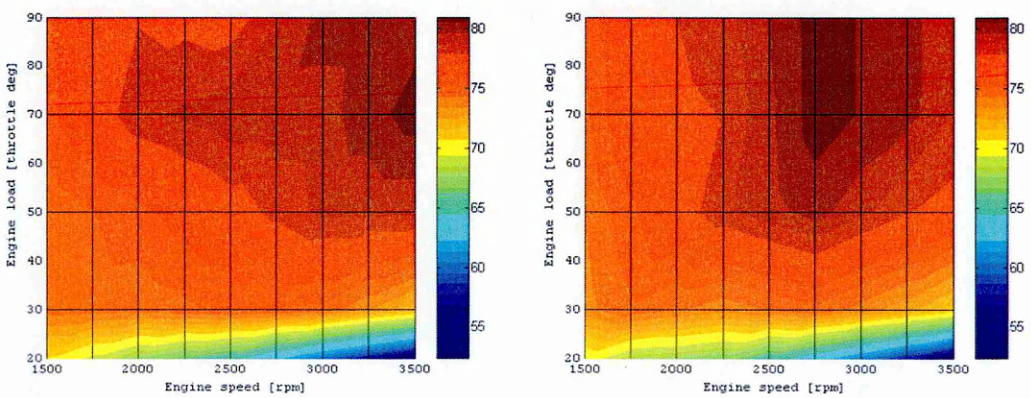

Figure V-VI. Measured engine torque with petrol (left) and CCLIS LPG system (right).

The results from the measurements are presented in the Figure V-VI. It is shown that the engine brake torque for both fuels is comparable. The engine brake torque is slightly higher during petrol operation (1-2%), but there is not a significant difference in any part of the engine operating range.

Engine torque was also measured for the PCLIS system using different pipe lengths and diameters. The pipe system details are explained in Table V-III. Using the smaller diameter PCLIS system, the injection duration was slightly increased in order to achieve a stoichiometric mixture. This was due to the effect of pressure in the pipe on the injector flow rate, where the pressure in the coupling pipe is slightly higher than in the manifold resulting in a lower pressure difference across the injector flow area and consequently lower flow rate. This pressure effect reduces with increasing pipe diameter, and for the larger diameter pipes the injection duration was slightly

decreased, which was an indication of lower charge density when the PCLIS injector system was used.

Table V-III. Injector system configurations for LPG engine torque measurements.

Configuration	Type	Coupling pipe diameter [mm]	Coupling pipe lentgth [mm]
1	CCLIS	N/A	N/A
2	PCLIS	2	20
3	PCLIS	2	40
4	PCLIS	4	20
5	PCLIS	4	40

The results from the PCLIS torque measurements are presented in Figure V-VII. The measurements were taken at an engine rpm of 3000 and WOT. The results indicate two significant characteristics of the system; the engine produces higher torque using the CCLIS system when compared to the PCLIS system and the torque is further decreased when the coupling pipe diameter and length is increased. In the worst torque PCLIS case, the torque was 8% lower than that of CCLIS system.

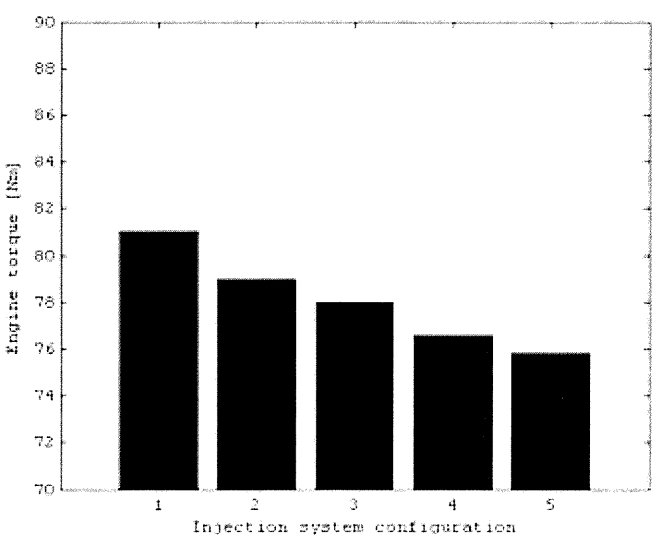

Figure V-VII. Measured engine torque using different LPG injector configurations (3000 rpm, WOT).

V.4.2 Cylinder temperature measurements

The cylinder temperatures were measured also on the engine at an rpm of 3000 and WOT. The cylinder temperatures are plotted in Figure V-VIII. The results show that the thermocouple is responding to the varying cylinder temperatures during the engine cycles; temperature is decreasing during the intake stroke due to the induction of colder charge, and increasing during the compression stroke due to increasing cylinder pressure.

It is also evident that the difference in mean cylinder temperatures between the injector being disabled and enabled is higher with the two injection systems, where all the fuel is vaporised in the manifold or in the cylinder. This is a clear indication of the presence of the charge cooling effect; the petrol and CCLIS system show lower cylinder charge temperatures than the PCLIS system. This suggests that a greater fraction of heat for the vaporisation is obtained from the intake air with the petrol and CCLIS systems than with the PCLIS system, where more energy used for vaporising the fuel is drawn as heat from the pipe walls rather than from the intake air.

Further, it is evident that the difference in the mean temperatures is higher with the CCLIS system when compared to petrol. This is assumed to be attributed to the higher latent heat of vaporisation of LPG. However, this difference is rather small compared to the PCLIS system.

Table V-IV. Results from cylinder temperature measurements.

Fuel	Injector config	ΔT cycle-high [°K]	ΔT cycle-low [°K]	ΔT mean [°K]	Std dev cycle-high [°K]	Std dev cycle-low [°K]	Std dev mean [°K]
Petrol	Standard MPI	14.73	12.69	**13.71**	3.03	2.79	2.91
LPG	CCLIS	15.96	14.19	**15.07**	3.52	3.38	3.45
LPG	PCLIS	6.20	4.33	**5.27**	3.65	3.63	3.64

Table V-IV summarises the results and shows the standard deviation of 50 consecutive engine cycles from cylinder charge temperature measurements.

a

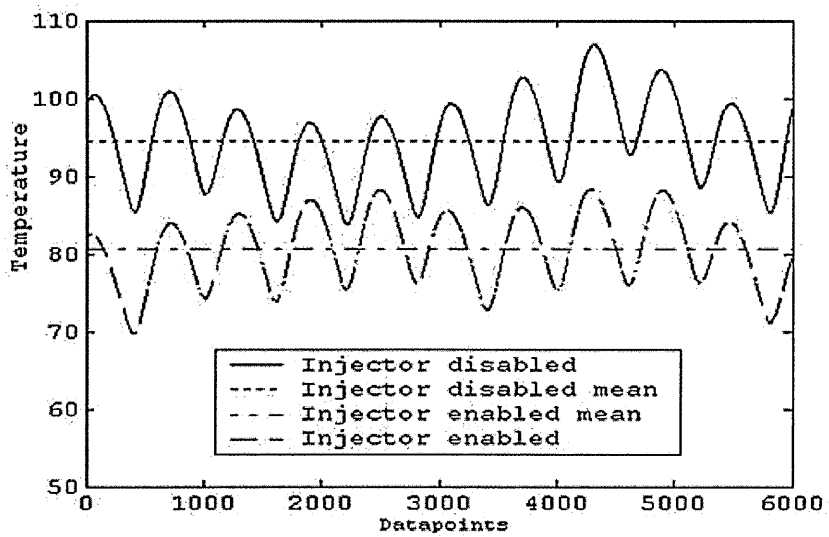

b

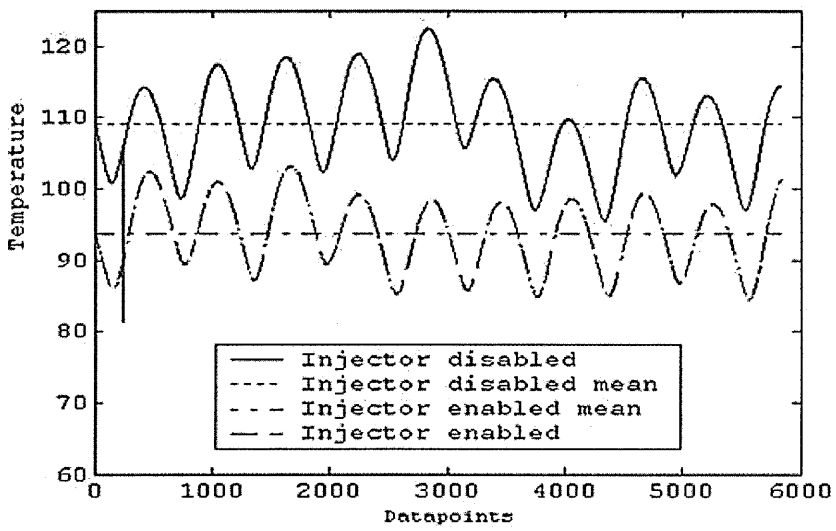

c

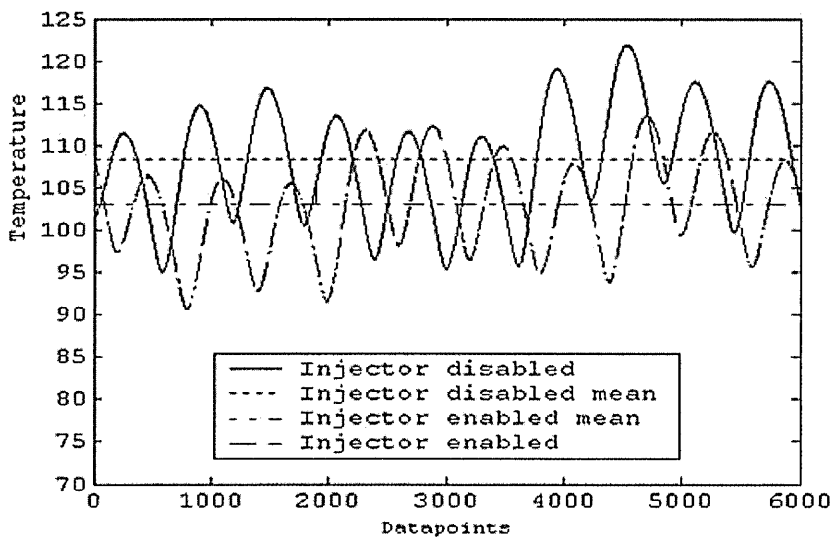

Figure V-VIII. Time history of non-combusting cylinder temperatures operating on petrol (a), CCLIS (b) and PCLIS (c) LPG system

V.4.3 Combustion analysis

V.4.3.1 Cylinder pressure measurements

Cylinder pressure – time histories from the engine operation with petrol and the three LPG injector configurations are shown in Figure V-IX. For each ignition setting, the cylinder pressure is calculated as an average of 100 consecutive successive engine cycles. For all the cases, the pressure diagrams show very similar behaviour with varying ignition timing.

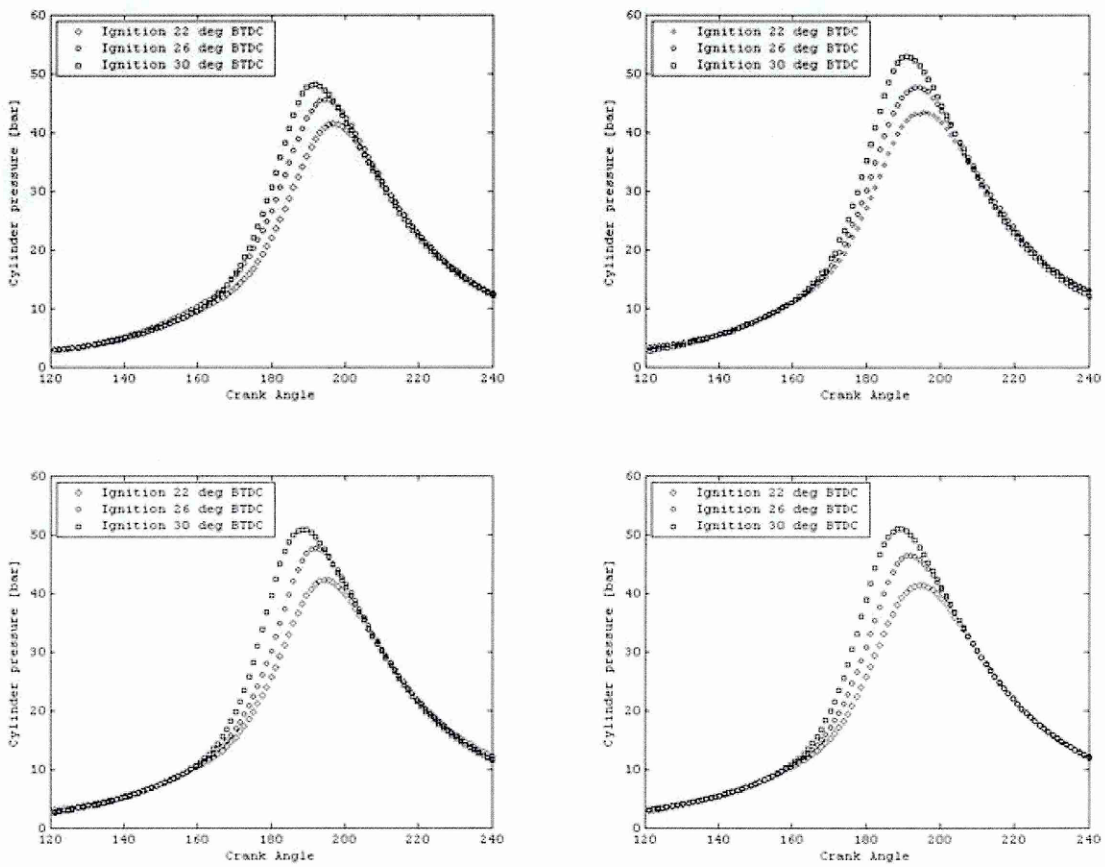

Figure V-IX. Cylinder pressure measurements with three ignition timings during engine operating on petrol (top left), CCLIS (top right), PCLIS 2 mm pipes (bottom left) and PCLIS 4 mm pipes (bottom right).

Figure V-X shows the engine torque measured simultaneously with the cylinder pressure measurements. The engine torque is the highest during petrol operation, but the torque produced during CCLIS operation is essentially the same, but occurs with different ignition timing. The torque produced by both PCLIS systems is lower than in the petrol and CCLIS case, and the peak torque occurs also in later ignition advance

compared to petrol peak torque. This behaviour is explained in Figure V-XI, which shows the peak cylinder pressures for each case plotted against ignition timing (left) and the corresponding the peak pressure timing, PPT (right). The results show that the peak pressures are very similar for all the LPG cases, while the peak pressures seem to be lower for petrol operation. The PPT plot demonstrates significant differences between LPG and gasoline, and also between different LPG injector configurations. During petrol operation, the peak cylinder pressure occurs considerably later than in any of the LPG configurations. Also, the PPT occurs later in the case of CCLIS case when compared to the PCLIS cases. Further, the peak cylinder pressure occurs later when the fuel is introduced to the manifold through a larger diameter coupling pipe. However, all the cases show a similar tendency when the ignition timing is retarded; the cylinder pressure magnitude decreases and the PPT occurs later.

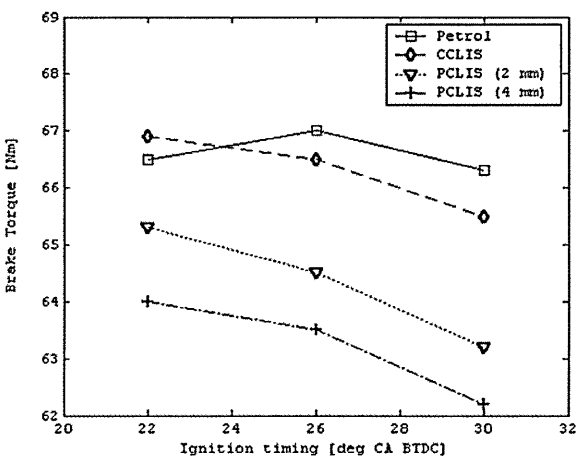

Figure V-X. Engine Torque.

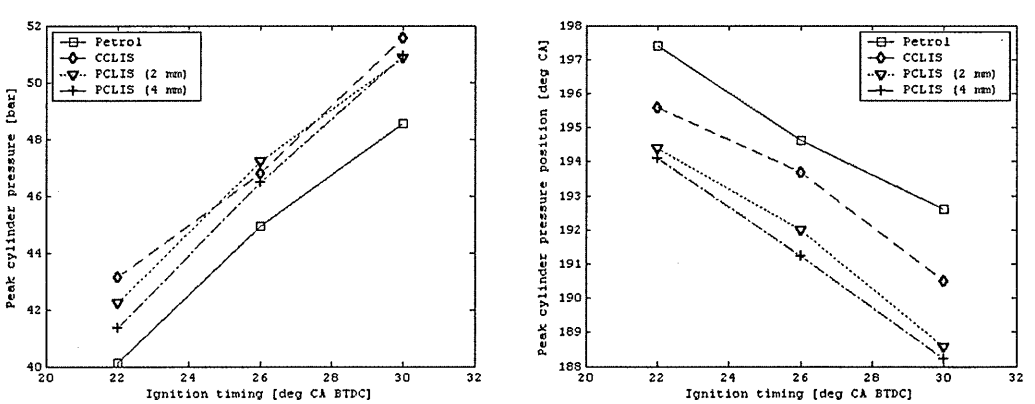

Figure V-XI. MBT – timing related cylinder pressure analysis.

V.4.3.2 Rate of heat release analysis

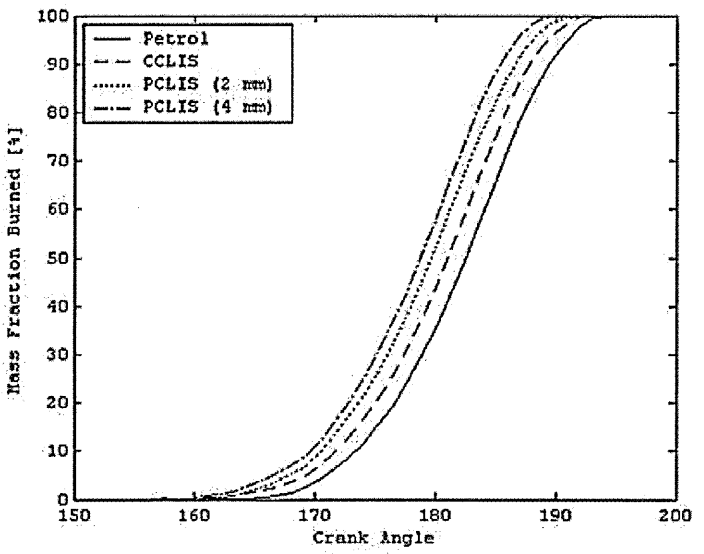

Figure V-XII. Mass Fraction Burned curves.

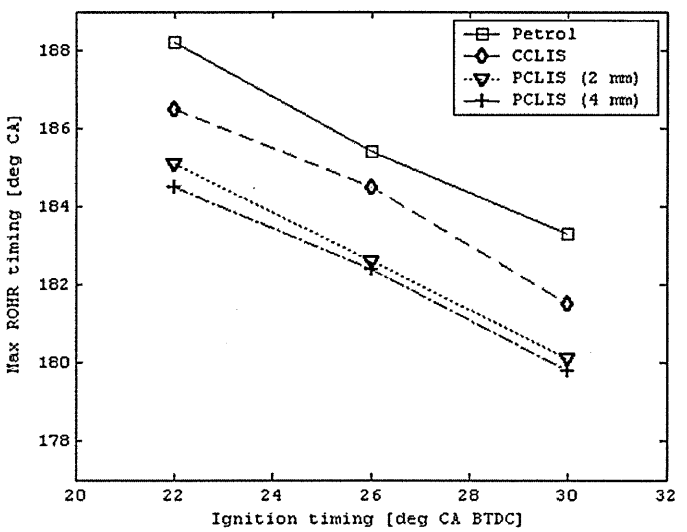

Figure V-XIII. MBT – timing related mass fraction burned analysis.

The mass fraction burned curves with the four different fuelling cases are shown in Figure V-XII. The curves indicate different combustion characteristics for each case. In the petrol and CCLIS case, the combustion is complete clearly later than in the case of PCLIS. The same is evident in Figure V-XIII, where the combustion phasing angle is plotted for each fuelling case using different ignition timings. It is observed that the

maximum rate of heat release occurs at a different phase when comparing the different fuelling case.

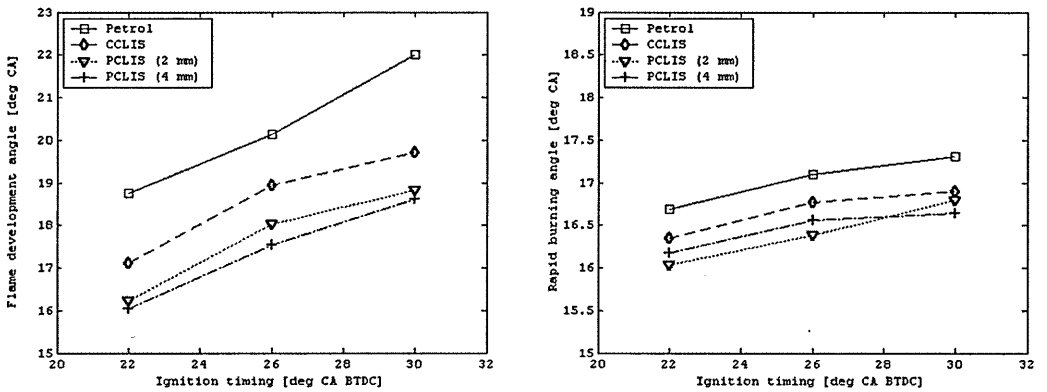

Figure V-XIV. Combustion progress related mass fraction burned analysis.

Figure V-XIV shows the flame development angles for each fuelling case (left) and corresponding rapid burning angles (right). It is observed that there is a considerable difference in the flame development angle between petrol, CCLIS and PCLIS cases. The flame development angle is significantly greater than any of the LPG cases. Also, the flame development angle is greater in the CCLIS case than the PCLIS case, while there is a only minor difference between the 2 mm and 4 mm PCLIS cases.

However, the differences in rapid burning angles are not hugely significant. The petrol operation shows slightly greater rapid burning angle than any of LPG cases, while there is hardly any difference between the three LPG cases.

V.5 DISCUSSION

V.5.1 Peak cylinder pressure and MBT – timing

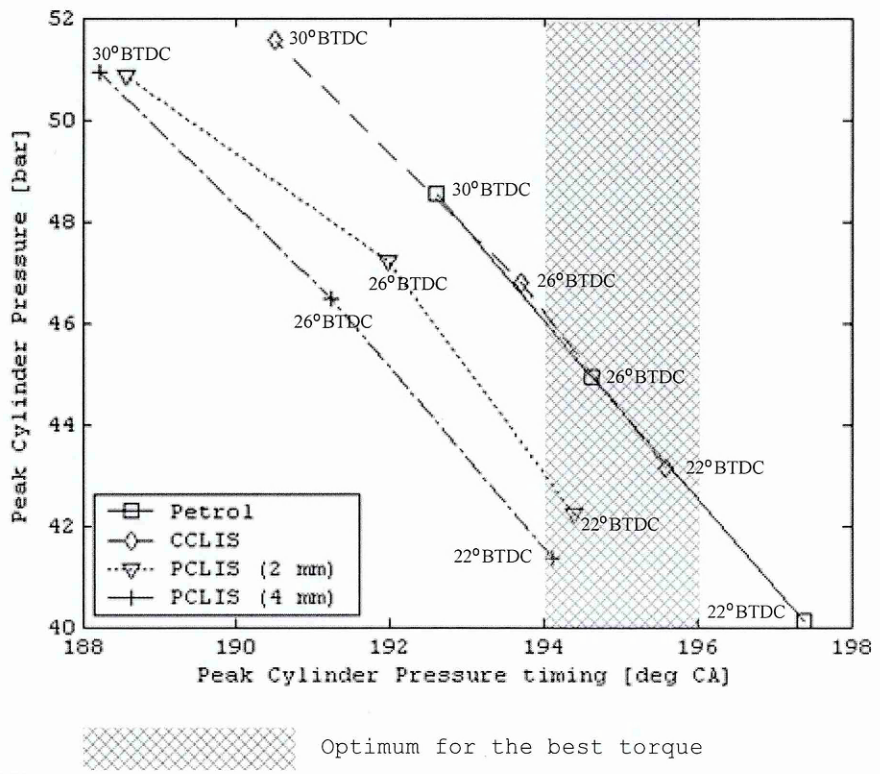

Figure V-XV. Optimum peak cylinder pressure timing.

The most significant observation in the cylinder pressure and torque measurements concerns of course the ignition timing. The effect of the ignition timing on the engine performance is illustrated in Figure V-XV and Figure V-XVI, where the peak cylinder pressure is plotted against the PPT and the combustion phasing angle, respectively. The figures clearly illustrate the following characteristics of the non-optimised bi-fuel system:

a. The slight difference in produced engine torque between CCLIS and petrol case observed in preliminary engine torque measurements can be explained by the different MBT – timing. The engine torque was measured using petrol MBT –timing, 24° CA BTDC. The figure shows that the peak pressure using ignition advance of 24° CA BTDC occurs in the optimum region for the best torque (which is 14-16° ATDC for most engines), in the case of petrol, but not

in the case of CCLIS. Also, the same observation is evident when the combustion phasing angles are compared. However, when the CCLIS advance was retarded, the peak pressure occurred in the optimum region, producing similar cylinder pressure than in the case of petrol. This indicates that similar torque is achievable with CCLIS LPG system as with petrol if the ignition is optimised for the LPG operation.

b. Though it is evident from both figures that the MBT – timing is different for PCLIS cases as well, compared to both CCLIS and petrol, it is evident that similar peak cylinder pressures are not achieved even if the ignition is retarded so that the peak pressure and combustion phasing angle occur at the optimum time relative to engine crank angle. This is suggested to be a result of lower charge density and hence lower amount of chemical energy released during combustion. An indication of lower charge density was evident in the cylinder temperature measurements associated with the PCLIS case, and also from the results of the spray imaging experiments described in Chapter IV, where significantly higher vapour content was observed in the case of PCLIS injection when compared to CCLIS injection.

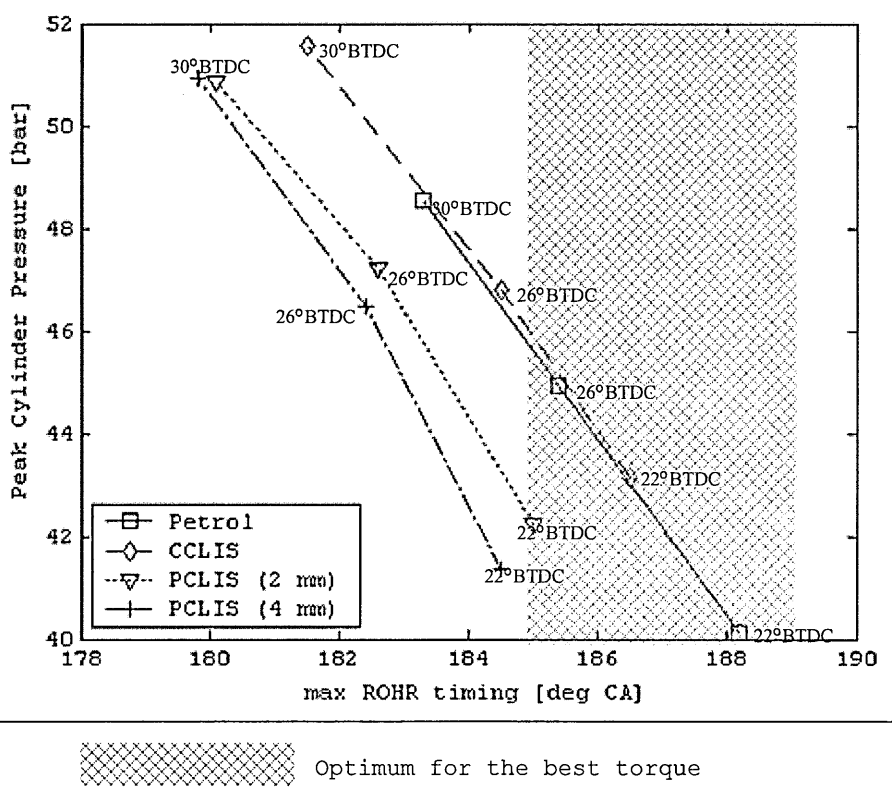

Figure V-XVI. Optimum for maximum rate of heat release timing.

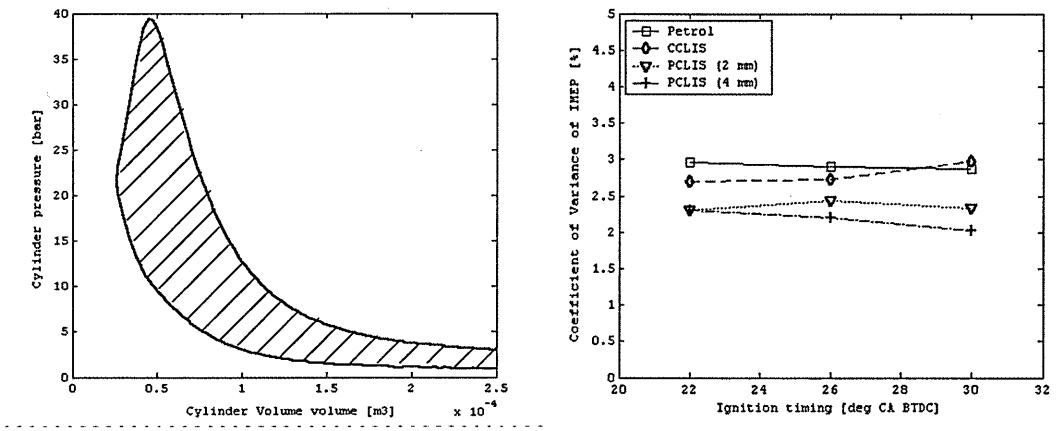

Figure V-XVII. Calculation of IMEP and COV_{IMEP} from the measured cylinder pressure data.

Covariance of Indicated Mean Effective Pressure (COV_{IMEP}) is a useful quantity to express the variation of both cylinder pressure and the peak pressure timing. The term indicated work (W_i) describes the work output per cylinder per mechanical cycle and can be expressed as the shaded area in the p-V diagram (Figure V-XVII on left). The Indicated Mean Effective Pressure ($IMEP$) is the indicated work per cylinder swept volume (V_d) and can be defined as:

$$IMEP = \frac{W_i}{V_d} \qquad \textbf{Equation V-VI}$$

COV_{IMEP} of the cylinder pressure measurements is presented in Figure V-XVII on right. The plot shows that the variance is small for each case, and also that the variance is higher for petrol and CCLIS case.

V.5.2 Combustion progress

As discussed in Chapter II, the flame propagation through the combustion chamber, and therefore the mass fraction burned profile, in SI engines is primarily affected by the combustion chamber geometry, the flow field characteristics and the unburned mixture composition and state.

In this discussion, the first two aspects mentioned above will not be considered because the geometrical parameters of the research engine are assumed to be independent on the fuel and injector configuration. Hence, the differences in the mass

fraction burned profiles are considered to be attributed to differences in unburned mixture characteristics.

The observations made in the previous section concerning the differences in the mass fraction burned curves leading to differences in the measured torque can be summarised as follows:

1. Petrol and CCLIS LPG produces higher cylinder peak pressures when compared with the both PCLIS LPG configurations
2. Petrol overall burning duration is longer than that of LPG
3. Differences in burning durations between petrol and LPG are mainly due to longer flame development time, but the rapid burning duration is slightly longer as well
4. The overall burning duration is longer for CCLIS LPG than for PCLIS cases and is due to longer flame development time, although there is also a minor difference in the rapid burning angle
5. The overall burn duration is longer for the 2 mm PCLIS case compared to the 4 mm PCLIS case, but it is only due to the longer flame development time and there is only a negligible difference in the rapid burning angle

The relevant differences between different fuels and injector configurations can be summarised as follows:

1. The fuel characteristics (mainly energy density, vaporisation rate and reaction rate) differ from petrol to LPG.
2. The unburned mixture is at a lower initial temperature for the CCLIS case when compared to the PCLIS case.
3. The fuel is introduced as liquid in the manifold in the case of CCLIS, while in the case of PCLIS the fuel is partly vapour when it enters in the manifold.
4. In the 2 mm PCLIS case, the liquid fuel concentration is slightly higher than in the case of 4 mm PCLIS when entering the manifold (Chapter IV).

The similar peak cylinder pressures between CCLIS and petrol cases can be attributed to two parameters. The similar peak pressure is expected because the energy densities

of stoichiometric LPG and stoichiometric petrol are very similar, and also because the mixing mechanics of the two fuel systems are similar. As a consequence, the mixture temperature is low at the end of the induction process and the density and mass of the inducted fuel is in a similar proportion. This is also evident when the peak cylinder pressures of CCLIS and PCLIS cases are compared. The peak pressure is lower in the case of PCLIS, which is a result of higher intake temperatures and higher vapour fractions of the intake air and consequently lower charge density compared with the CCLIS case.

As discussed in Chapter II, the laminar flame speed of propane is considerably higher than that of average petrol (Metghalchi and Keck, 1980; Metghalchi and Keck, 1982). Flame speed is also largely dependant on the flame temperature, which in turn depends on the unburned mixture temperatures. This is also evident from the results comparing CCLIS and PCLIS systems and explains the higher flame speed in the case of PCLIS system.

The flame development angle largely depends on the local mixture composition in the vicinity of the spark plug, while the rapid burning angle is affected by the mixture composition of the entire combustion chamber. Therefore, the greater flame development angle is an indication of mixture non-uniformities near the spark plug, while the rapid burning angle is not affected by these non-uniformities as the mixture through the entire combustion chamber is stoichiometric. This is evident when comparing the CCLIS and PCLIS cases, where the main differences in burn rates were due to the longer flame development angles while the rapid burn rates were very similar in duration. The observation therefore indicates that the mixture is more homogenous in the case of PCLIS when compared to CCLIS case. It also explains the differences in flame development angles between the 2 mm and 4 mm PCLIS cases, suggesting that the mixture is more uniform when using larger diameter coupling pipes.

This result compares with the results of Abd-Alla et al. (2003), discussed in detail in Chapter II. It was noticed that the mass fraction burned curves showed significant differences in combustion progress between petrol and vapour LPG (mixer-type), which were attributed to the larger flame development angle and which compares

with the results presented in this study. These results clearly indicate that the mixture in the vicinity of the spark plug was less homogenous in the case of petrol resulting in longer flame kernel development. Similar results were obtained by Homeyer et al, (2002) where vapour mixer-type system was compared to LPLI system (also described in Chapter II). It was noted that the MBT timing was more advanced than with mixer-type system, which appeared to be a result of longer ignition delay with the LPLI system. This was attributed solely to lower unburned mixture temperatures with the LPLI system and the authors did not comment on the influence of the mixture formation on flame development duration.

The observation compares well also with the study of Oh et al. (2002) and Lee Y et al. (2004), which are both discussed in detail in Chapter II. It was noticed that if the fuel is injected very early and it vaporises fully in the intake manifold, the fuel distribution in the combustion chamber is consequently more homogeneous resulting in small flame development angles. When the fuel was injected later, just before IVO, a stratified charge resulted in the cylinder. Further, it was noticed that the flame development angles were significantly higher in the case of late CVI injection, which was attributed to ill-stratification, where the spark-plug was surrounded by lean mixture This was thought to be due to incomplete fuel mixing with the air in the manifold.

In the experiments described in this chapter, the fuel in all cases was injected just before the IVO. In the case of CCLIS and petrol, it is suggested that the larger flame development angle in the case of CCLIS and petrol is caused by charge stratification, non-uniformities in the AFR in the combustion chamber, and in particular, the lean mixture in the vicinity of the spark plug. This stratification is not so significant in the case of PCLIS, because the fuel is essentially premixed in the intake manifold, and the mixing is spread through the entire engine cycle. Therefore the fuel that enters the cylinder is already mixed with the intake air, unlike in the case of CCLIS and petrol, where vaporisation possibly still occurs during the intake stroke, and fresh air enters the cylinder after the fuel causing the stratification.

V.6 CONCLUSIONS

1. A non-optimised bi-fuel injection system was demonstrated in a 4-cylinder engine operated on a dynamometer. The results showed that the engine can be operated by both CCLIS and PCLIS injector configurations.
2. The measured differences in in-cylinder temperatures between the cases were the injector was enabled and disabled were higher in the case of petrol and CCLIS when compared with PCLIS in non-combusting cycles. This indicated that the charge temperature was lower in the case of petrol injection and CCLIS injection and the charge cooling effect was evident.
3. There was a slight difference in engine torque between spark-optimised petrol operation and non-optimised CCLIS operation. From the mass fraction burned analysis and investigation of the cylinder pressure data, it was concluded that this difference is attributed to the different MBT – timing of the fuels. When the ignition advance was reduced in the CCLIS case to the CCLIS MBT – timing, the cylinder pressure and the engine brake torque were the same as in the petrol case the spark timing optimised for petrol.
4. The torque was lower for the PCLIS case when compared with CCLIS and the petrol case. This was again partly explained by the different combustion phasing and the consequent difference in MBT – timing, but optimising the ignition advance for the PCLIS system resulted in lower peak pressures and engine brake torques than with petrol. This indicated that the effect of charge cooling was responsible for the higher torque in the case of CCLIS and petrol.
5. The differences in combustion phasing were attributed to greater flame development angles with the CCLIS and PCLIS cases. This was suggested to be due to in-cylinder charge stratification during petrol and CCLIS operation, while in the PCLIS operation the mixture was essentially premixed in prior to entering the cylinder. This suggestion is supported by the results from spray imaging experiments presented in Chapter IV, where it was demonstrated that in the PCLIS case, the fuel vaporises partly in the coupling pipes resulting in long travelling times. As a consequence, the fuel enters the manifold during the entire engine cycle. Also, the lower charge temperatures result in longer flame development time.

VI. PREMATURE VAPORISATION IN THE FUEL RAIL

VI.1 ABSTRACT

The primary purpose of this work was to develop an alternative method to control the critical heat transfer to the fuel rail in liquid LPG injection systems. The approach was to develop a sensor, which could detect the vaporisation event and could give the control unit the opportunity to respond by means of pressure or flow rate control, or switching the fuels. Premature vaporisation in the fuel rail results in inevitable and critical errors in fuel metering leading to deterioration of engine performance and emissions.

An optical sensor installed in the fuel line was developed for the purpose. The device uses a simple infrared emitter diode and phototransistor pair to distinguish between vapour phase and liquid phase fuels, but also to detect small bubbles in the fuel rail.

The application of the sensor was tested and validated in the liquid injection LPG vehicle. The sensor successfully detected the events occurring when the saturation temperature in the fuel rail was reached. More importantly, the sensor detected small bubbles migrating with the liquid fuel. These bubbles were suggested to have been formed in local hotspots and the presence of them in the liquid fuel was evident while the fuel temperature was still below the saturation temperature. This behaviour is not easy to detect or predict by any other sensors or measurement techniques, and it also gives the control unit warning before the detrimental complete fuel vaporisation in the fuel rail occurs. Even without the suggested feedback control strategy, the device has a great potential in research and development, where the knowledge of bubble formation can be used to study the effect of different fuels, pressures, flow rates, fuel rail configurations or engine and ambient conditions to the heat transfer characteristics.

One of the major advantages of this newly developed sensor is the very low cost, which enables the device to be used in production LPG conversion systems. Essentially, this chapter describes in detail the development and evaluation of this prototype sensor, which has a total material cost of £2.61.

VI.2 INTRODUCTION

The objectives of the work described in this chapter are to demonstrate a device which can be used for premature vaporisation control in liquid injection LPG engines and to study the mechanics of vapour bubble formation in the LPG fuel line. As described in Chapter II, this heat transfer problem is considered to be one of the major issues concerning liquid injection LPG systems. Vapour bubble formation in the fuel supply line affects significantly on AFR control and hence engine performance and emissions.

The most important measures concerning the fuel phase change process are obviously the fuel rail pressure and the fuel temperature. If the pressure in the fuel rail falls below saturation pressure or the fuel temperature increases above saturation temperature, the fuel starts vaporising. Preventing these circumstances can be challenging for several reasons. First, the fuel composition might vary significantly and this affects the saturation properties. Secondly, the vaporisation in the fuel rail starts locally because either the temperature or the fuel pressure is not uniform in the fuel line. Location of the high temperature "hot spots" in the fuel rail depend solely on the engine geometry and operating conditions, which might affect the heat transfer characteristics to the fuel rail and to the fuel. The local variation in fuel pressure in the fuel line, apart from the pressure fluctuation which results from the injection valve opening and closing, is mainly determined by the fuel rail and the injector geometry.

The detection and observation of these conditions by the simple means of a pressure and temperature sensor is difficult because the non-uniformity of both the pressure and the temperature in the fuel line. The vaporisation starts by local bubble formation. Some bubbles grow and form a local vapour plug. However, some of the bubbles are small and spherical and migrate with the fuel flow. The method of detecting the premature vaporisation proposed in this chapter is based on the detection of these small migrating bubbles.

VI.3 MATERIALS AND METHODS

VI.3.1 Development of vapour bubble detection device

An optical method to detect vapour bubbles was applied because of simplicity and low cost of the hardware required and wide availability of components. Standard infra red (IR) light sources were chosen to limit the radiation wavelength. Because the absorption properties of propane were not known at the early stages of the development process, the initial idea was to use an infrared light source and detector, to distinguish the fuel phase in the fuel line. The initial experiment was based on the idea that the liquid propane would "block" the infrared absorption, and the detector would get the signal from the infrared source only when there is vapour in the line. However, as soon as the experiment was properly set up and the right pair of infrared emitter and a phototransistor was found, it was evident that the device works based on a different physical phenomenon. The liquid propane, with a very simple molecular structure, does not absorb the wavelengths emitted by the infrared emitter diode, and there is not much difference in the phototransistor output if the medium between the emitter and the collector is liquid or vapour.

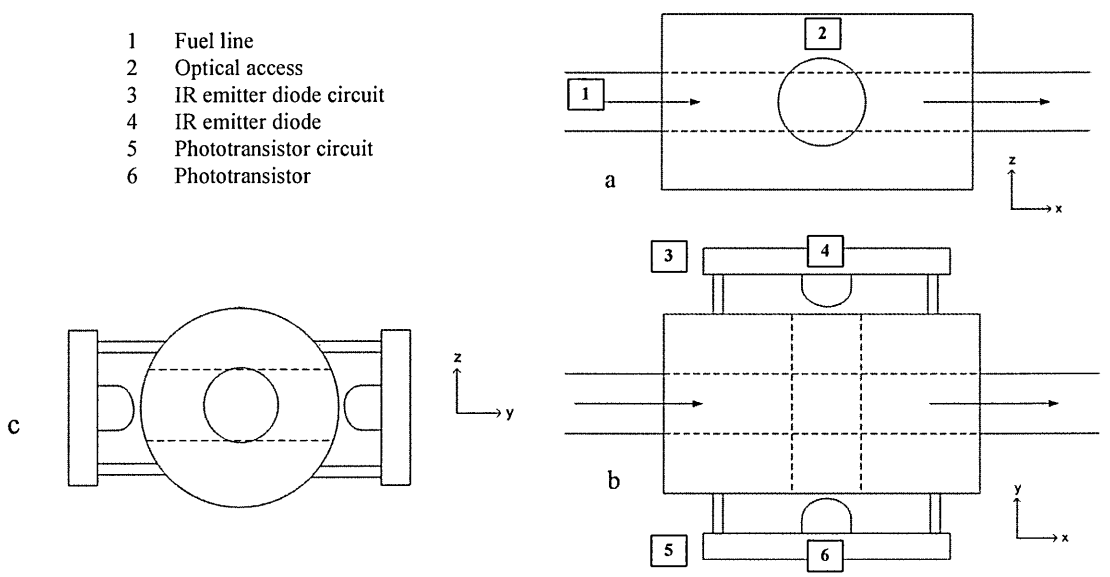

Figure VI-I. Schematic diagram of the bubble detection device, front view (a) without the diode and transistor circuits, top view (b) and side view (c) with the diode and transistor circuits.

The prototype device was constructed from a cylindrical aluminium case. A Perspex window was installed on each side of the cylinder to enable optical access for the

infrared emitter and the phototransistor. The electronics were fixed to the main body with adjustable bots and nuts. Figure VI-I illustrates the construction of the device.

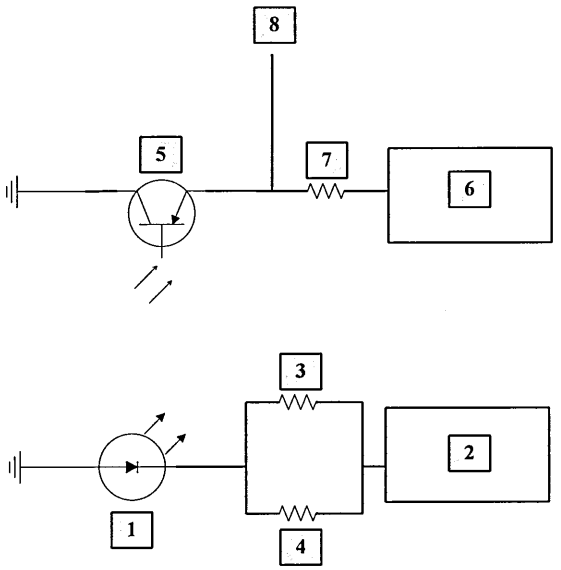

1 IR emitter diode (Siemens SFH487)
2 Pulse generator 0-1.5V
3 Resistor 12 ohm
4 Resistor 12 ohm
5 Phototransistor (Siemens SFH309)
6 Power supply 5 V
7 Resistor 1k ohm
8 Transistor output 0-5V

Figure VI-II. Circuit diagram of vapour bubble detection device circuit.

A simplified circuit diagram of the emitter and collector is provided in Figure VI-II. The photodiode and the transistor were chosen to be able to achieve maximum radiant intensity. A high power emitter diode was chosen, of which maximum radiant intensity is 300mW/sr. The maximum relative spectral emission is at 880 nm. Figure VI-III illustrates the most relevant characteristics of the emitter diode. From the figures it becomes evident that the radiant intensity depends on following parameters:

1) *Emitter current.* This is adjusted by supply voltage and resistors. By increasing current, the radiant intensity is increased
2) *Duty cycle.* The supply voltage is pulsed, the maximum permissible current depends on the period and the pulse width. By decreasing the pulse width and the duty cycle, more current can flow through the emitter.

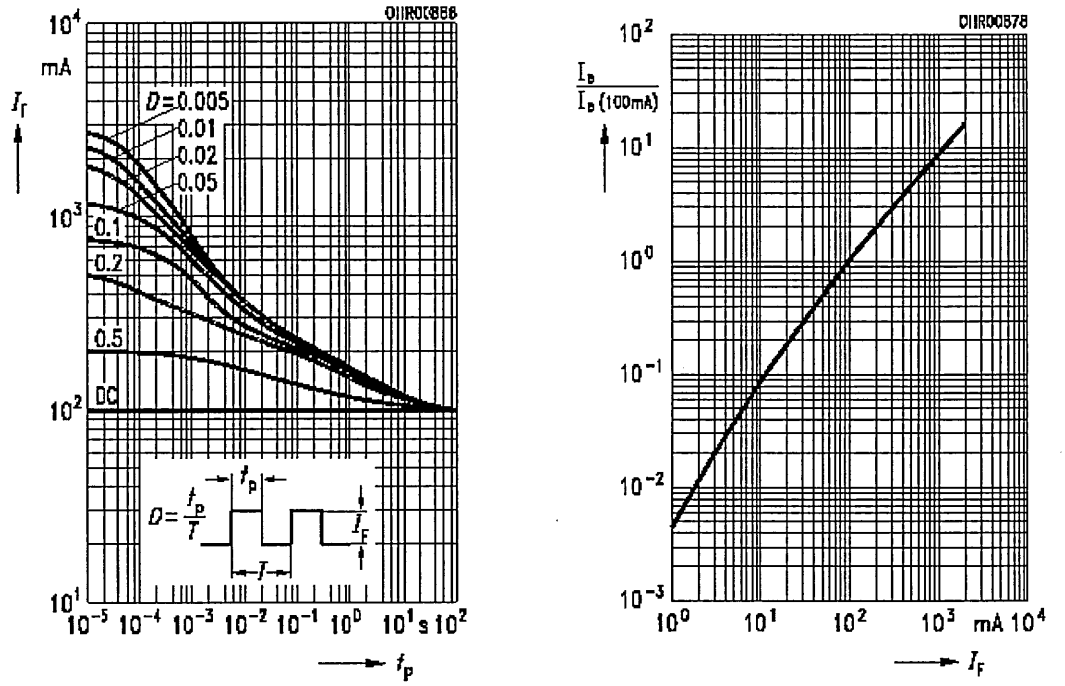

Figure VI-III. Permissible pulse handling capability (left) and radiant intensity (right) of the SFH487 emitter diode (adapted from the manufacturer's data sheet).

The phototransistor was chosen for its wide acceptance angle. The wavelength of maximum photosensitivity (850nm) is near to the emitter diode spectral emission, the spectral range of photosensitivity is from 420 nm to 1130 nm.

In the experiments, a pulse generator was used to generate the supply voltage for the emitter. The phototransistor was supplied by 5 Volt DC. The circuit was configured so that when there is no current from the phototransistor emitter to collector (no infrared connection between the two circuits), the output voltage is 5 Volts. The more current there is from emitter to collector, the less the output voltage is. When the infrared emitter is placed very close to transistor, an output voltage near to 0 V is detected.

During the initial experiments, the sensor was placed in a propane line so that the fuel flows through the sensor element, and liquid propane was circulated in the system with a pump. The fuel line was equipped with a drain line, from which the fuel was vented to the atmosphere. Vapour bubbles were generated in the fuel line and therefore inside the detector casing by opening a ball valve in the drain line.

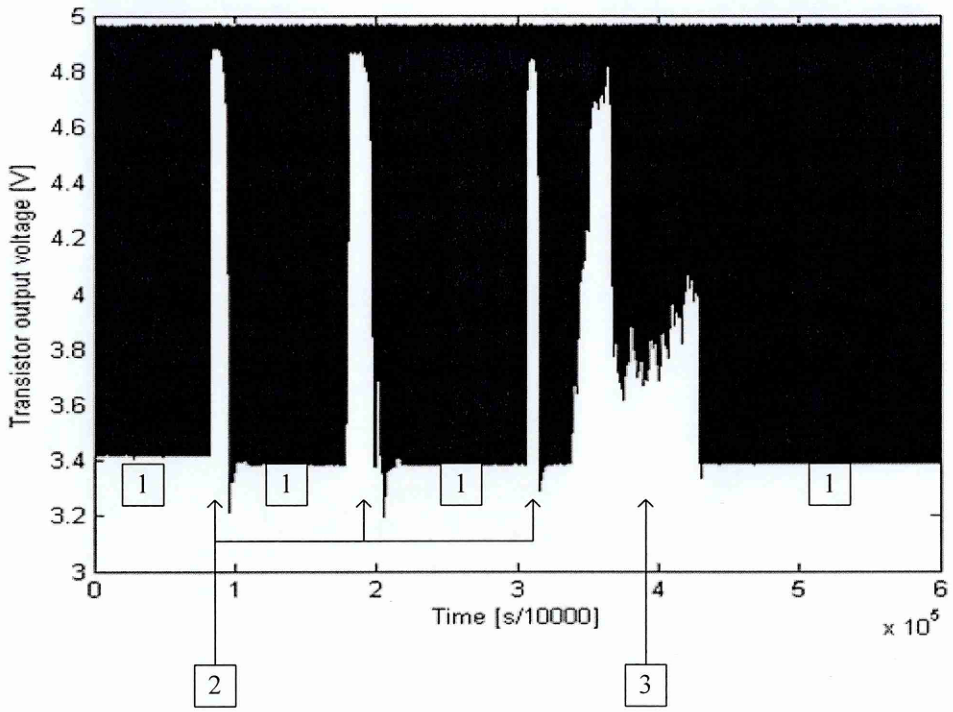

Figure VI-IV. Transistor output voltage during initial vapour bubble detection experiments.

Figure VI-IV shows the results from the vapour bubble detection device tests. The time history is 60 seconds (x-axis) and signal recorded was the phototransistor output voltage (black line). The explanations for the numbers in the figure are as follows:

1) The emitter diode supply voltage is 0 - 1.5 Volts, with period of 1.1 ms and pulse width of 0.1 ms. Therefore, the duty cycle is just less than 10 %, or, D=0.1 in Figure VI-III. Transistor output, when there is only flowing liquid propane in the fuel line, is fluctuating between 0 and 3.4 V corresponding to the fluctuations of the emitter supply voltage.
2) The drain line was opened fully. The transistor does not detect the infrared light very well because the fuel line is full of vapour bubbles and the emitted light refracts.
3) The drain line was opened carefully, in order to introduce small individual bubbles. The bubbles which resulted were small but visible. The signal shows that the signal interrupts, but the transistor output is higher that in case 2.

The difference in the infrared signal is due to light refraction caused by the bubbles, rather than absorption as initially was thought. From these initial experiments it can

be concluded that a vapour bubble detection device has successfully distinguished two different state of fuel in the duel line; a pure liquid and a liquid accompanied by vapour bubbles. This is distinguished by both the magnitude of the transistor signal voltage and the fluctuation of the minimum output voltage. Further, a simplifying assumption can be made that the magnitude and the fluctuation of the minimum voltage are relative to the amount of refraction and the amount of light refraction is relative to the amount and size of the bubbles.

VI.3.2 Experimental set-up

To demonstrate the application of the developed sensor, further experiments were carried out in a vehicle operating on liquid LPG injection. A 1993 model year Rover 812 was equipped with identical liquid pipe-coupled LPG injection system as used in the engine dynamometer tests described in Chapter V, with the exception that the vapour bubble detection device was installed in the fuel return line along with various other sensors (see Table VI-I) and the fuel was pressurised with only one pump in order to introduce vapour bubble formation in lower temperatures. The data from the sensors were acquired to a laptop computer using a National Instruments DAQ 6026 data acquisition card via SCB-2345 connector block.

Table VI-I. Sensors used in the premature vaporisation experiments.

Physical measure	Sensor Manufacturer	Sensor Model	Sensor Type
Fuel temperature (rail in and out)	Omega	K-type	Thermocouple
Fuel tank pressure	Keller	PA-22M	Pizoresistive
Injector current	LEM HEME	PR20	
Exhaust oxygen (rich/lean)	Bosch (Nissan)		Switch
Fuel rail pressure	Keller	PA-22M	Pizoresistive
Fuel flow (rail in)	Floscan 20		Turbine

The vehicle was run both with petrol and LPG and the fuels were switched with a series of relays. The injection of the both fuels was controlled by the OEM ECU. Injection strategy of the ECU was a multipoint, but non-sequential with lambda feedback control. The LPG injectors were equipped with the flow area restrictors described in Chapter III, but the available pressure range was not wide enough to compensate the fuelling, and the closed-loop lambda control of the ECU was too slow to be able to correct the fuelling. As a result, the engine was operating in richer than

stoichiometric AFR. However, this was considered insignificant for the experiments described in this chapter.

The vehicle was started from cold (5-7°C) and the ambient temperature was the same during each test. Three sets of measurements were taken. For the first set, the fuel rail pressure was set to approximately 7 bar, which was 2 bar above the fuel saturation pressure in the tank. The vehicle was operated with LPG, and 10 seconds of data was recorded once in every 30 seconds. The vehicle was stationary, but the engine speed was maintained in constant 2000 rpm in order to minimise the time for the engine warm-up and minimise the heat transfer from the engine to the cold ambient air. The data acquisition from the sensors was not continuous because of the limitations set by the memory of the laptop computer and high data sampling rate required by the vapour bubble detector output. The measurement was continued until the temperature in the fuel rail increased to a level, where it completely vaporised and the engine did not get enough fuel to run.

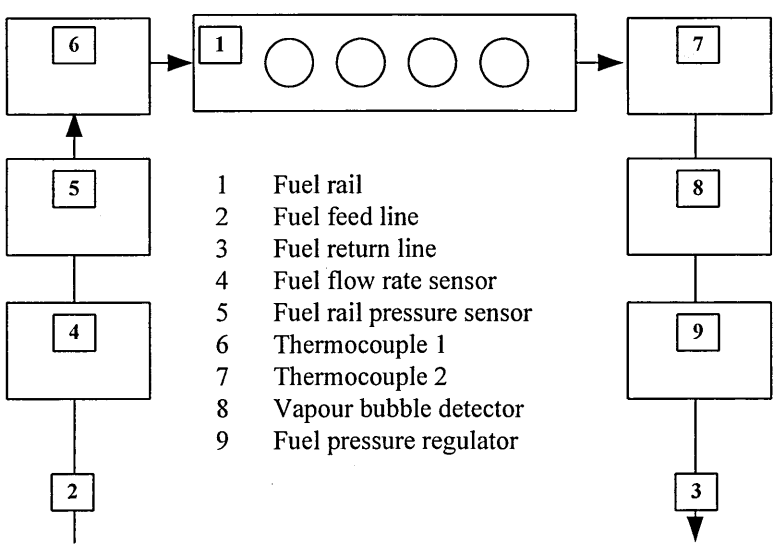

Figure VI-V. Fundamental diagram of the sensor configuration in the engine bay.

The same measurements were repeated also for the fuel rail pressures of 8.3 bar and 9 bar, with the intention to keep all the other system parameters the same for each set of measurements.

VI.4 RESULTS

Figure VI-VI shows the measured engine bay temperature during the three tests. The thermocouple was placed between the engine block and the remote fuel rail, approximately 20 mm away from the fuel rail. The plot demonstrates similar engine bay temperature evolution during the three experiments.

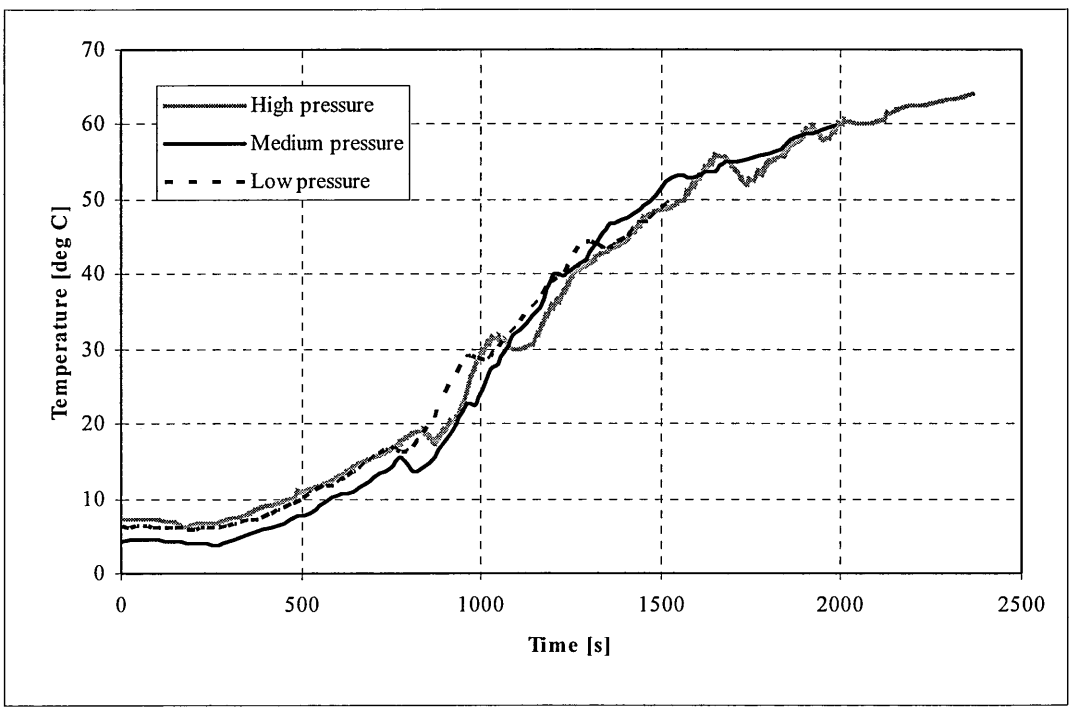

Figure VI-VI. Engine bay temperature.

Figure VI-VII shows the simultaneous time history of the fuel outlet temperature, which shows a clear difference in the temperature between the three fuel pressures. The highest rail pressure case also has the highest temperature, while in the lowest fuel pressure case the fuel temperature rises more slowly. This indicates that the heat transfer rate is higher for the high pressure and low flow rate case.

Figure VI-VIII shows the plot of the averaged lowest voltage value of the vapour bubble detector output. There is clear difference in the voltage between the different fuel pressures at the end of the measurement period, showing that the lowest pressure fuel starts vaporising earlier than the higher fuel pressure. This transition in the signal in all the cases is very strong. However, there is another, less radical transition evident

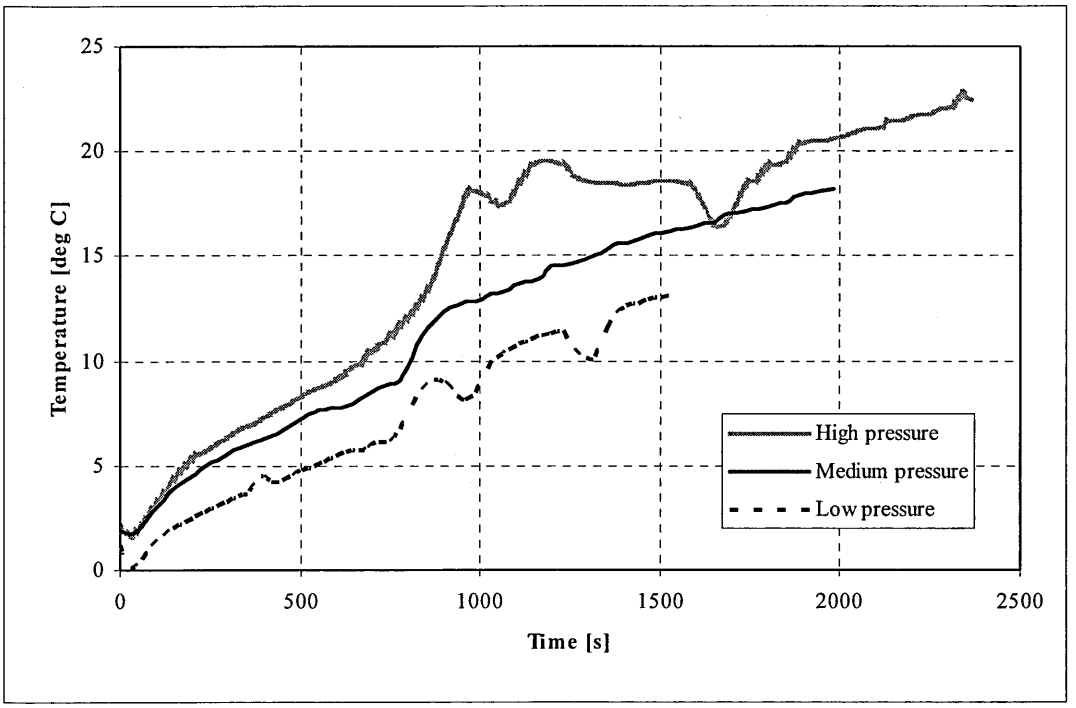

Figure VI-VII. Fuel temperature in the fuel rail.

the plot. This occurs approximately 800 seconds after the start of the measurements, when the signal gets weaker (voltage increases), but only slightly. After this transition the signal stays at approximately the same level until complete vaporisation occurs.

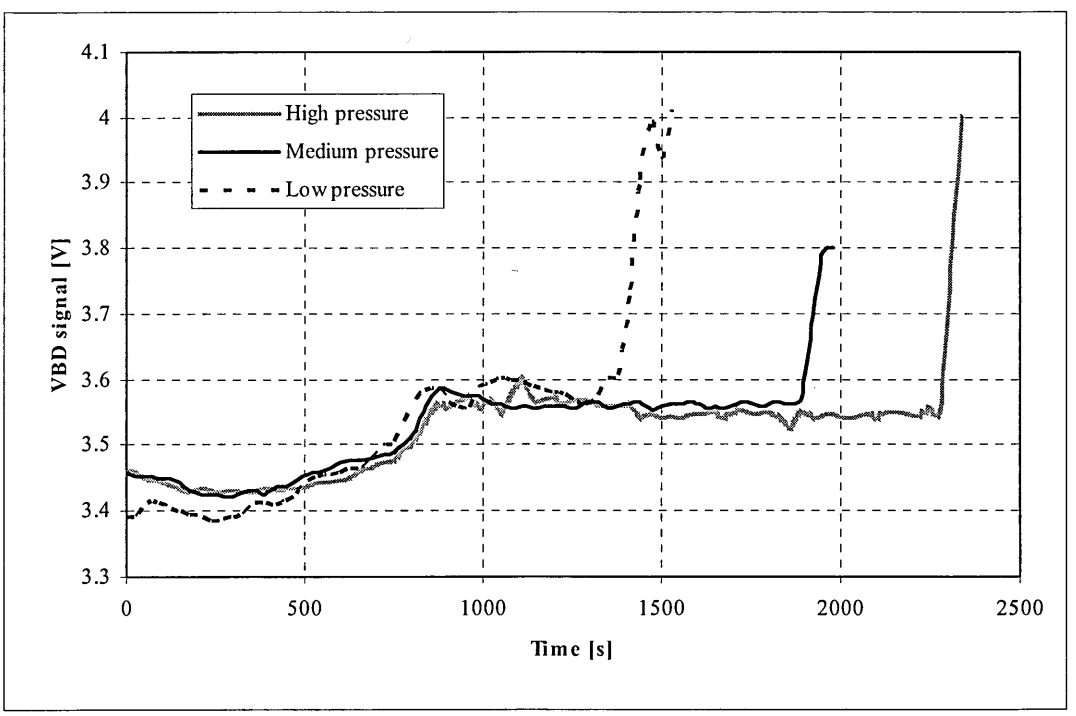

Figure VI-VIII. Vapour bubble detector minimum voltage.

This behaviour is also evident in the Figure VI-IX, where the standard deviation of the average minimum vapour bubble detector voltage is plotted. The standard deviation rises sharply simultaneously with the voltage value at the time of complete vaporisation. Also, simultaneously with the less significant transition period observed in the detector voltage, there is a small but clear increase in the standard deviation plot.

Another interesting observation is that, unlike the complete vaporisation, the smaller transition period seems to occur at the same time for all fuel pressure cases. There is only a slight time difference which suggests that this decay in the emitter diode signal accompanied with the increase in the standard deviation, occurs earlier for the low pressure case. This behaviour is further discussed in the following section.

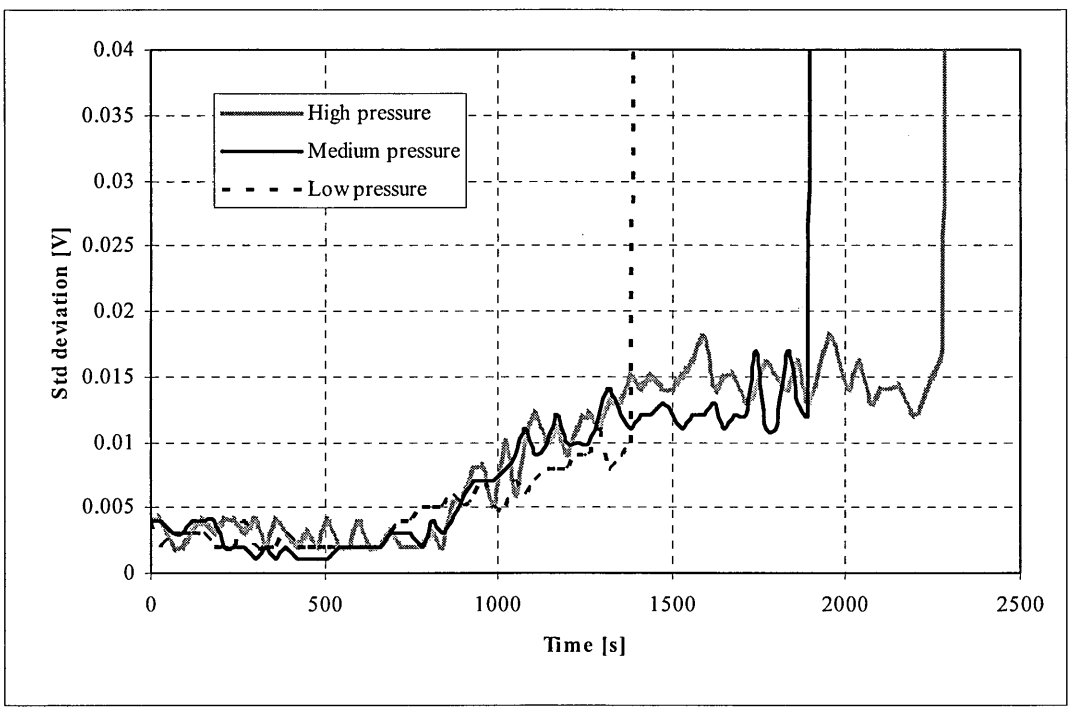

Figure VI-IX. Vapour bubble detector minimum voltage standard deviation.

VI.5 DISCUSSION

Figure VI-X shows the results of the experiments plotted with the propane saturation curve. The series B plots show the temperatures against the pressures of the complete vaporisation event detected by the vapour bubble detector device. The three markers represent the lowest, average and highest fuel rail pressure value observed during the 10 second measurement period. The fuel rail pressure fluctuation is due to the injector opening and closing. The two adjacent sets of markers for each rail pressure are from two consecutive sets of measurements, between which the vapour bubble detector output significantly changes.

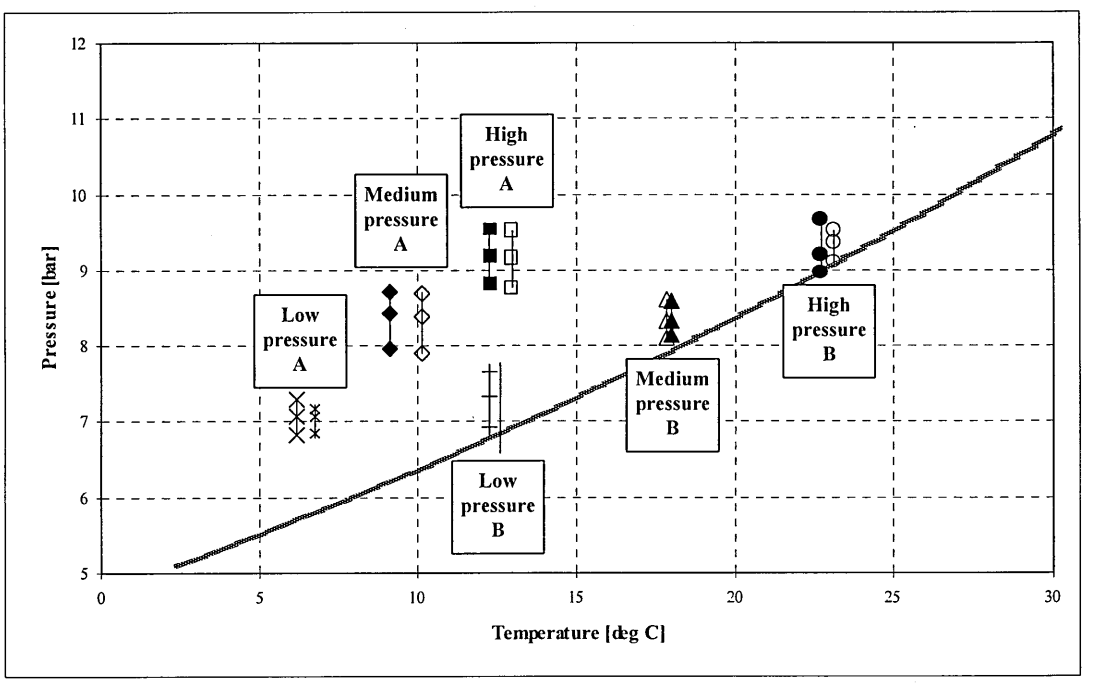

Figure VI-X. Vapour bubble detector output plotted with the propane saturation curve.

The series B plots clearly shows that the complete vaporisation detected by the device occurs when the temperature rises close to the saturation temperature, which demonstrates that the device is capable of distinguishing the phase change event.

However, in the case of complete vaporisation, the detection of the event does not prevent the consequent effect on the fuel metering and hence the engine performance and emissions. During the experiments, it was observed that the complete vaporisation event was very sudden and the effect of fuel metering was so radical that

severe misfiring was evident because of the too lean mixture. This condition should clearly be avoided.

The series A points in the Figure VI-X represent the state of the fuel when the weaker transient condition is detected by the vapour bubble detector. The locations of the points in the figure indicate that this transient occurs when the fuel rail temperature measured by the thermocouples is still well below the propane saturation temperature. Also, it is noticeable that in the fuel temperature trace in Figure VI-VII, there is significant temperature rise at the same time, but the temperature is not the same for all the pressure cases. Instead, this transient seems to correspond more to the saturation properties, which are evident in Figure VI-X. Even though some temperature-dependency is expected in the IR light emission detected by the collector due to temperature-dependency of the absorption properties and refractive index of the fluid, the detector output indicating the weak transient condition can not be explained only by the temperature transient because

a. the detector output voltage or the standard deviation does not respond to temperature gradient anywhere else during the measurement
b. the temperature transient occurs at different temperatures under different pressures

Taking into account these considerations, it is suggested that the weak transient is caused by small migrating vapour bubbles passing the IR light path. This suggestion is supported by the evident saturation property-dependency of the transient event. However, the temperature at which the event occurs does not have a constant relationship with the saturation temperature, i.e. in lower fuel pressure the temperature difference between the point A and B (in Figure VI-X) is not consistent with the three fuel pressures. In lower pressure, this temperature difference (which also corresponds to temporal difference evident in Figure VI-VIII and Figure VI-IX) is significantly smaller than in the high pressure cases. This suggests that the small vapour bubbles are formed somewhere in the fuel rail

a. where the temperature is locally significantly higher than the average fuel temperature

b. where the temperature increases significantly faster than the average fuel temperature (and is not affected by the flow rate) and the engine bay temperature
c. where the high temperature area is so small that it does not affect the average fuel temperature significantly, i.e. the heat transfer rate in the spot is less significant than the average radiation and conduction to the fuel rail

Therefore, it is suggested that the small bubbles form in a local "hot spot", which is affected by the significantly higher heat transfer rate from the engine than the average heat transfer to the fuel. This could from a fuel rail contact to the engine block. In any case, the crucial consideration is if the vapour bubbles form in the vicinity of the injector needle or if the bubbles are big enough to cause a vapour lock at the injector tip location, which would have an affect on the fuel metering. During the experiments described in this chapter, no deterioration in engine performance was observed as a result of the weak transient condition detected by the bubble detector. However, as explained previously, the mixture was richer than stoichiometric during the experiments, and it is completely possible that there was a small tendency for the mixture to have become weaker as a result of the small bubbles. If this was the case, it would have been noticed if a wide-band lambda sensor would have been used during these experiments, which is one of the major point of criticisms towards the experiments the author would like to address. The validation of the vapour bubble detector and the effect of the small bubbles on the engine performance would only have been properly studied if the above mentioned exhaust gas monitoring method was used. However, the detection of small bubbles is very useful from the engine control point of view, the detector signal gives the control unit the possibility to react (whether it is done by increasing the boost pressure or the flow rate using an additional pump or switching to petrol operation or some other method) before the complete vaporisation and the consequent deterioration in engine performance and emissions occur.

Further, it was evident from the results that the fuel flow rate has a significant effect on the heat transfer from the engine to the fuel, although it is also evident that the most significant factor in preventing the premature vaporisation in the fuel rail is the fuel pressure. In the type of pump – regulator system used in the experiments, the

higher pressure is achieved at the cost of decreased fuel flow rate and the consequent higher heat transfer to the fuel, even the few bar higher pressure resulted in significantly longer time from the starting of the cold engine until the fuel vaporised completely.

The ambient conditions in which the experiments were carried out were supposed to have been the "worst case scenario" in terms of the fuel premature vaporisation, when the ambient temperature was relatively cold and consequently the tank pressure was also low (in saturation pressure). The engine bay temperature increased to a very high level relative to the tank pressure, which essentially remained in the same ambient temperature (and saturation pressure). The pressure increase between the tank and the fuel rail was limited by the boost pressure of the pump. In these experiments only one pump was used in order to limit the boost pressure. These conditions (low ambient temperature and low boost pressure) were chosen for the experiments in order to create the conditions where vapour bubbles were most likely to form and premature vaporisation was most likely to occur. From the results presented in this chapter it is evident that this was indeed the case, and it is clear that the use of only one standard pump with a boost pressure of 4 bar is not adequate in liquid injection LPG systems, as it was not particularly difficult to get the fuel to vaporise in the fuel rail. It is true though that the engine revolutions were significantly higher than normal idle conditions in order to enhance the engine temperature rise, and the vehicle was stationary to prevent heat transfer to cold air flow for the same reason, but the saturation conditions were reached, even considering these "artificial" conditions, very fast. It is appropriate to emphasize that the liquid injection system developed in this work applies the twin pump system, with twice the boost pressure available, but the similar vaporisation experiments for this system is left for future work.

VI.6 CONCLUSIONS

The major conclusions from the work described in this chapter can be summarised as:

1. A low cost device to detect vapour bubbles in the LPG fuel line was successfully designed and developed.

2. The initial tests carried out suggested that the device is capable of detecting a phase change in the fuel line (distinguishing between vapour and liquid LPG fuel), but also detecting single vapour bubbles migrating with the liquid fuel in the fuel rail.

3. From the experiments performed on a liquid injection LPG vehicle, it was proved that the sensor was capable of detecting the complete phase change which occurs in the fuel rail when the fuel temperature increases above the saturation pressure. This was proved using three different fuel pressures.

4. The experiments in the vehicle showed that the sensor is also capable of detecting small vapour bubbles, which are formed in local hot spots and migrated with the liquid fuel, before the fuel temperature reaches saturation conditions.

5. The experiments showed that the fuel flow rate has a significant effect on the heat transfer to the fuel, but also that the fuel pressure is more significant factor when considering the prevention of premature vaporisation.

6. The standard single pump system is not adequate to prevent premature vaporisation in the fuel rail

VII. DISCUSSION

The main motivation for the work described in this thesis was to:

a. Improve engine performance of aftermarket LPG conversion systems
b. Study the combustion and performance characteristics of non-optimised LPLI bi-fuel systems
c. Improve mixture control in aftermarket LPG conversion systems
d. Improve engine calibration and OBD compatibility in aftermarket conversion systems
e. Improve control over in-system vaporisation in liquid injection LPG systems

This chapter describes the achievements of the work and the significance of the findings. While solutions to improving the mixture formation, preventing backfires, and improving engine performance by using liquid injection systems were found, implementing these solutions in commercial conversion systems requires some further practical engineering efforts as is explained later in this chapter. For preventing the premature vaporisation in the fuel rail, more than one method was found to improve the existing systems. Furthermore, a significant improvement in the knowledge and understanding some system processes, like mixture formation in non-optimised LPLI engines, vaporisation and fluid transport in pipe-coupled injection systems and vapour bubble formation was also gained. However, one of the major system requirement, the fuelling control and OBD compatibility could not be adequately tested within the time and budget of this study.

A significant part of the work presented in this thesis was to evaluate the performance of two alternative injector configurations. From the results it is quite obvious that the favourable system in terms of engine control and performance to use in the bi-fuel is the CCLIS system. PCLIS system has got several disadvantages compared to CCLIS system. Possibly the most crucial is the effect of coupling pipes on fuelling control. The results from the spray imaging showed that the combined effect of fuel vaporisation and the pressure fluctuation in the pipes due to the injector opening and closing caused a significant transport delay in fuel flow through the pipes and

consequently, the fuel that is injected to the pipes does not reach the cylinder during the same cycle This affects the engine operation in several ways.

VII.1 IMPROVEMENT IN THE ENGINE PERFORMANCE

The engine performance with CCLIS system was found to be 0.5-2% lower than the performance during petrol operation. The reduction in performance is due to different combustion characteristics of LPG, and the performance was also found to be similar to petrol when the ignition timing was be optimised for LPLI operation. This result showed that the newly developed aftermarket conversion system offers a significant benefit in engine performance when compared to existing systems.

The evaluation of the developed injection system by combustion analysis in 4-cylinder test engine showed some important aspects of LPG combustion which were not previously reported in scientific literature. Even though the vapour injection bi-fuel aftermarket conversion technology is in some aspects highly developed, it was not in prior knowledge that the encountered engine power loss of 10%, reported in several studies, is actually a combined result from loss in volumetric efficiency and ill combustion phasing. However, the power loss due to ill phasing in the combustion is not that severe in the LPG injection system, where the fuel is injected directly to the manifold. This was suggested to be partly a result of lower charge temperatures and partly mixture stratification in the combustion chamber, which actually is considered to be a negative characteristic of an engine which is designed to operate in the stoichiometric AFR. Considering a non-optimised LPG bi-fuel system, this mixture stratification and the consequent increase in combustion duration is actually very beneficial, because the combustion duration is similar to that of petrol, and hence the combustion phasing and MBT – timing is also similar to that of petrol.

Another interesting finding from the combustion analysis was that as the combustion duration was shorter for the partly pre-vaporised systems (PCLIS), to achieve the MBT – timing, the ignition was retarded. In prior knowledge, it has been claimed that the engine performance can be improved, compared to petrol, with LPG systems due to higher octane rating by advancing the ignition, but only in spark-optimised LPG conversion engines. This is based on the fact that often in production engines the

ignition timing is retarded from the MBT – timing in order to avoid knock, while this limitation is not necessary in LPG engines because of the higher knock resistance. However, it appears that the LPG operation in non-optimised systems actually benefits from the knock-limited ignition timing of petrol engines, when the ignition is retarded from the petrol MBT – timing. Retarding the ignition shifts the combustion phasing closer to the LPG MBT – timing.

The engine experiments showed that the engine performance is reduced by approximately 5 % with the PCLIS configuration when compared to petrol operation. Even though the comparison with the vapour injection system in the same engine was not completed due to time constraints, the results found in literature suggests that most vapour injection systems have a 10% power loss compared to the petrol operation. This suggests that there is performance benefit associated with the PCLIS configuration in comparison with the vapour injection system. This was also evident from the cylinder temperature measurements, when a reduction in cylinder temperature was accounted for during PCLIS operation, indicating that the performance improvement is due to the charge cooling effect. The charge cooling effect is not possible with vapour injection systems. Also, the apparent intake air cooling during PCLIS operation was further evidence that the fuel flow in the pipe-coupled system is essentially two-phase flow.

VII.2 IMPROVEMENT IN MIXTURE CONTROL

The spray images from the PCLIS system suggested that the fuel starts vaporising in the coupling pipes resulting in longer fuel travelling times through the pipe. It was evident that the fuel continued arriving in the constant volume chamber through the entire injection (and engine) cycle. This observation leads to first point of criticism concerning the system requirements. In modern petrol engines, one of the most crucial parameters in emissions control is the accurate and fast AFR control. This is implemented in MPI engines by sequential injection, which means that the fuelling of each cylinder can be controlled independently. One of the main motivations for the development of the new aftermarket conversion system was to achieve similar sequential fuel metering with LPG operation. Even though the present vapour injection systems are called sequential because there are four injectors, the systems do not offer the same benefit than petrol because of the considerably longer injection durations. However, it is apparent that the PCLIS system does not offer any improvement towards more sequential mixture formation.

Also, the long fluid travelling times in the PCLIS lead to the situation where the intake manifold is filled with LPG fuel due to inaccurate injection timing. This was also evident during the engine experiments when some backfiring was experienced during PCLIS operation. One of the main motivations of the project was to develop an aftermarket conversion bi-fuel system which prevents the backfiring problem associated in vapour injection systems. The PCLIS does not offer any benefit in terms of reducing the backfiring when compared to vapour injection system.

There was a significant variation in the fuel flow density during the injection operation period, which suggested that the density of fuel entering the manifold varied through the engine cycle. This will address a problem during engine transients, when either the engine speed or load changes (or both). Consequently, the injection duty cycle and period changes and also the phasing of the higher density part of the fuel flow enter the manifold at different part of the cycle relative to the intake valve opening. This makes the engine operation worse when comparing the vapour injection system, where the fuel injected through the pipes is essentially uniform, and the mass of fuel entering to the cylinder in transient conditions can be controlled by controlling

the injection duration and injection timing. Also, during the spray imaging, significant cycle-to-cycle variations were observed. This causes a potential problem even in steady state engine operation, if the intake valve closing coincides with the high density and high cycle-to-cycle-variation part of the fuel flow entering the manifold and cylinder. As transient conditions were not measured during the engine experiments, these potential problems were not accounted for during the engine experiments. However, it is obvious that the use of PCLIS configuration is not offering any improvement in mixture control when compared to the vapour injection system. Concerning the success of the study on PCLIS configuration it is apparent that even though the system did not meet the initial system requirements and did not show required improvements in all areas, this type of system has not been evaluated in scientific literature before, and the knowledge and understanding of partly pre-vaporised mixture formation systems was significantly increased as a result of this study.

However, the measurements showed that when using the CCLIS system, the mixture formation process is similar to that of petrol, and the mixture could be controlled as accurately as petrol. There was no backfires encountered during engine operation due to accurate mixture control. Therefore, it was demonstrated that the mixture formation was significantly improved compared to vapour injection systems, but this was only achieved with CCLIS system.

However, further discussion is appropriate concerning injection timing. The engine experiments were carried out by using only one injection timing, where the start of the injection was timed just prior to IVO. Petrol MPI engines however, use a range of injection timings, depending on the engine speed and load conditions, though usually injection timing is very close to IVO. This injection timing has presumably an effect on mixture control, and especially possible backfire events. The injection timing also affects the vaporisation and therefore mixture stratification in the combustion chamber and to the charge cooling effect. Therefore, a point of criticism has to be addressed towards the engine experiments, a further study on injection timing would have possible revealed some further evidence on the mixture formation and combustion processes.

VII.3 IMPROVEMENT IN FUELLING CALIBRATION AND OBD COMPATIBILITY

Another major motivation for the development of the new aftermarket conversion bi-fuel system was to use a fuelling control method that would not interfere with the OBD unit.

During the engine experiments, the suggested control method could not be properly tested. This was due to financial constraints of the project. The evaluation of the OBD compatibility would have required:

1. Flow rate reducing additional orifice components that would have met the accurate design specifications, or injectors with smaller original flow rates.
2. Vehicle testing using OEM injection control unit and vehicle emission testing on a vehicle dynamometer.

This was not possible for implementation within the project, and therefore the evaluation of the control method is limited to the discussion in this chapter.

The objective was to use the same control unit to control both petrol and LPG operation. This was the primary reason, why engine experiments were carried out with no optimisation of the ignition or injection timing being used. However, because a satisfactorily performing hardware based flow rate control method was not found for the purpose of these experiments, the injection duration for LPG operation was adjusted. This was possible because a programmable control unit was used instead of the OEM control unit. The stoichiometric injection map for LPG is similar to that of petrol, and it was assumed that providing that the injector orifice area can be mechanically adjusted, the fuelling can be controlled with the original petrol control unit. It is considered that using different flow rate injectors would be a better option than using any additional components.

However, as explained previously in Chapter I and Chapter III, the operation of the proposed control system depends on two factors; the adaptive learning capability of the petrol ECU and the mechanical functionality of the flow rate adjustment method. There are several issues, why the adaptive control algorithms in the ECU play very

significant role in the success of this type of bi-fuel control method. Firstly, the injection pressure during LPG operation is significantly higher than with petrol. The injectors behave very differently at higher pressures than at lower pressures, even though this is partly compensated by using low impedance injectors with LPG. The effect of the injection pressure on injector opening duration and hence the injector flow rate particularly in short injection durations is more significant at higher injection pressures, and therefore the relationship between the flow rates is not linear through the range of injection durations. Secondly, the injector flow rate changes slightly with the LPG injection system, because the injection pressure is not referenced to the manifold pressure. Therefore, even though the LPG fuelling would be hardware-calibrated (with the aid of injector orifice and fuel pressure), the ECU still needs to compensate these variations in injector flow rates.

Even though the fuelling control and calibration method was not demonstrated with the actual OBD system, the concept of a single control unit was demonstrated. The use of this type of method does not depend on the injector configuration used, and therefore it is also fair to say that both the CCLIS and PCLIS configurations offer a benefit over the vapour injection system in OBD compatibility.

VII.4 IMPROVEMENT IN PREVENTING PREMATURE VAPORISATION

The general issue in all LPLI systems, fuel vaporisation in the fuel rail, was considered in two independent approaches:

a. Using a fuel pumping system that improves the efficiency of the pumps and produces higher pressure than the conventional LPLI fuel pressure systems.
b. Developing a method to detect vapour bubbles in the fuel rail.

The prior knowledge in scientific literature consists mainly of reducing the heat transfer to the fuel. The present study showed that using the standard LPLI pump system, where the fuel is pressurised three to four bar above the saturation pressure of the fuel in the tank, is not adequate to prevent the vaporisation. This measurement was carried out in a vehicle, which was operated with the LPLI system. Due to time constraints involved, the study using the suggested improved pumping system was not completed. However, the new pumping system was used in all engine experiments and no issues in premature vaporisation were encountered.

However, an obvious issue with the suggested pumping system is its low efficiency. The pumps used in the system are operated by electric motors, and therefore be powered from the vehicle battery. The highest power demand of the pumps occur when both the ambient and tank temperature, and hence the pressure are the lowest, and the boost pressure requirement is the highest. This is also when the vehicle battery is working least efficiently, and it is the most likely situation that the battery is not capable of providing required current to the pumps. Another solution would be to use a mechanical pump. However, mechanical pumps are not suitable for aftermarket conversions, because they require modifications to the engine itself, since a driving belt is required to operate the pump.

Another, additional solution to the premature vaporisation problem was developed. This method involved development of a sensor, which can detect both complete vaporisation in the fuel rail and the formation of the small vapour bubbles in local hot spots. The sensor was primarily developed for control purposes; adding a simple feed-

back to the bi-fuel switch could make it possible for the vehicle to switch over to petrol operation in case of detection of vapour bubbles in the fuel rail.

The developed sensor improves existing systems significantly. While no suggested feed-back control method to switch fuelling exists, it has been reported that the state of fuelling has been monitored using thermocouples and fuel pressure sensors during engine experiments. This method, however, introduces several possible errors in the measurements. Firstly, the fuel composition varies significantly, which means that the fuel saturation properties vary, and the limit to vaporisation is always only an estimation. Secondly, the thermocouples measuring the flowing fuel temperature, and the pressure sensor installed in the fuel line measure only the global conditions. Vapour bubbles start forming locally in areas where the temperature rises significantly faster than global fuel temperature, or where the local pressure is lower than the global pressure. These conditions will not be detected from the information provided by the thermocouple and the pressure sensor. Also, the thermocouple and pressure sensor are more expensive and require signal monitoring from two channels.

VIII. CONCLUSIONS

VIII.1 CONCLUSIONS

Conclusions for the work described in this thesis are:

1. A prototype of a novel bi-fuel aftermarket conversion system was developed. The motivation for the development was to improve the present aftermarket conversion bi-fuel vehicle systems mainly by improving mixture formation and control, improving the engine performance during LPG operation and improving the LPG fuelling control method.

2. The prototype system is designed to use the original petrol control unit to control both petrol and LPG fuelling, and the LPG fuelling is calibrated by the installer with only changing two hardware settings. Therefore in the system, only the injector flow rates are calibrated, while all the other engine control parameters are optimised only for petrol, also during LPG operation. This is believed to improve both the calibration procedure and OBD compatibility.

3. A liquid injection system was designed for the aftermarket conversion system. The system uses low impedance fuel injectors and a novel fuel pump system concept was developed to both make it possible to use a petrol control unit to control LPG fuelling, and also to increase the margins to saturation conditions in the fuel rail.

4. The fuel spray characteristics of two alternative injector configurations, PCLIS and CCLIS injector systems were measured in a constant volume chamber. The results showed that while the CCLIS system showed significant improvement in mixture control compared to presently available aftermarket conversion systems in terms of achieving accurate sequential AFR control, the PCLIS system did not show any significant improvement in terms of AFR control.

5. The results from the imaging experiments indicated also that PCLIS configuration does not offer any significant improvements to the present vapour injection systems in terms of preventing backfires. However, an improvement was evident with the CCLIS system.

6. Both CCLIS and PCLIS systems showed approximately 5 – 10% improvement in engine power compared to vapour injection systems.

7. The system evaluation by engine experiments showed that the CCLIS system is capable of producing engine brake torque of 0.5-2% lower than petrol when all the engine control aspects, with the exception of the AFR, is optimised for petrol operation. The reduction in engine power was attributed to the different combustion characteristics of LPG and petrol, which resulted in different combustion phasing.

8. The engine experiments also showed that the engine brake torque was 5% lower with PCLIS operation compared to petrol operation. This reduction in engine power was attributed both to ill combustion phasing and decrease in volumetric efficiency due to different mixture formation process of PCLIS and CCLIS systems.

9. The charge cooling effect was evident also when in-cylinder temperatures of non-combusting cycles were measured both with the injector enabled and disabled. The results of three injection systems (petrol, CCLIS and PCLIS) were compared. The results indicated that the CCLIS system offered the greatest benefit in charge cooling, while the benefit was significantly lower with PCLIS than petrol or CCLIS.

10. The combustion duration was longer with the CCLIS that with the PCLIS system, which indicated that mixture stratification occurs in the case of CCLIS.

11. A vapour bubble detection device was developed in order to overcome the problem of premature vaporisation, which is considered a major issue with all

LPLI systems. The sensor was tested in a LPLI vehicle using fuel pressures typical to a conventional tank-pressure-referenced LPLI system. The sensor, which is based on infra-red emitter detector technology, was able to detect the complete phase change in the fuel rail, when the global saturation conditions in the fuel rail were met. It was also noticed that before the global saturation, small vapour bubbles started forming in a local hot-spot. The sensor was also able to detect these migrating small bubbles.

12. From the experiments premature vaporisation experiments, it was evident that a conventional tank-pressure-referenced fuel pressurising system is not adequate to prevent the vaporisation conditions in the fuel rail. It is concluded that the twin-pump system developed within the work presented in this thesis increases the margins to the vaporisation curve significantly, especially at low ambient temperatures.

VIII.2 RECOMMENDATIONS

The CCLIS system showed significant benefits compared to vapour injection system. However, the installation of the LPG injectors to the manifold requires very careful design of the injectors pods. A suggested configuration of bi-fuel CCLIS injector pod is illustrated in (Figure VIII-I). The injector pod accommodates both the original petrol injector and the LPG injector. While all the petrol injection equipment is original, an adapter is installed to the manifold to connect both injectors to the manifold. Adapters act also as injector pods, which take care of the fuel supply to the side-feed LPG injectors. Pods are connected to each other with flexible pipes, similar to the ones used in the prototype CCLIS configuration described in Chapter III.

The most challenging issue concerning the suggested CCLIS bi-fuel configuration is to make the adapter/pod component universal. The main problem is that the adapter/pod presented in this work is only designed for engines in which the petrol injectors are a top-feed type; the fuel rail with bottom-feed injectors are of very different size and shape. Another issue will obviously be the physical space available in the manifold, which is often limited by the air filter and the petrol fuel rail and pressure regulator. Another issue is the varying size of the original petrol injector hole in the manifold, though the bottom o-ring of a typical MPI injector seems to be fairly standardised.

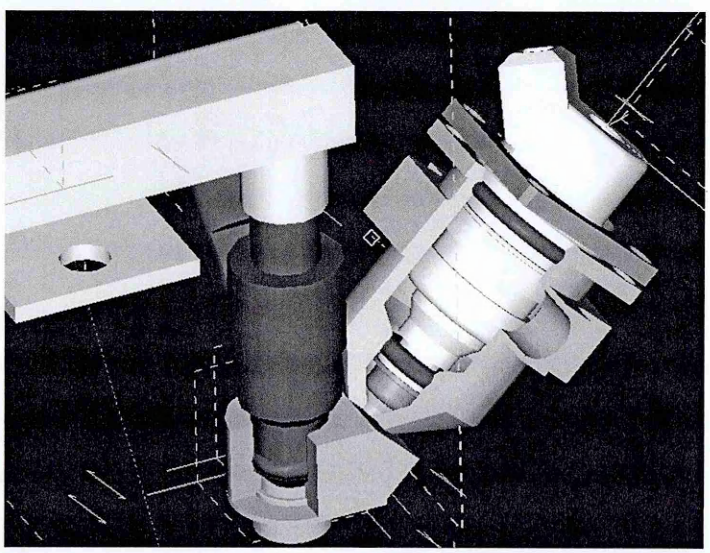

Figure VIII-I. Design for CCLIS bi-fuel arrangement. (I-DEAS model courtesy of Eric Lepot)

Another practical recommendation regarding the aftermarket system is the design of the injector orifice flow restrictor. During this thesis work it was noticed that even though the idea of using additional components for the injector is attractive because only one type of injector could be used for any type of vehicles, the design and manufacturing of these additional components would be very demanding, and therefore, very expensive. The critical dimensions of the additional flow restrictor are:

1. The centre of the orifice area has to be accurately aligned with centre of the original injector hole.
2. The orifice area diameter and shape is not allowed to vary from sample to sample.
3. The orifice outlet shape is not allowed to vary from sample to sample.
4. The face of the orifice component has to form a seal with the face of the injector tip.

Considering these requirements, it is obvious that the manufacturing tolerances of the component are very small. This inevitably leads to extensive quality monitoring efforts. Also, the component is very small to handle. Therefore, it is strongly recommended that rather than using additional flow restrictors, the several different flow rate injectors are bought from the supplier. Therefore, a consistent quality is assured.

If the practical issues described above are solved, the CCLIS system is completely ready to be installed in a vehicle. The vehicle should be controlled with a modern OBD engine control unit. It is of course recommended that several different make and model of vehicles will be used in order to evaluate the control system performance. The evaluation should be carried out on a vehicle dynamometer, where engine performance and tailpipe emissions using standard driving cycles can be measured.

VIII.3 FUTURE WORK

The future work suggested here could be divided under two titles; the work concerning the MPI LPLI aftermarket conversions systems and the work concerning future LPG systems.

VIII.3.1 Bi-fuel LPLI conversions

The obvious next stage of the work is to complete the implement hardware issues suggested in this chapter and complete the full emissions testing for a bi-fuel vehicle.

The work could be though carried on an engine dynamometer as well. There are several issues which are worth investigating in a non-optimised system; the effect of injection phasing is possibly the most obvious factor to affect the performance and emissions of the system. Also, carrying out the combustion analysis for the complete engine speed and load range would be essential, though time-consuming. The PCLIS system could be further investigated, there are several factors in designing the system which were not covered by this study. The effect of the pipe length, ambient temperature and the pipe material on the rate of vaporisation and travelling time would be important to investigate. Also, an alternative imaging method (for example LSD), which would provide more quantitative information on the state of the emerging fuel, could be applied.

VIII.3.2 DISI engines

The natural continuity for this work would be to study the mixture formation and combustion in a DISI engine. The most interesting and challenging aspect seems to be the high temperatures in the fuel injector; the success of an LPG system depends largely on preventing the premature vaporisation in the fuel rail and inside the injector. Although the injection pressures are significantly higher with the DISI system compared to MPI system, the critical temperature of 97°C would limit the operation. A DISI LPG engine should be optimised for LPG use.

LIST OF REFERENCES

Aakko, P, Nylund N-O. Particle emissions at moderate and cold temperature using different fuels. *SAE Technical Paper Series, 2003-01-2385.* 2003.

Abd-Alla, T, Pucher, G R, Bardon, M F, Gardiner, D P. Effects of spark characteristics on engine combustion with gasoline and propane. *SAE Technical Paper Series, 2003-01-3264.* 2003.

Acedo, E, Acosta, O, Angulo, A, Enriquez, O, Krishnaswamy, H K, Loya, R, Perez, J, Olson, S A, Saenz, S, Vega, F, Villalobos, J A, Worth, B, Robbins, C and Wicker, R B 1997 UTEP LPP-FI propane challenge vehicle. *SAE Special Publications, v 1360.* 1998.

Alger, T, Huang, Y, Hall, M, Matthews, R. Liquid film evaporation off the piston of a direct injection gasoline engine. *SAE Technical Paper Series, 2001-01-1204.* 2001.

Anderson, E, Wandrie, H, Celmins, J, Bouboulis J, Botha, C, Dalton, J, Klug, D, Kish, T Sljivar, S and Sullivan, J A Y. The GMI fuel injected propane conversion vehicle. *SAE Special Publications, v 1360.* 1998.

Andersson, J D, Wedekind, B. G. A, Hall, D, Stradling, R, Wilson, G. DETR/SMMT/CONCAWE Particulate Research Programme: Light duty results. *SAE Technical Paper Series, 2001-01-3577.* 2001.

Andersson, P and Eriksson, L. Cylinder air charge estimator in turbocharged SI engines. *SAE Technical Paper Series, 2004-01-1366.* 2004.

Annand, W J D. Heat transfer in the cylinders of reciprocating internal combustion engines. *Proceedings of Institution of Mechanical Engineers, Part D, v 177, n 36, p 397-990.* 1963.

Badr, O, Alsayed, N, Manaf, M. A parametric study on the lean misfiring and knocking limits on gas-fuelled spark ignition engines. *Applied thermal engineering, v 18, n 7, p 579-594.* 1998.

Bauer, Horst. Gasoline-engine management . Stuttgart, Robert Bosch, 1st Edition. 1999.

Bauer, Horst. Gasoline-engine management . Plochingen Germany, Robert Bosch GmbH and copublished by Profesional Engineering Publishing Ltd, 2nd Edition. 2004.

Bechtold, R L. Alternative fuels guidebook : properties, storage, dispensing and vehicle facility modifications. Warrendale, Society of Automotive Engineers.1997.

Bella, G, Pontoppidan, M, and Rocco, V. Mixture formation in SI-engine intake systems: a simplified theoretical model with experimental verification. *American Society of Mechanical Engineers, Internal Combustion Engine Division (Publication) ICE, v 26, n 3, p 19-33.* 1996.

Berckmuller, M, Tait, N, Greenhalgh D A. The time history of the mixture formation process in a lean=burn stratified-charge engine. *SAE Technical Paper Series, 961929.* 1996.

Bilcan, A, Le Corre, O, Tazerout, M, Ramesh, A, Ganesan, S. Characterization of the LPG-diesel, dual-fuel combustion. *SAE Technical Paper Series, 2001-28-0036.* 2001.

Bood, J, Bengtsson, P-E, Mauss, F, Burgdorf, K, Denbratt, I. Knock in spark-ignition engines: end-gas temperature measurements using rotational CARS and detailed kinetic calculations of the autoignition process. *SAE Technical Paper Series, 971669.* 1997.

Boyan, X, Furuyama, M. Jet characteristics of CNG injector with MPI system. *JSAE review, v 19, n 3, p 229-234.* 1998.

Brasoveanu, D and Gupta, A K. Effect of pressure and velocity distribution on propane and air mixing under reacting and reacting conditions. *SAE Technical Paper Series, 1999-01-2604. 1999.*

Brunt, M F J and Emtage, A L. Evaluation of burn rate routines and analysis errors. *SAE Technical Paper Series, 970037.* 1997.

Brunt, M F J, Rai, H, Emtage, A L. The calculation of heat release energy from engine cylinder pressure data. *SAE Technical Paper Series, 981052. 1998.*

Chang, C-C, Lo, J-G, Wang, J-L. Assessment of reducing ozone forming potential for vehicles using liquefied petroleum gas as an alternative fuel. *Atmospheric Environment, v 35, n 35, p 6201-6211. 2001.*

Chen, Z , Konno, M, Goto, S. Study on homogenous premixed charge CI engine fueled with LPG. *JSAE Review, v 22, n 3, p 265-270.* 2001.

Chiriac, R, Apostolescu, N. Cyclic variability patterns in a spark ignition engine fueled with LPG. *SAE Technical Paper Series, 2004-01-1920.* 2004.

Chiu, J and Matthews, R. The Texas Project: Part 2 - control system characteristics of aftermarket CNG and LNG conversions for light-duty vehicles. *SAE Technical Paper Series, 962099.* 1996.

Cho, H, Lee, J, Lee, K. Measurements of cycle resolved air-fuel ratio near the spark plug in a spark ignition engine. *Proceedings of the Institution of Mechanical Engineers, Part D: Journal of Automobile Engineering, v 214, n 4, p 421-434.* 2000.

Chun, K M, Heywood, J B. Estimating Heat-Release and mass of mixture burned from spark-ignition engine pressure data. *Combustion Science and technology, v 54 , p 133-143.* 1987.

Cipollone, R, Villante, C. A/F and liquid-phase control in LPG-injected, spark-ignition ICE. *SAE Technical Paper Series, 2000-01-2974.* 2000a.

Cipollone, R, Villante, C. A dynamical model for the design of LPG liquid phase injection system. *American Society of Mechanical Engineers, Internal Combustion Engine Division (Publication) ICE, v 35, n 2, p 29-37.* 2000b.

Cortese, M, Xue, A, Peddieson, J, Jennings, P, Sellers, K, Chai, J and Munukutla, S. Modeling of the Fuel Line Wave Propagation Induced by the Injector Operation. *SAE Technical Paper Series, 2000-01-563.* 2000.

Cottrill, J. Evaluation of automotive oxygen sensors for steady-state air/fuel ratio control and its OBD characteristics on natural gas engines. *Engine Division ASME, ICE Spring Technical Conference of the ASME Internal Combustion.* 1999.

Daniels, C F. The comparison of mass fraction burned obtained from the cylinder pressure signal and spark plug ion signal. *SAE Technical Paper Series, 980140.* 1998.

Dill, S, Anderson, E, Taylor, B, Dunbar, B, Baker, M, Tischler, T, Wandrie, H, Cheroudi, B and Barak, P. Conversion of engine fuel system from gasoline injection to liquid propane

injection. *SAE Special Publications, v 1360.* 1998.

Dutczak, J and Golec, K. Spark ignition engine fuelled by means of liquid propane-butane injection. *SAE Technical Paper Series, 2002-01-1689.* 2002.

Egnell, R. Combustion diagnostics by means of multizone heat release analysis and NO calculation. *SAE Technical Paper Series, 981424.* 1998.

Eichelberg, G. Some new investigations on old engine problems. Engineering, v 148, p 463-547. 1939.

Emi, M, Suzuki, Y, Yamada, Y, Ishii, H, Kimura, S, Ogawa, H, Enomoto, Y. Development of thin film thermocouple for measurement of instantaneous heat flux flowing into the cast iron combustion chamber wall. *JSAE Review, v 23, n 3, p 379-382.* 2002.

Energy Savings Trust. Road fuel gases and their contribution to clean low-carbon transport. EST. 2003.

Eriksson, L. Requirements for and a systematic method for identifying heat-release model parameters. *SAE Technical Paper Series, 980626.* 1998.

European Union. http://europa.eu.int/comm/environment/air/legis.htm#transport. Accessed 20/9/2004. 2004.

Fansler, T D, Stojkovic, B, Drake, M C and Rosalik, M E. Local fuel concentration measurements in internal combustion engines using spark-emission spectroscopy. *Applied Physics B: Lasers and Optics, v 75, n 4-5, p 577-590.* 2002.

Ferrera, M, Gerini, A, Casacci, C. Advanced electronic controlled lpg liquid injection system for automotive applications. *SAE Technical Paper Series, 1999-24-0028.* 1999.

Frith, A M, Gent, C R and Beaumont, A J. Adaptive control of gasoline engine air-fuel ratio using artificial neural networks. *IEE Conference Publication, n 409, p 274-278.* 1995.

Gatowski, J A, Balles, E N, Chun, K M, Nelson, F E, Ekchian, J A, Heywood, J B. Heat release analysis of engine pressure data. *SAE Technical Paper Series, 841359.* 1984.

Gerini, A, Monnier, G, Bonetto, R. Ultra low emissions vehicle using LPG engine fuel. *SAE Technical Paper Series, 961079.* 1996.

Gimbres, D, Boree, J, Bazile, R, Charnay, G. Effect of air-pulsed flow on the mixture preparation for the optimization of natural gas SI engine. *SAE Technical Paper Series, 1999-01-2905.* 1999.

Guezennec, Y G and Hamama, W. Two-zone heat release analysis of combustion data and calibration of heat transfer correlation in an I.C. engine. SAE Technical Paper Series, 1999-01-0218. 1999.

Guibet, J C. Fuels and engines : technology, energy, environment. Paris , Editions Techip. 1999.

Heywood, John B. Internal combustion engine fundamentals. McGraw-Hill. 1988.

Homeyer, C, Choi, G H, Kim, J H. Effects of different LPG fuel systems on performances of variable compression ratio single cylinder engine. *American Society of Mechanical Engineers, Internal Combustion Engine Division (Publication) ICE, v 39, p 369-375.* 2002.

Hyun, G, Lee, D, Goto, S. KIVA simulation for mixture formation processes in an in-cylinder-injected LPG SI engine. *SAE Technical Paper Series, 2000-01-2805.* 2000.

Hyun, G, Oguma, G, Goto, S. CFD study of an LPG DI SI engine for heavy-duty vehicles. *SAE Technical Paper Series, 2002-01-1648.* 2002.

Imatake, N, Saito, K and Morishima S. Quantitative Analysis of Fuel Behaviour in Port-Injection Gasoline Engines. *SAE Technical Paper Series, 971639.* 1997.

Jaasma, S. Heat balance improvements for LPI systems. *SAE Technical Paper Series, 1999-25-0155.* 1999.

Jermy, M C, Greenhalgh, D A. Planar dropsizing by elastic and fluorescence scattering in sprays too dense for phase Doppler measurement. *Applied Physics B: Lasers and Optics, v 71, n 5, p 703-710.* 2000.

Kang, K, Kim, C, Lee, J, Lee, D, Jung, N, Rhee, J, Ko, E, Kang, J. Performance and emissions of an 11L LPG MPI engine for city buses. *SAE Technical Paper Series, 2002-01-0448.* 2002.

Kang, K, Kim, C, Lee, J, Lee, D, Jung, N, Rhee, J, Ko, E, Kang, J. Development of an llL heavy-duty engine for city bus using LPG MPI system. *SAE Technical Paper Series, 2001-08-0038* . 2001b.

Kang, K, Lee, D, Oh, S, Kim, C. Performance of an liquid phaseLPG injection engine for heavy-duty vehicles. *SAE Technical Paper Series, 2001-01-1958.* 2001a.

Kawahara, N, Tomita, E, Kamakura, H. Transient temperature measurement of gas using fiber optic heterodyne interferometry. *SAE Technical Paper Series, 2001-01-1922.* 2001.

Kim, C U and Bae, C S . Speciated hydrocarbon emissions from a gas-fuelled spark-ignition engine with various operating parameters. *Proceedings of the Institution of Mechanical Engineers, Part D: Journal of Automobile Engineering, v 214, n 7, p 795-808.* 2000.

Kim, C, Lee, D, Oh, S, Kang, K, Choi, H, Min, K. Enhancing performance and combustion of an LPG MPI engine for heavy duty vehicles. *SAE Technical Paper Series, 2002-01-0449.* 2002.

Kim, C, Oh, S, Lee, Y, Kang, K, Lee, D. Characteristics of icing phenomenon on injector in a liquid phase LPG injection SI engine. *SAE Technical Paper Series, 2003-01-1919.* 2003.

Kim, I, Lee, D, Goto, S. Combustion Process Modelling using a mechanism in an LPG Lean-burn SI engine . *SAE Technical Paper Series, 1999-01-3481.* 1999.

Knubben, G and van der Geld, C W M. Drop size distribution evolution after continuos or intermittent injection of butane or propane in a confined air flow. *Applied Thermal Engineering, v 21, p 787-811.* 2001.

Le Moyne, L and Moine, X. Application of a physical model in engine control: compensation of wall wetting by fluid mechanics. *International Journal of Vehicle Design, v 22, n 3, p 216-226.* 1999.

Lee, D, Goto, S, Kim, I, Motohashi, M. Spectroscopic investigation of the combustion process in an LPG lean-burn SI engine. *SAE Technical Paper Series, 1999-01-3510.* 1999b.

Lee, D, Shakal, J, Goto, S, Ishikawa, H. Flame speed measurements and predictions of propane, butane and autogas at high pressures. *SAE Technical Paper Series, 982448.* 1998.

Lee, E, Park, J, Huh, K Y, Choi, J and Bae, C. Simulation of fuel/air mixture formation for heavy duty Liquid phase LPG injection (LPLI) engines. *SAE Technical Paper Series, 2003-01-0636.* 2003.

Lee, S-W, Kusaka, J, Daisho, Y. Spray characteristics of alternative fuels in constant volume chamber (comparison of the spray characteristics of LPG, DME and n-dodecane). *JSAE Review, v 22, n 3, p 271-276.* 2001.

Lee, S-W, Tananka, D, Kusaka, J, Daisho, Y. Two-dimensional laser induced fluorescence measurement of spray and OH radicals of LPG in constant volume chamber. *JSAE Review, v 23, n 2, p 195-203.* 2002.

Lee, S-W, Kusaka, J, Daisho, Y. Mixture formation and combustion characteristics of directly injected LPG spray. *SAE Technical Paper Series, 2003-01-1917.* 2003.

Lee, Y, Kim, C, Oh, S, Kang, K. Effects of injection timing on mixture distribution in a liquid-phase LPG injection engine for a heavy-duty vehicle. *JSME International Journal, Series B: Fluids and Thermal Engineering, v 47, n 2.* 2004.

Lee, D, Shakal, J, Goto, S, Ishikawa, H, Ueno, H, Harayama, N. Observation of flame propagation in an LPG lean burn SI engine. *SAE Technical Paper Series, 1999-01-0570.* 1999a.

Lentz, H P. Mixture Formation in Spark-Ignition Engines. Springer-Verlag / Society of Automotive Engineers 1992.

Li, D T, Xiong, R., Xue, H. Temperature measurement in the swirl chamber of an IDI engine using Moire deflectometry. *Applied Thermal Engineering, v 19, n 5, p 543-554.* 1999.

Li, L, Wang, Z, Deng, B, Han, Y, Wang, H. Combustion and emissions characteristics of a small spark-ignited LPG engine. *SAE Technical Paper Series, 2002-01-1738.* 2002.

Lippert, A M, El Tahry, S H, Huebler, M S, Parrish, S E, Inoue, H, Noyori, T. Development and optimization of a small-displacement, spark-ignition, direct-injection engine~Full-load operation. *SAE Technical Paper Series, 2004-01-0034.* 2004.

Lutz, B R, Stanglmaier, R H, Matthews, R D, Cohen, J, Wicker, R. Effects of fuel composition, system design, and operating conditions on in-system vaporization and hot start of a liquid-phase LPG injection system. *SAE Technical Paper Series, 981388.* 1998.

Lynch, D and Smith W J. Comparison of AFR calculation methods using gas analysis and mass flow measurement.. *SAE Technical Paper Series, 971013.* 1997.

Matthews, R D, Chiu, J, Zheng, J, Wu, D-Y, Dardalis, D, Shen, K, Roberts, C, Hall, M.J, Elizey, J.L, Mock, C, Wicker, R.B, Jaeger, R. Texas Project: Part 1 - emissions and fuel economy of aftermarket CNG and LPG conversions of light-duty vehicles. *SAE Technical Paper Series, 962098.* 1996.

Metghalchi, M and Keck, J C. Laminar burning velocity of propane-air mixtures at high temperature and pressure. *Combustion and Flame, v 38, p 143-154.* 1980.

Metghalchi, M and Keck, J C. Burning velocities of mixtures of air with methanol, iso-octane and indolene at high pressure and temperature. *Combustion and Flame, v 48, p 191-210.* 1982.

Moraal, P E. Adaptive compensation of fuel dynamics in an SI engine using a switching EGO sensor. *Proceedings of the IEEE Conference on Decision and Control,*

v 1, p 661-666. 1995.

Namazian, M, Hansen, S, Lyford-Pike, E, Sanchez-Barsse, J, Heywood, J, Rife, J. Schlieren visualization of the flow and density fields in the cylinder of a spark-ignition engine. *SAE Technical Paper Series, 800044.* 1980.

Newkirk, M S, Smith, L R, Payne, M E and Segal J S. Reactivity and exhaust emissions from an EHC-equipped LPG conversion vehicle operating on butane/propane fuel blends. *SAE Technical Paper Series, 961991.* 1996.

Oguma, M, Goto, S, Sugiyama, K, Kajiwara, M, Mori, M, Konno, M, Yano, T. Spray characteristics of LPG Direct Injection Diesel Engine. *SAE Technical Paper Series, 2003-01-0764.* 2003.

Oh, S, Kim, S, Bae, C, Kim, C, Kang, K. Flame propagation characteristics in a heavy duty LPG engine with liquid phase port injection . *SAE Technical Paper Series, 2002-01-1736.* 2002.

Oh, S, Lee, Y, Kang, K, Woo, Y, Bae, C. Fuel stratification in a liquid-phase LPG injection engine. *SAE Technical Paper Series, 2003-01-1777.* 2003.

Ortmann, R, Arndt, S, Raimann, J, Grzeszik, R; Wurfel, G. Methods and analysis of fuel injection, mixture preparation and charge stratification in different direct-injected SI engines. SAE Technical Paper Series, 2001-01-0970. 2001.

Ouelette, P and Hill, P. Visualization of natural gas injection for a compression ignition engine. *SAE Technical Paper Series, 921555.* 1992.

Paulsen, H and Valland, H. A new method for time-resolved full-field measurement of local average gas concentration during fuel-injection. *SAE Technical Paper Series, 960829.* 1996.

Raina, A, Midkiff, K C, Bell, S R and Carl, D. Characterization of the effects of methane and propane mixtures on performance and emissions in a spark-ignited engine. *ASME, Sparing Technical Conference, 98-ICE-108.* 1998.

Rakopoulos, C D and Mavropoulos, G C. Experimental instantaneous heat fluxes in the cylinder head and exhaust manifold of an air-cooled diesel engine. *Energy Conversion and Management, v 41, n 12, p 1265-1281.* 2000.

Rassweiler, G and Withrow, L. Motion pictures of engine flames correlated with pressure cards. *SAE Transactions, v 33, p 185-204.* 1938.

Ristovski, Z.D, Morawska, L, Bofinger, N D and Hitchins, J. Submicrometer and supermicrometer particulate emission from spark ignition vehicles. *Environmental Science and Technology, v 32, n 24, p 3845-3852.* 1998.

Ryu, J and Song, J. Emissions performance of Korean vehicles with different vehicle specification, mileage and fuel. *Proceedings of the Institution of Mechanical Engineers, Part D: Journal of Automobile Engineering, v 216, n 6, p 523-529.* 2002.

Salomons, M L, Dale, J D, Checkel, MD, Booth, N P, Krug, T, Ratke, T A, Erickson, D, Berg, I, Altimas, T and Apparao S. Development of University of Alberta entry in the 1997 Propane Vehicle Challenge. *SAE Special Publications, v 1360.* 1998.

Schiessl, R and Maas, U. Analysis of endgas temperature fluctuations in an SI engine by laser-induced fluorescence. *Combustion and Flame, v 133, n 1-2, p 19-27.* 2003.

Settles, G S. Schlieren and shadowgraph techniques : visualizing phenomena in transplant media. Springer, Berlin. 2001.

Shayler, P J, Wiseman, M W, Ma, T. Improving the determination of mass fraction burnt. *SAE Technical Paper Series, 900351.* 1990.

Shehata, M.S. Combustion characteristics of spark ignition engine fuelled by LPG. *American Society of Mechanical Engineers, Internal Combustion Engine Division (Publication) ICE, v 37, n 2, p 147-156.* 2001.

Shiraishi, H, Ipri, S L and Cho, D. CMAC neural network controller for fuel-injection systems. *IEEE Transactions on Control Systems Technology, v 3, n 1, p 32-38.* 1995.

Sierens, R . Experimental and theoretical study of liquid LPG injection. *SAE Technical Paper Series, 922363.* 1992.

Sjoberg, M and Dec, J E. An investigation of the relationship between measured intake temperature, BDC temperature, and combustion phasing for premixed and DI HCCI engines. *SAE Technical Paper Series, 2004-01-1900.* 2004.

Smith, W J, Timoney, D J, Lynch, D P. Emissions and efficiency comparison of gasoline and LPG fuels in a 1.4 litre passenger car engine. *SAE Technical Paper Series, 972970.* 1997.

Sobiesiak, A, Hoag, A, Battoei-Avarzaman, M. Injector durability and emissions from liquid LPG port-injected spark ignition engine. *SAE Technical Paper Series, 2003-01-3090.* 2003.

Stanglmaier, R, Strubhar, J, Roberts, C, Mine, K, Lutz, B, Wheeler, L, Diller, T, Wu, D-Y, Matthews, R and Hall M. Design and development of the University of Texas at Austin's 1997 Propane Vehicle Challenge entry. *SAE Special Publications, v 1360.* 1998.

Stodart, A, Aitchison, I and Lapetz, J. Emissions performance of bi-fuel CNG and bi-fuel LPG passenger cars using sequential multi-point injection systems. *SAE Technical Paper Series, 2001-01-1195.* 2001.

Stone, R. Introduction to internal combustion engines. Houndmills, Macmillan, 3rd Edition. 1999.

Stone, C R and Green-Armytage, D I. Comparison of methods for the calculation of mass fraction burnt from engine pressure-time diagrams. *Proceedings of Institution of Mechanical Engineers, Part D, v 201, p 61-67.* 1987.

Sugiyama, K, Kajiwara, M, Iwami, M, Mori, M, Oguma, M, Kinoshita, K, Goto, S. Performance and emissions of a DI diesel engine operated with LPG and cetane-enhancing additives. *SAE Technical Paper Series, 2003-01-1920.* 2003.

Tanaka, M, Warashina, M, Itano, Y, Tsujimoto, Y, Wakamatsu, S. Effects of super-light-duty gasoline and LPG-fueled cars on 16 ambient hydrocarbons at roadsides in Japan. *Chemosphere - Global Change Science, v 3, n 2, p 199-207.* 2001.

Tang, X, Asik, J R, Meyer, G M. Optimal A/F ratio estimation model (synthetic UEGO) for SI engine cold transient AFR feedback control. *SAE Technical Paper Series, 980798.* 1998.

Thobois, L, Lauvergne, R, Gimbres, D, Lendresse, Y. The analysis of natural gas engine combustion specificities in comparison with isooctane through CFD computation. *SAE Technical Paper Series, 2003-01-0009.* 2003.

Van Beeck, J P A J, Zimmer, L, Riethmuller, M L. Global rainbow thermometry for mean temperature and size measurement of spray droplets. *Particle and Particle Systems Characterization, v 18, n 4, p 196-204.* 2001.

Varde, K S. Ignition delay and emissions characteristics of a methanol-diesel fueled engine at low charge temperatures. *SAE Technical Paper Series, 920037.* 1992.

Watson, H C and Gowdie, D R R. The systematic evaluation of twelve LP gas fuels for emissions and fuel consumption. *SAE Technical Paper Series, 2000-01-1867.* 2000.

Woo, Y, Yeom, K, Bae, C, Oh, S, Kang, K. Effects of stratified EGR on the performance of a liquid-phase LPG injection engine. *SAE Technical Paper Series, 2004-01-0982.* 2004.

World LP Gas Asscociation. http://www.worldlpgas.com/. Accessed 20/9/2004. 2004.

Woschni, G. A universally applicable equation for the instantaneous heat transfer coefficient in the internal combustion engines. *SAE Transactions, v 76, p 3065-3083.* 1967.

Wu, D-Y, Matthews, R.D, Popova, E T, Mock, C. The Texas Project, Part 4~Final results: emissions and fuel economy of CNG and LPG conversions of light-duty vehicles. *SAE Technical Paper Series, 982446.* 1998.

Wu, D.-Y, Matthews, R.D, Zheng, J, Shen, K, Chiu, J, Mock, C, Jaeger, S. Texas Project: Part 3 - off-cycle emissions of light-duty vehicles operating on CNG, LPG, Federal Phase 1 reformulated gasoline, and/or low sulfur certification gasoline. *SAE Technical Paper Series, 962100.* 1996.

Wyszynski, L, Stone C R, Kalghatgi, G T. The volumetric efficiency of direct and port injection gasoline engines with different fuels. *SAE Technical Paper Series, 2002-01-0839.* 2002.

Yildiz, D, van Beeck, J P A J, Rithmuller, M I. Global Rainbow Thermometry applied to a flashing two-phase jet. *von Karmann Institute Publication* . 2002.